Design and Characterization of Broad Band and Multi-Band Slot Ring Antennas

By

Carlos A. Jaramillo Henao

A thesis submitted in partial fulfillment of the requirements for the degree of

MASTER OF SCIENCES

in

ELECTRICAL ENGINEERING

UNIVERSITY OF PUERTO RICO
MAYAGÜEZ CAMPUS

2004

Approved by:

_____	_____
José Colom Ustáriz, Ph.D. Member, Graduate Committee	Date
_____	_____
Sandra Cruz Pol, Ph.D. Member, Graduate Committee	Date
_____	_____
Rafael Rodríguez Solís, Ph.D. President, Graduate Committee	Date
_____	_____
Isidoro Couvertier, Ph.D. Chairperson of the Department	Date
_____	_____
David González Barreto, Ph.D. Representative of Graduate Studies	Date

Abstract

In this thesis, the Design of Experiments technique is applied to characterize rectangular slot ring antennas in terms of their physical dimensions and relative permittivity of the substrate. Several 2^5 factorial designs were simulated in two different electromagnetic simulators, Momentum and Designer, to collect data for the statistical analysis. Three different approaches were used to identify the most influential factors in the antenna response. The first one was an intuitive approach using a geometrical representation of the DOE input factors. This approach allowed to identify the factors that affected the antenna resonance frequency, multiband operation, impedance bandwidth and return loss. The second approach was based on a linear regression model that was applied to the return loss response. Confidence frequency bands based on the adjusted determination coefficient were presented; in these bands the linear regression models were reliable to identify the significant factors in the antenna response. Finally, several linear models for different resonance frequencies and antenna input impedance were computed using punctual responses and two replicates of the same design. In order to validate the simulations some prototypes were fabricated and tested.

Resumen

En esta tesis se utilizó la técnica de diseño de experimentos para caracterizar antenas rectangulares de anillo en términos de sus dimensiones físicas y la permitividad relativa del substrato. Se simularon varios diseños factoriales de 2^5 en dos simuladores electromagnéticos diferentes, Momentum y Designer, con el objetivo de reunir datos para el análisis estadístico. Se aplicaron tres diferentes tipos de análisis para identificar los factores más influyentes en la respuesta de la antena. El primero fue un análisis intuitivo utilizando una representación geométrica de los factores de entrada del diseño de experimentos. Este método permitió identificar los factores que afectaban la frecuencia de resonancia de la antena, operación de multi banda, ancho de banda de la impedancia de entrada y las perdidas de retorno. El segundo análisis fue basado en un modelo de regresión lineal que fue aplicado a la respuesta de perdidas de retorno. Se definieron bandas de confianza con base en el coeficiente de determinación ajustado; en estas bandas los modelos de regresion lineal eran confiables para identificar los factores significantes en la respuesta de la antena. Finalmente, en el tercer método se calcularon modelos lineales para la frecuencia de resonancia y la impedancia de entrada de la antena utilizando respuestas puntuales y dos replicas del mismo diseño. Para validar las simulaciones se fabricaron y se midieron algunos prototipos.

Acknowledgments

I would like to thank Dr. Rafael Rodriguez Solis for his patience and critical review to this thesis.

Special thanks, to the professors of my graduate committee: Dr. José Colom Ustáriz, Dr. Sandra Cruz Pol, Dr. David Gonzalez Barreto because their participation in this work was very important to me.

I would also thank to my family, specially my mom for her prayers.

This work was sponsored by the National Science Foundation CARREER Award ECS-0093650.

Table of Contents

List of Tables..... *x*

List of Figures..... *xiii*

Chapter 1. Introduction..... 1

Section 1.1 Justification..... 1

Section 1.2 Objectives..... 2

Section 1.3 Project Description..... 2

Section 1.4 Work Organization..... 3

Chapter 2. Literature Review and Background..... 4

Section 2.1 Antenna Configuration and Characteristics..... 4

Section 2.1.1 Slot-line Characteristics…… 5

Section 2.2 Enhancement to the Slot Antenna Basic Configuration…..... 7

Section 2.3 Applications……..... 9

Section 2.4 Coplanar Waveguide Transmission Line……..... 11

Section 2.5 Design of Experiments (DOE)……..…… 12

Section 2.5.1 Basic Definitions……..….. 13

Section 2.5.2 General Guidelines to Design Experiments……..... 13

Section 2.6 Simulation Software……..…… 14

Section 2.7 Summary..... 15

Chapter 3. Methodology..... 16

Section 3.1 Design Method……..... 16

Section 3.1.1 CPW Transmission Line Design…….....16

Section 3.2 DOE for the RSRA……..... 18

Section 3.2.1 DOE for RSRA with Parasitic Ring Outside the Feeding Antenna..... 18

Section 3.2.2 DOE for RSRA with Parasitic Ring Inside the Feeding Antenna…….. 23

Section 3.2.3 DOE for RSRA with Parasitic Ring Outside and Inside the Feeding Antenna..... 24

Section 3.3 Linear Regression Model for RSRA…….……. 25

Section 3.3.1 Model Adequacy Checking..... 29

Section 3.3.2 Hypothesis Testing in Linear Regression..... 30

Section 3.3.2.1 Testing for Significance of Regression……..... 30

Section 3.3.2.2 Determination Coefficient and Adjusted Determination Coefficient….. 32

Section 3.3.2.3 Testing Hypotheses on Individual Regression Coefficients…..... 33

Section 3.3.3 Application Example.…….…… 37

Section 3.4 DOE Using Punctual Responses.……... 40

Section 3.5 Antenna Fabrication and Testing.……..…… 44

Section 3.6 Summary..... 44

Chapter 4. Results and Discussions..... 46

Section 4.1 First Approach: Intuitive Analysis……..... 46

Section 4.1.1 RSRA with the Parasitic Ring outside the Feeding Antenna……..…… 46

Section 4.1.1.1 Effects of Changing the Substrate Permittivity on the Resonance Frequencies and Return Loss Response……... 46

Section 4.1.1.2 Effects of Changing the Slot Width (W) on the Resonance Frequencies and Return Loss Response…….…….. 49

Section 4.1.1.3 Effects of Changing the Feeding Antenna Perimeter (L_1) on the Resonance Frequencies and Return Loss Response……..... 51

Section 4.1.1.4 Effects of Changing the Distance (W_s) Between the Parasitic Ring and the feeding Antenna on the Resonance Frequencies and Return Loss Response……... 52

Section 4.1.1.5 Effects of Changing the Length of the Open Circuit Stub (L_s) on the Resonance Frequencies and Return Loss Response…….… 53

Section 4.1.1.6 Summary of the Effects……... 54

Section 4.1.2 RSRA with the Parasitic Ring inside the Feeding Antenna……..... 54

Section 4.1.2.1 Effects of Changing the Substrate Permittivity on the Resonance Frequencies and Return Loss Response……..... 54

Section 4.1.2.2 Effects of Changing the Slot Width (W) on the Resonance Frequencies and Return Loss Response……..... 55

Section 4.1.2.3 Effects of Changing the Feeding Antenna Perimeter (L_1) on the Resonance Frequencies and Return Loss Response……..….... 56

Section 4.1.2.4 Effects of Changing the Distance (W_s) Between the Parasitic Ring and the feeding Antenna on the Resonance Frequencies and Return Loss Response……..…. 58

Section 4.1.2.5 Effects of Changing the Length of the Open Circuit Stub (L_s) on the Resonance Frequencies and Return Loss Response…….…… 59

Section 4.1.2.6 Summary of the Effects……... 60

Section 4.2 Second Approach: Linear Regression Analysis…….…… 60

Section 4.2.1 RSRA with the Parasitic Ring outside the Feeding Antenna…..... 60

Section 4.2.2 RSRA with the Parasitic Ring inside the Feeding Antenna…..... 64

Section 4.3 Third Approach: DOE Using Punctual Responses……..... 67

Section 4.3.1 RSRA with Parasitic Ring outside the Feeding Antenna…… 68

Section 4.3.1.1 First Resonance Frequency……..……..... 71

Section 4.3.1.2 Input Impedance at First Resonance Frequency…….. 74

Section 4.3.1.3 Second Resonance Frequency…..……..... 77

Section 4.3.1.4 Input Impedance at Second Resonance Frequency....…….. 79

Section 4.3.1.5 Third Resonance Frequency……...…. 80

Section 4.3.1.6 Input Impedance at Third Resonance Frequency……..... 83

Section 4.3.1.7 Model Optimization……..... 85

Section 4.3.2 RSRA with Parasitic Ring inside the Feeding Antenna…….…. 88

Section 4.3.2.1 First Resonance Frequency……..…… 91

Section 4.3.2.2 Input Impedance at First Resonance Frequency……..… 94

Section 4.3.2.3 Second Resonance Frequency…..……... 94

Section 4.3.2.4 Input Impedance at Second Resonance Frequency....…….. 96

Section 4.3.2.5 Third Resonance Frequency……..….. 98

Section 4.3.2.6 Input Impedance at Third Resonance Frequency……... 101

Section 4.3.2.7 Model Optimization……... 104

Section 4.3.3 Characterization Summary…… 106

Section 4.4 Matching Technique……..... 108

Section 4.5 RSRA Case 3……... 109

Section 4.5.1 Superposition of Responses……..… 109

Section 4.5.2 Impedance Scaling Varying W_{s2} in the RSRA Case 3……. 110

Section 4.5.3 Impedance Scaling Adding Multiple Parasitic Rings in the RSRA Case 3……..... 110

Section 4.6 RSRA Electric Field Distribution, Radiation Pattern and Gain……..… 112

Section 4.7 Antenna Testing……... 115

Section 4.8 Summary 119

Chapter 5. Conclusions and Recommendations 120

Section 5.1 Conclusions 120

Section 5.2 Recommendations 121

References 122

Appendix A..…… 125

Appendix B……. 127

List of Tables

Table 3.2.1. CPW Transmission Line Parameter Results……. 17

Table 3.2.2. Factors and Levels for RSRA Case 1……... 19

Table 3.2.3. Design Matrix of 2^5 Full Factorial with two Center Points…….. 21

Table 3.3.1. Frequency Ranges where the Model coefficient is ≠ 0 and its location in the Model…… 34

Table 3.3.2. Behavior of the coefficients in the frequency band from 5.5 to 6 GHz…… 37

Table 3.4.1. RSRA Case 1 Design Summary……... 40

Table 3.4.2. ANOVA for the First Resonance Frequency…… 42

Table 4.1.1. Values of λ_g according to expressions (4.1.1) and (4.1.2)…… 48

Table 4.1.2. Summarized effects of the Main Factors when they were changed from Low to High Level……..... 54

Table 4.1.3. Summarized effects of the Main Factors when they were changed from Low to High Level……..... 60

Table 4.2.1. Confidence Bands……..… 62

Table 4.2.2. Betas, Codified and Natural Factors with low impact in the response…..… 63

Table 4.3.1. First and Second Replicate. Designer and Momentum Results…… 69

Table 4.3.2. First and Second Replicate. Designer and Momentum Results…… 71

Table 4.3.3. ANOVA for the First Resonance Frequency…… 72

Table 4.3.4.Values for the First Resonance Frequency Simulated in Designer and Momentum and the Resonance Frequency obtained from the Model…….……..… 73

Table 4.3.5. ANOVA for the Input Impedance at First Resonance Frequency……..... 76

Table 4.3.6.Values for the Input Impedance at First Resonance Frequency Simulated in Designer and Momentum and the Input Impedance obtained from the Model……...… 76

Table 4.3.7. ANOVA for the Second Resonance Frequency……..... 78

Table 4.3.8. ANOVA for the Input Impedance at Second Resonance Frequency…… 79

Table 4.3.9. ANOVA for the Third Resonance Frequency……...… 81

Table 4.3.10.Values for the Third Resonance Frequency Simulated in Designer and Momentum and the Resonance Frequency obtained from the Model…..……..… 82

Table 4.3.11. ANOVA for the Input Resistance at Third Resonance Frequency……. 84

Table 4.3.12.Values for the Input Impedance at Third Resonance Frequency Simulated in Designer and Momentum and the Input Impedance obtained from the Model……...… 84

Table 4.3.13. Constraints for the Responses……. 86

Table 4.3.14. Solutions for the Optimization……...……. 86

Table 4.3.15. First and Second Replicate. Designer and Momentum Results…….. 89

Table 4.3.16. First and Second Replicate. Designer and Momentum Results……..… 90

Table 4.3.17. RSRA Case 2 Design Summary……. 91

Table 4.3.18. ANOVA for the First Resonance Frequency…… 92

Table 4.3.19.Values for the First Resonance Frequency Simulated in Designer and Momentum and the Resonance Frequency obtained from the Model…….……..… 93

Table 4.3.20. ANOVA for the Second Resonance Frequency…..…..... 95

Table 4.3.21. ANOVA for the Input Impedance at Second Resonance Frequency…..… 97

Table 4.3.22. ANOVA for the Third Resonance Frequency……..…. 99

Table 4.3.23.Values for the Third Resonance Frequency Simulated in Designer and Momentum and the Resonance Frequency obtained from the Model…..……... 100

Table 4.3.24. ANOVA for the Input Resistance at Third Resonance Frequency…….... 102

Table 4.3.25.Values for the Input Impedance at Third Resonance Frequency Simulated in Designer and Momentum and the Input Impedance obtained from the Model…….…... 103

Table 4.3.26. Constraints for the Responses……... 104

Table 4.3.27. Solutions for the Optimization……...……..…. 104

List of Figures

Figure 2.1.1. Feeding techniques in a slot antenna……..... 5

Figure 2.1.2. Field and current distribution……..... 6

Figure 2.2.1. Impedance scaling by multiple slots…….. 7

Figure 2.2.2. Geometry of a circular slot ring antenna with microstrip feed……..… 9

Figure 2.4.1. CPW geometry and electric field distribution……..... 11

Figure 3.1.1. Top and side view of RSRAs…….…. 16

Figure 3.1.2. CPW Transmission line and design parameters……...… 17

Figure 3.2.1. RSRA with parasitic ring outside the feeding antenna……..... 18

Figure 3.2.2. Geometrical representation for 2^5 full factorial design……... 22

Figure 3.2.3. RSRA with parasitic ring inside the feeding antenna…….. 23

Figure 3.2.4. RSRA with parasitic ring inside and outside the feeding antenna…….. 24

Figure 3.3.1. Simulated and estimated return loss for different designs……...… 28

Figure 3.3.2. Plot of residuals for the first frequency point…….. 29

Figure 3.3.3. F_0 value and F statistic……. 31

Figure 3.3.4. Determination coefficient and adjusted determination coefficient……. 32

Figure 3.3.5. t_0 value and t statistic for individual regression coefficients……...… 35

Figure 3.3.6. β's codified values……... 36

Figure 3.3.7. Beta codified values in the interest band……. 39

Figure 3.3.8. Simulated designs……..... 39

Figure 3.3.9. Determination coefficients…….. 40

Figure 3.4.1. Normal probability plot of the effects for the first resonance frequency.... 42

Figure 3.4.2. Plot of residuals for first resonance frequency response……. 43

Figure 4.1.1. Input reactance and return loss for two experiments……... 49

Figure 4.1.2. Input reactance and return loss for two experiments……... 50

Figure 4.1.3. Input reactance and return loss for two experiments……... 51

Figure 4.1.4. Input reactance and return loss for two experiments……... 52

Figure 4.1.5. Input reactance and return loss for two experiments……... 53

Figure 4.1.6. Input reactance and return loss for two experiments……... 55

Figure 4.1.7. Input reactance and return loss for two experiments……... 56

Figure 4.1.8. Input reactance and return loss for two experiments……... 57

Figure 4.1.9. Input reactance and return loss for two experiments……... 58

Figure 4.1.10. Input reactance and return loss for two experiments……. 59

Figure 4.2.1. Determination Coefficient for 15 regressors and confidence bands…...… 61

Figure 4.2.2. t_0 value and t statistic for individual regression coefficients……... 62

Figure 4.2.3. β's codified values……...… 64

Figure 4.2.4. Determination Coefficient for 15 regressors and confidence bands…...… 65

Figure 4.2.5. t_0 value and t statistic for individual regression coefficients……... 65

Figure 4.2.6. β's codified values……...… 67

Figure 4.3.1. Plot of residuals for the first resonance frequency…….. 74

Figure 4.3.2. Normal probability plot of the effects for the input impedance at first resonance frequency……. 75

Figure 4.3.3. Plot of residuals for Zin_1 at resonance ……..…….. 77

Figure 4.3.4. Normal probability plot of the effects for the second resonance frequency…….. 77

Figure 4.3.5. Plot of residuals for the second resonance frequency……..... 78

Figure 4.3.6. Normal probability plot of the effects for the input impedance at second resonance frequency…….. 79

Figure 4.3.7. Plot of residuals for the input impedance at second resonance frequency.. 80

Figure 4.3.8. Normal probability plot of the effects for the third resonance frequency... 81

Figure 4.3.9. Plot of residuals for the third resonance frequency……. 82

Figure 4.3.10. Normal probability plot of the effects for the input impedance at third resonance frequency…….. 83

Figure 4.3.11. Plot of residuals for the input impedance at third resonance frequency… 85

Figure 4.3.12. Graphical representation of factors and responses for the first row of table 4.3.14……. 87

Figure 4.3.13. Normal probability plot of the effects for the first resonance frequency.. 92

Figure 4.3.14. Plot of residuals for the first resonance frequency……..... 93

Figure 4.3.15. Normal probability plot of the effects for the second resonance frequency…….…. 95

Figure 4.3.16. Plot of residuals for second resonance frequency……. 96

Figure 4.3.17. Normal probability plot of the effects for the input impedance at second resonance frequency…….…. 97

Figure 4.3.18. Plot of residuals for the input impedance at second resonance frequency……..... 98

Figure 4.3.19. Normal probability plot of the effects for the third resonance frequency…….. 99

Figure 4.3.20. Plot of residuals for the third resonance frequency……. 100

Figure 4.3.21. Normal probability plot of the effects for the input impedance third resonance frequency……..... 102

Figure 4.3.22. Plot of residuals for the third resonance frequency……. 103

Figure 4.3.23. Graphical representation of factors and responses for the first row of table 4.3.26……... 105

Figure 4.3.24. Characterization summary..…… 106

Figure 4.3.25. Flow chart design guide……...…… 107

Figure 4.4.1. RSRA Case 2. Effects of increasing W_t for design b……...…. 108

Figure 4.5.1. Illustration of the superposition property……..… 109

Figure 4.5.2. Impedance secaling varying W_{s2} for the RSRA case 3……..... 110

Figure 4.5.3. Impedance scaling adding multiple exterior rings……..... 111

Figure 4.6.1. Electric field distribution on the substrate side for the RSRA design (1) at 5.6 GHz……... 112

Figure 4.6.2. Radiation pattern for design (1) at 5.6 GHz xz and yz plane…… 113

Figure 4.6.3. Radiation pattern for design (1) (case 2) at 5.6 GHz xz and yz plane…… 114

Figure 4.6.4. Radiation pattern for design (1) (case 3) at 5.6 GHz xz and yz plane…… 115

Figure 4.7.1. Simulated and measured return loss for the RSRA case 1…… 116

Figure 4.7.2. Simulated and measured return loss for the RSRA case 2……..... 117

Figure A.1. T test for three factor interaccions……... 125

Figure B.1. Determination coefficients for 5 regressors……. 127

Chapter 1. Introduction

1.1 Justification

The wireless communications industry has had an explosive growth in the last two decades. This growth has shown that wireless channel is a reliable mechanism to transport data, voice, and video. It is expected that this revolution in wireless communication will continue in the next few years. Therefore, it will be necessary to use higher bandwidths, simultaneous access to different systems through the same device, and data rates on the order of megabits per second to satisfy the demand of audio and video transmission from everywhere. For instance, the data rates in Third (3G) and Fourth Generation (4G) Cellular systems are 2.4 Mbps and 20 Mbps respectively. Consequently, a major concern in the antenna design is to characterize antennas that can provide wide bandwidth or multiple band operation.

The need for different kinds of traffic and highly mobile networks requires special antennas. This is the case of smart antenna arrays that can automatically optimize their radiation pattern depending of the scenario, in order to improve radio link performance. In addition, these antennas must be small and low profile in order to keep terminal size and weight small enough. Also, low profile antennas do not affect vehicle aerodynamics; this parameter is very important in mobile and aircraft applications.

An antenna structure that can be used in smart antenna arrays and fulfills the above requirements is a Slot Ring Antenna (SRA). However this antenna is usually

narrow band and few techniques have been published to address the problem of increasing the impedance bandwidth or multiband operation. In order to overcome this narrow bandwidth and to achieve a better impedance bandwidth (VSWR<2) in the operating point, some techniques, such as adding parasitic elements to a SRA and varying its dimensions are investigated in this research. In addition, it is investigated the fact that some of these techniques produce multiple resonances or tuning agility.

1.2 Objectives

The main objective of this research is the partial characterization of a concentric slot ring antenna array (CSRAA) using two different substrates. This characterization will be based on design of experiments (DOE) and should predict antenna performance according to different design specifications. With this characterization it is possible to find out the effect of changing either the antenna dimensions or the relativity permittivity of the substrate in the antenna response. In addition, identify the most influential variables and where to set these variables in order to optimize the antenna response. Finally, based on the characterization results, simplified linear models will be developed.

1.3 Project Description

This thesis presents the characterization of CSRAA in terms of the antenna dimensions and the relativity permittivity of the substrate. DOE is used as the tool for this characterization. The data collected for the DOE analysis is from electromagnetic simulations using Method of Moments commercial software. In order to have two

replicates of the same experiment; two different electromagnetic simulators, Ansoft's Designer and Agilent's Momentum are used. With the DOE analysis it is possible to establish linear models for specified RSRA parameters. Linear models provide computationally inexpensive approximations to engineering simulations models. In order to validate the simulations some prototypes will be fabricated and measured at the Radiation Laboratory at the University of Puerto Rico at Mayagüez.

1.4 Work Organization

A literature review is presented in Chapter 2. This chapter deals with the basic configuration and characteristics of slot antennas, slot lines and coplanar waveguide transmission lines. In addition, the software used in the simulations and in the analysis of the data is introduced and a short review of DOE theory is presented. Chapter 3 explains how the antenna was designed, simulated, characterized and how its responses were analyzed. Finally, it explains how the antennas were implemented and measured. Chapter 4 explains the results of the simulations, measured of prototypes and linear models obtained from the DOE analysis. Finally, Chapter 5 presents conclusions of the characterization and recommendations for future research.

Chapter 2. Literature Review and Background

2.1 Antenna Configuration and Characteristics

A slot antenna is a metallic sheet with a narrow slot that is either over a substrate or air. The other side of the dielectric is with or without any metallization. The slot can be of different shapes such as circles, and squares, for example. There are basically two ways to feed this antenna. The first way is using a microstrip line feeding the slot on the opposite side of the substrate; in this case, the fields of the line excite the slot. The microstrip line can be short-circuited with the edge of the slot or open-circuited. This configuration is shown in Figure 2.1.1(a). However this feeding possibility is not compatible with monolithic fabrication which means that is not possible to integrate the antenna and solid state devices in a single block. A variation to this technique is using a stripline instead of a microstrip line. The other way is using Coplanar Waveguide (CPW) transmission lines. This technique has lower radiation loss and less dispersion than microstrip lines. A CPW line feeding alternative is shown in Figure 2.1.1(b). Other CPW line feeding variations, such as offset-fed slot antenna and capacitively or inductively coupled slot antenna are considered in [1]. In the CPW-fed configuration it is easier to place lumped components and it is not necessary to drill holes through the substrate to reach the ground plane. For instance, an advantage of this configuration is the possibility to have an antenna-mixer structure. Since CPW lines are used to feed the antenna in this research a deeper analysis is considered later in this same chapter.

Some of the advantages of this antenna are low profile, low weight and easy fabrication. A single slot antenna presents an input impedance of nearly 500 Ω at its first resonance frequency and bandwidth in the order of 5-30% for a VSWR<2.

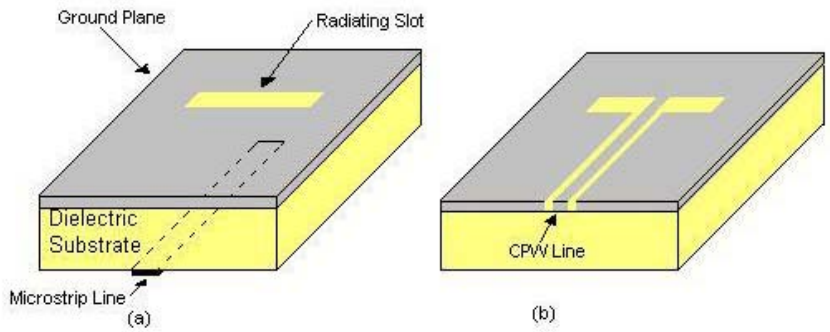

Figure 2.1.1. Feeding techniques in a Slot Antenna. (a) Microstrip line feeding. (b) CPW line feeding

One of the earliest works published about slot antennas was done in 1961 by Johnson and Jasik [2]. They considered a slot antenna as a rectangular slot in a thin metallic sheet. The electric field distribution in the slot was calculated using a complementary wire dipole antenna with the electric and magnetic field interchanged. The antenna radiates on both sides of the sheet. Also, as in wire antennas, a slot in a metallic sheet will be resonant when it is a half wavelength long (λ/2). One variation to a simple slot is an annular slot; in this case the complementary structure is a wire loop.

2.1.1 Slot-line Characteristics

In the slot-line shown in Figure 2.1.2 (a), the wave propagates along the slot with the electric field component oriented across the slot in the plane of metallization on the dielectric substrate; the magnetic field is perpendicular to the slot; the mode of propagation is non-TEM [3].

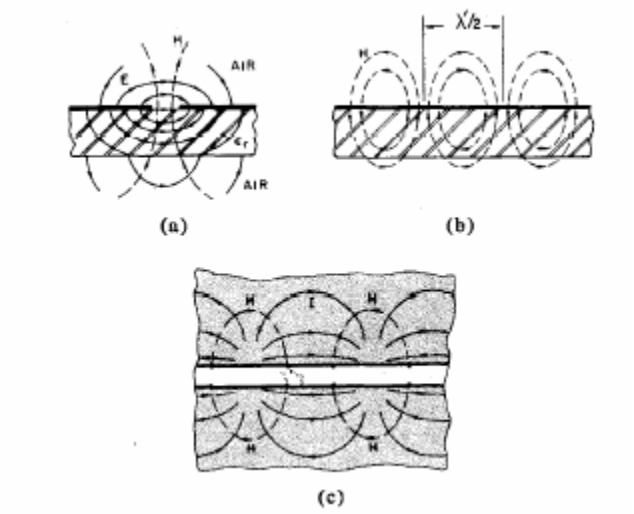

Figure 2.1.2. Field and current distribution. (a) Field distribution in cross section. (b) H field in longitudinal section. (c) Current distribution on metal surface. (Taken from [3])

Figure 2.1.2 (b) shows that the magnetic field curves and returns to the slot at half-wavelength intervals. The field components are confined to the substrate and they are on both sides of the substrate and the metallization layer; the energy is distributed between the substrate and the air regions.

Figure 2.1.2 (c) shows the current paths on the conducting surface. The surface-current density is greatest at the edges of the slot and decreases with distance from the slot. In slot lines, the characteristic impedance Z_0 and the phase velocity v are not constant since the non-TEM nature of the slot line mode. In contrast, in microstrip lines Z_0 and v are almost independent of frequency because of their quasi-TEM propagation mode. Another important feature of slot lines is that they have no cutoff frequency unlike waveguides.

For a slot line to be practical as an antenna, radiation must be maximized. This is achieved using a low ε_r substrate which cause that the energy does not concentrate in the

substrate but it radiates through the space. In [4] Janaswamy and Schaubert present empirical formulas to calculate the slot wavelength and the characteristic impedance of wide slots etched on an electrically thin substrate of low dielectric constant ε_r.

2.2 Enhancement to the Slot Antenna Basic Configuration

Some papers have been written about changing some antenna physical characteristics in order to improve bandwidth, multiple resonance or tuning agility. These changes go from varying the slot width or the slot shape to the addition of varactors or PIN diodes switches.

As it was mentioned before, a single slot antenna presents high input impedance, however this impedance can be scaled down using folded slots [5]. Figure 2.2.1 shows the impedance scaling with the number of slots.

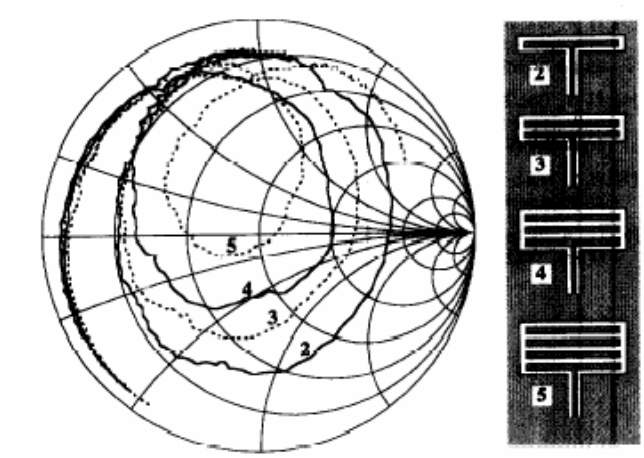

Figure 2.2.1. Impedance scaling by multiple slots. Taken from [5]

Furthermore, in [6] it is shown that a loop antenna in a rectangular slot shape has a wider bandwidth than a single slot. In both cases the slots are fed using CPW line.

In addition, in [7], Misra and Chowdry worked with a complementary structure using microstrip antennas instead slot antennas. The authors have designed a Concentric Microstrip Triangular Ring antenna (CMTRA) using the log-periodic principle. The CMTRA array is fed by a 50 Ω microstrip line. Results, using the finite-difference time-domain (FDTD), show that the bandwidth of the CMTRA is increased with respect to the single triangular-ring antenna. This feature is very attractive not only for CMTRA but also Slot Ring Antennas (SRA) because in both cases the bandwidth is increased without changing antenna's dimensions.

Circular (annular) slot rings have been used with varactor diodes to change the antenna polarization state and radiation pattern [8] and rectangular slot rings have been made tunable using varactor diodes in [9]. Gupta [10] has presented a frequency-reconfigurable rectangular ring slot antenna fed by a single slot line or CPW line. The tuning is carried out changing the perimeter of the slot ring using PIN diode switches.

Other work about tunable SRA is reported by Tehrani and Chang [11]. They analyzed a slot ring antenna with one microstrip electromagnetic coupling as it is shown in Figure 2.2.2. In this work, the microstrip feed is ignored and the slot-ring antenna is considered as a transmission line. As a result of this, the operating frequency is the frequency at which the circumference of the slot ring antenna becomes one guided wavelength of the slot. Simulated and experimental results show that multiple operating frequencies can be obtained when the microstrip open-circuited stub AC, as shown in Figure 2.2.2 varies among 4.85 mm, 16.85 mm and 46.85 mm. Similarly, the effect of

changing w_s is studied and the results show that it is possible to improve the performance characteristics of the antenna impedance and excite multiple operating frequencies.

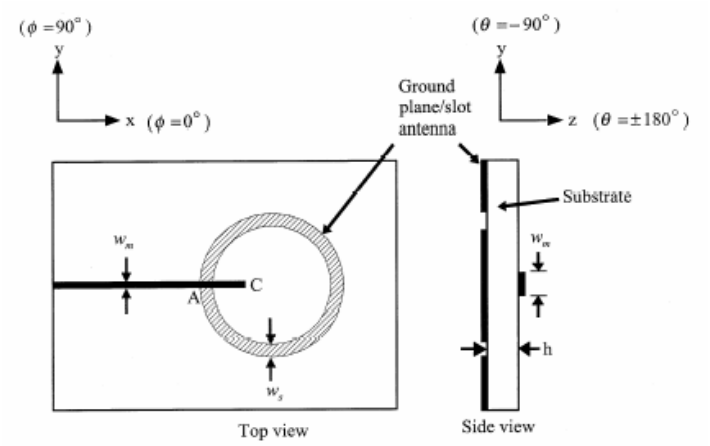

Figure 2.2.2. Geometry of a circular slot ring antenna with microstrip feed. w_m=2.16 mm, w_s=2.9 mm, slot ring mean circumference = 93.3 mm (Taken from [11])

2.3 Applications

Slot ring antennas have been used in applications such as millimeter wave receivers, transmitters, imaging arrays, aircraft landing systems, automotive anti-collision systems and satellite communication systems. They have been mainly used in mobile communications, since they can radiate power at low elevation angles [12].

There are many applications reported of SRA in the design and implementation of balanced mixer receivers. In [13] Tong and Blundell have used a SRA in the development of a magic slot balanced mixer. In this work, the mixer, antenna and local oscillator are incorporated in a single unit. Since a full wave analytical study of the SRA has not been developed, a qualitative description is presented. The geometric shape of the SRA is a square. This antenna has been designed to operate at around 2.5 cm wavelength. The slot antenna is fed by two 50 Ω microstrip lines at the center of two

opposite sides of the square. This design has good radiation impedance, flat frequency response and well behaved diffraction limited radiation patterns over the bandwidth.

Other application in which SRA is suitable for implementing a balanced mixer is presented in [14]; again Tong and Blundell developed a solution for radiation patterns of the different operating modes of an annular slot antenna printed on a dielectric half space.

In addition, Sthephan, Camilleri, and Itoh [15], reported another integrated planar antenna-mixer structure for use at millimeter-wave frequencies. They applied the Garlekin's method in the Hankel transform domain in order to calculate the radiation pattern. Also, they investigated the performance of the structure on a high dielectric constant substrate; the investigation showed that it is practical to fabricate the structure on a thin GaAs wafer.

Furthermore, Raman and Rebeiz in [16] used single and dual polarized SRAs on a silicon dielectric lens. Since these antennas are fed using CPW line; they are compatible with uniplanar mixers and low noise amplifiers. These antennas were fabricated and measured at millimeter-wave frequencies (90-100 GHz). The measured millimeter-wave patterns agreed with the theoretical results. Finally, a 2 x 2 SRA array for monopulse applications was presented by the authors. The antennas are placed on a dielectric lens in order to eliminate power loss to substrate modes and increase antenna directivity. It is worth mentioning that aircraft landing systems and automotive collision avoidance sensors are based on these monopulse applications. Further information of slot ring antennas integrated with amplifiers and mixers can be found in [17] and [18].

2.4 Coplanar Waveguide Transmission Line

Coplanar lines are transmission lines where all the conductors are in the same plane [19]; i.e. slotline, coplanar waveguide and coplanar strip. As it was mentioned at the beginning of the chapter, in coplanar lines it is possible to connect active and passive circuit components in shunt from the conducting strip to the ground plane on the same side of the substrate and it is not needed to drill holes through to the substrate to reach the ground plane.

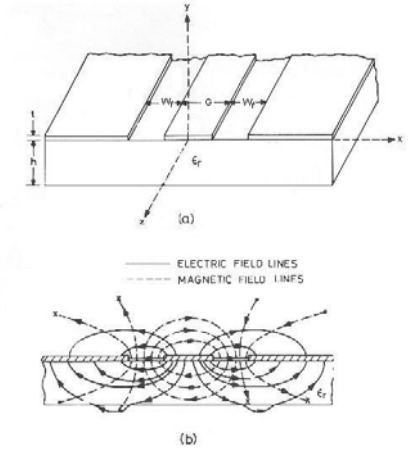

Figure 2.4.1. (a) CPW geometry. (b) Electric and magnetic field distributions in CPW. (Taken from [19])

The coplanar waveguide consists of two slots each of width W_f printed on a dielectric substrate. The central conductor width is denoted by G as it is shown in Figure 2.4.1 (a). The electric and magnetic field distributions are shown in Figure 2.4.1 (b). The mode of propagation in the CPW becomes non-TEM because a longitudinal component of the magnetic field is present.

CPW is used as a feed line in patches, slots and folded slot antennas. The most practical method to feed a SRA is using CPW. In [20] M.H Yeh, P. Hsu and J.F. Kiang analyzed CPW-fed slot ring antenna using a spectral domain moment method. They also

studied other feed lines such as microstrips and striplines and inferred that the antenna with the CPW-fed has better performance than the others in terms of return loss and bandwidth.

2.5 Design of Experiments (DOE)

Design of Experiments has been used in the analysis of microstrip patches [21] and folded slot antennas [22]; it is a statistical technique that allows organizing experiments to extract information according to intentional changes in one or more input parameters [23]. Experiments play a major role in developing and improving products and process. The goal, in many cases, is to develop a robust process which is not affected by external sources.

2.5.1 Basic definitions

The input parameters in an experiment are called factors; they are controlled independent variable whose impact in the response wants to be known. These factors can be qualitative such as kind of material, machine number, etc, or quantitative such as temperature, velocity etc. The levels or alternatives of the factors are set by the experimenter. In a factorial design 2^k the number of levels is two and in 3^k the number of levels is three. In both cases k is the number of factors. The combination of factors is known as treatment. A same treatment can be repeated during the experiment, this experimental condition is a replicate. The output variable that it wants to be measured is

the response. The objective of any experiment is to determine how the factors affect the response.

In addition, the factors can be fixed or random. In an experiment with fixed factors, the treatments are specifically chosen by the experimenter. In this situation the test of hypothesis is about the treatment means and the conclusions apply only to the factors levels considered in the analysis. The conclusions can not be extended to similar treatments that were not explicitly considered. This research works with fixed factors. On the other hand, in an experiment with random factors, the treatments are a random sample from a larger population of treatments. In this situation the conclusions can be extended to all treatments in the population.

In the Analysis of Variance (ANOVA) there are two assumptions that are followed; the first one is that the observations are adequately described by a linear regression model and the second is that the errors are normally and independently distributed with mean zero and constant but unknown variance σ^2. If these assumptions are valid, the ANOVA procedure is an exact hypothesis test of no difference in treatment means.

2.5.2. General Guidelines to Design Experiments

To use the statistical approach in designing and analyzing an experiment it is necessary to have a clear idea of what is to be studied, how to collect the data and how to analyze it. A recommended procedure is as follows.

- To establish the problem clearly

- To identify the response variable and to determine the most effective form to measure it
- To select to the factors of interest and the levels at which they will be prove.
- To determine the type of experiment that must be executed. To plan all the details.
- To carry out the experiment according to how it was planned.
- To analyze the data using a reliable tool
- Conclusions and design a new experiment if it is necessary.
- Run of validation or confirmation
- Recommendations.

2.6 Simulation Software

To collect data for the statistical analysis the electromagnetic simulator Ansoft's Designer [24] and Agilent's Momentum [25] will be used. These simulators are based on Method of Moments and use full wave electromagnetic functions for planar analysis based on Maxwell's equations. They compute the input impedance and radiation characteristics for arbitrary shape antennas.

Designer also integrates with Ansoft's Optimetrics module for optimization of planar circuits and antennas. Optimetrics allows Designer users to perform parametric analysis, optimization, and sensitivity analysis. With Optimetrics, design variations can be analyzed, components can be optimized, and DOE studies can be automated [24]. ADS

Line Calc [25] is used to calculate the dimensions of the CPW transmission line on base of input parameters such as Frequency, substrate relative permittivity, and thickness.

In addition, Stat-Ease's Design Expert is used for data analysis. This software helps to find the critical factors that lead to breakthrough improvements and to optimize the antenna response [26].

2.7 Summary

This chapter presented a literature review of slot antennas and slot ring antennas. First of all, the antenna's basic configuration and characteristics such as the field distribution, radiation pattern, etc were explained. Second, some enhancements to the basic configuration were presented on base to preview publications. Third, some applications of slot ring antennas were exposed. These applications go from millimeter wave transmitters-receivers to satellite communications systems. Fourth, some characteristics of the CPW transmission line are explained. And finally, a short theory about DOE is given.

Chapter 3. Methodology

3.1 Design Method

In order to reduce the SRA input impedance and to increase the antenna bandwidth, three different structures of rectangular slot ring antennas (RSRA) were proposed with a parasitic ring inside and/or outside the feeding antenna. In addition, it was necessary to implement a slot in the RSRA that is labeled as open circuit stub in order to match the RSRA's input impedance to 50 Ω. These antennas are shown in Figure 3.1.1.

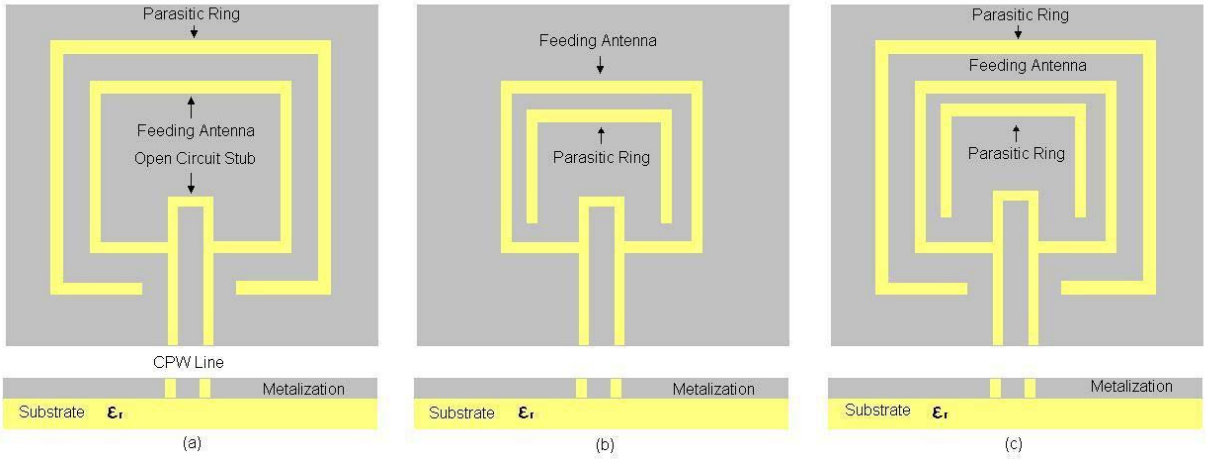

Figure 3.1.1. Top and side view of RSRAs. (a) RSRA with parasitic ring outside feeding antenna. (b) RSRA with parasitic ring inside feeding antenna. (c) RSRA with parasitic rings outside and inside feeding antenna

3.1.1 CPW Transmission Line Design

The CPW transmission line and its design parameters are shown in Figure 3.1.2. Two different substrates and substrate's thicknesses were considered in this research in order to support the antenna's metallization layer. The first one had a relative

permittivity (ε_r), of 3 and a thickness, (H), of 0.76 mm; and the other had a relativity permittivity 6.15 and a thickness of 0.635 mm. In this figure are also shown, the fed slot width (G), the fed conductor width (W_f), and the length of the feeding slot (L).

The CPW transmission line feeding of the RSRA was calculated using ADS Line Calc. This software allows to either fix G or W_f to a desired value. G was fixed to 0.25 mm, the line characteristic impedance, (Z_0), to 50 Ω, the electric length, (φ), of 90°, and the design frequency to 5.77 GHz. This center frequency is used by the industrial, scientific and medical (ISM) radio bands, they are license-free and in recent years these bands have been used in wireless LANs and Bluetooth applications.

The results are shown in Table 3.2.1.

Table 3.2.1. CPW Transmission Line Parameter Results

Permitivity ε_r	Thickness H (mm)	W_f (mm)	L (mm)
3	0.76	2.2442	10.2921
6.15	0.635	0.611	7.9167

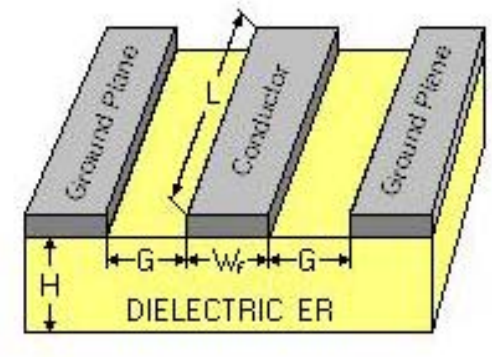

Figure 3.1.2. CPW Transmission Line and Design parameters

3.2 DOE for the RSRA

Three different cases were considered depending whether the parasitic ring was outside or inside the feeding antenna. Also, the general guidelines to design experiments, given in Chapter 2, were followed.

3.2.1 DOE for RSRA with Parasitic Ring Outside the Feeding Antenna, Case 1

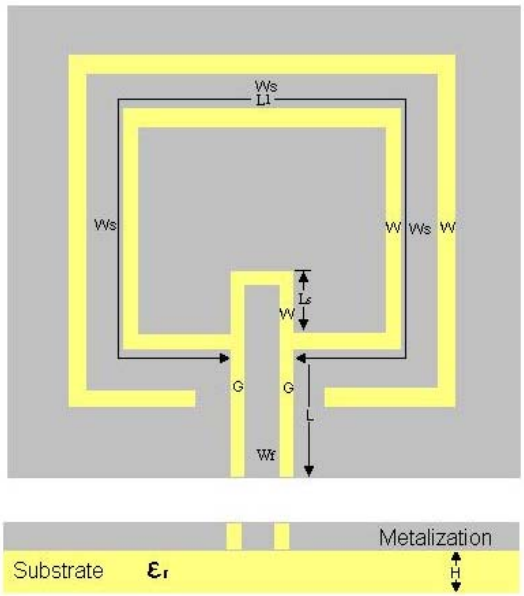

Figure 3.2.1. RSRA with Parasitic Ring Outside the feeding Antenna

In Figure 3.2.1 it is shown the RSRA Case 1 with nine design parameters. These parameters are: the substrate permittivity (ε_r), the substrate thickness (H), the perimeter of the feeding antenna (L_1), the slot width (W), the length of the open circuit stub (L_s), the fed slot width (G), the fed conductor width (W_f), the length of the feeding slot (L), and the distance between the parasitic ring and the feeding antenna (W_s).

In order to characterize this antenna using DOE it is necessary to carry out a 2^k full factorial; where k is the number of factors or design parameters. The factors that were considered in this design with its respective levels are shown in Table 3.2.2.

Table 3.2.2. Factors and Levels for RSRA Case 1

Factor	Low level	High level
ε_r	3	6.15
W	0.25 mm	1 mm
L_1	41.54 mm	87.62 mm
W_s	1 mm	2 mm
L_s	2 mm	4 mm

From experience, it is known that these levels can give meaningful results. The other factors such as W_f and G were established before on Section 3.1.1.

According to the number of factors, the factorial design considered was a 2^5 full factorial. A potential concern in a two level factorial design is the assumption of linearity of the factor effects. Generally, in this kind of factorial experiments, the first order model is assumed. A second order model could proof to be more adequate. There is a method to prove this assumption, which consists of adding center points. These center points are only for quantity factors (i.e. W, L_1, W_s, L_s); in this project ε_r is considered as a qualitative factor and does not have center points because this value can be either 3 or 6.15. According to [27] a substrate with a permittivity of 4.575 is not available.

Table 3.2.3 shows the design matrix for the 2^5 full factorial design. The five factors are presented with their respective physical dimensions (a low level and a high level). The

center points are in the last two rows. In this table upper case letters such as A, B, C, D, and E are the codified factors that represent the 5 factors of this design. That is A represents to ε_r, B represents to W, C represents to L_1, D represents to W_s and E represents to L_s. Lower case letters are assigned to the runs. Because in the first design the five factors are in low level, this design is noted as *(1)*. In the same way, in the second design only factor A is in high level, then this design is noted as *a*; and so forth.

The software Design Expert allows creating 2^k factorial design. Based on the levels of each factor, it is possible to obtain a design matrix as shown in Table 3.2.3 and the response data that it wants to be analyzed. It is important to notice that the order of collecting data should be random. Since the collected data was from simulations, the order of the runs does not need to follow a random pattern.

Each design from Table 3.2.3 was simulated in Ansoft's Designer and Agilent's Momentum in order to have two replicates of the same experiment. The frequency range went from 1 GHz to 10 GHz. The total number of simulations for Case 1 was 68. The simulation time for each design depends on its complexity, the range of frequency and the sample points. On average, this simulation time in Ansoft's Designer was 15 minutes and in Agilent's Momentum was 30-45 minutes in a computer with an Intel XEON processor at 2.20 GHz.

Table 3.2.3 Design matrix of 2^5 full factorial with two center points

Design	ε_r (A)	W (mm) (B)	L_1 (mm) (C)	W_s (mm) (D)	L_s (mm) (E)
(1)	3	0.25	41.54	1	2
a	6.15	0.25	41.54	1	2
b	3	1	41.54	1	2
ab	6.15	1	41.54	1	2
c	3	0.25	87.62	1	2
ac	6.15	0.25	87.62	1	2
bc	3	1	87.62	1	2
abc	6.15	1	87.62	1	2
d	3	0.25	41.54	2	2
ad	6.15	0.25	41.54	2	2
bd	3	1	41.54	2	2
abd	6.15	1	41.54	2	2
cd	3	0.25	87.62	2	2
acd	6.15	0.25	87.62	2	2
bcd	3	1	87.62	2	2
abcd	6.15	1	87.62	2	2
e	3	0.25	41.54	1	4
ae	6.15	0.25	41.54	1	4
be	3	1	41.54	1	4
abe	6.15	1	41.54	1	4
ce	3	0.25	87.62	1	4
ace	6.15	0.25	87.62	1	4
bce	3	1	87.62	1	4
abce	6.15	1	87.62	1	4
de	3	0.25	41.54	2	4
ade	6.15	0.25	41.54	2	4
bde	3	1	41.54	2	4
abde	6.15	1	41.54	2	4
cde	3	0.25	87.62	2	4
acde	6.15	0.25	87.62	2	4
bcde	3	1	87.62	2	4
abcde	6.15	1	87.62	2	4
Centerpoint	3	0.63	64.58	1.5	3
Centerpoint	6.15	0.63	64.58	1.5	3

The response (i.e. Return Loss, Resonance Frequency, Input Impedance at resonance, etc) was analyzed using different approaches. An intuitive approach to

analyze DOE responses is using the geometrical representation of a 2^5 full factorial design shown in Figure 3.2.2. Each corner of the small squares represents a design or simulation run. Also, in this figure the center points are represented. It is possible to determine the effect to changing each factor or its interactions with other factors, according to the change on the response. A second approach was using a linear regression model like the one described in Section 3.3. The last approach was using punctual responses such as the resonance frequency or the antenna's input impedance at resonance. This response was analyzed using Stat-Ease's Design Expert that calculated the effects and the regressions coefficients for the 2^5 factorial design; this approach is described in Section 3.4. The results of each analysis are discussed in Chapter 4.

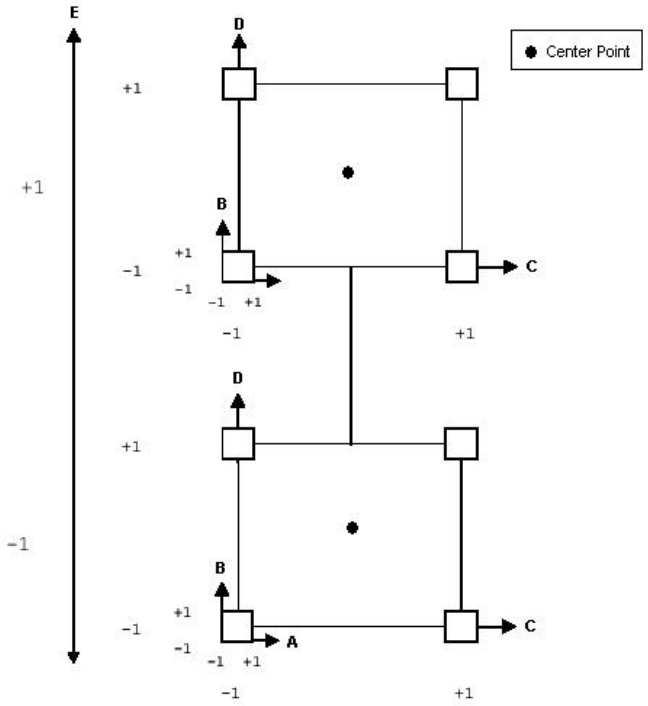

Figure 3.2.2. Geometrical representation for 2^5 full factorial design

3.2.2 DOE for RSRA with Parasitic Ring Inside the Feeding Antenna, Case 2

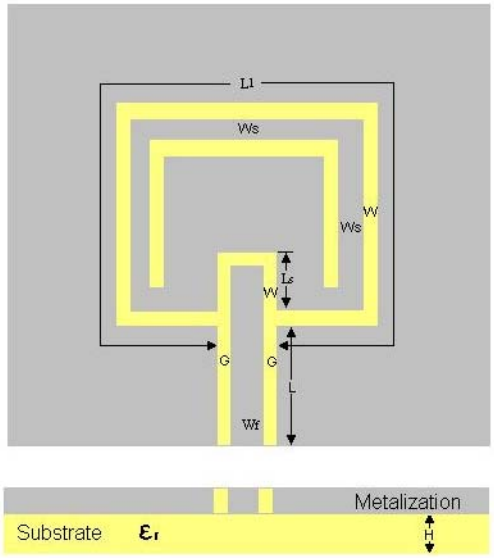

Figure 3.2.3. RSRA with Parasitic Ring Inside the feeding Antenna

In Figure 3.2.3 it is shown the RSRA Case 2. The DOE procedure that it was followed was similar than the procedure followed in Case 1. This configuration has the same design parameters as Case 1, consequently Tables 3.2.2 and 3.2.3 are also valid in this case.

Each design from Table 3.2.3 was simulated in Ansoft's Designer and Agilent's Momentum under similar conditions as Case 1. The total number of simulations for Case 2 was 68. Their responses were analyzed and the results of the analysis are discussed in Chapter 4.

3.2.3 DOE for RSRA with Parasitic Ring Outside and Inside the Feeding Antenna, Case 3

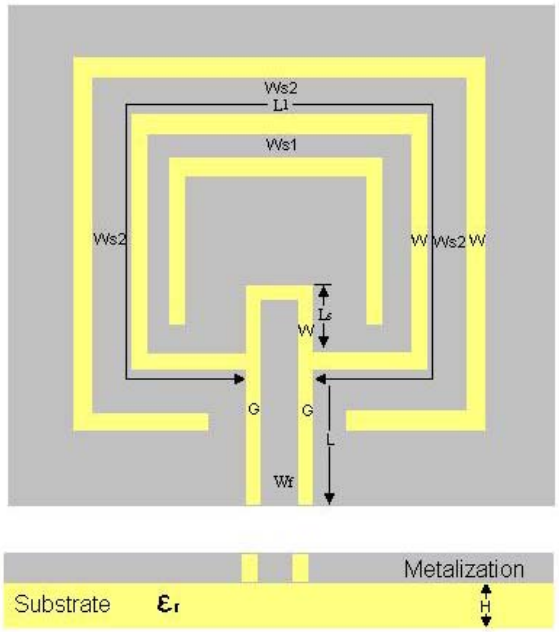

Figure 3.2.4. RSRA with Parasitic Ring Inside and outside the feeding Antenna

In Figure 3.2.4 it is shown the RSRA Case 3. This design corresponds to the union of Case 1 and 2. The new variables in Case 3 are Ws_1 and Ws_2. Where, Ws_1 is the distance between the inside parasitic ring and the feeding antenna. Ws_2 is the distance between the outside parasitic ring and the feeding antenna. Some simulation results showed that Case 3 responses were the superposition of Case 1 and 2 responses. Consequently the characterization of those cases can be extended to Case 3. In addition, impedance bandwidth, and matching enhancements are achieved varying Ws_1 and Ws_2. All these results are analyzed and discussed in Chapter 4.

3.3 Linear Regression Model for RSRA

One of the objectives of this research is to identify the most influential factors in the antenna response. The fact that a factor it is more or less significant in the response it is related with its slope; the factor with the highest slope is the most significant. A method to determine these slopes and to establish a mathematical equation is the linear regression model. This model can work as a prediction tool or can be used to optimize the response of the antenna.

For five factors, the regression model is

$$y = \beta_0 + \beta_1 X_A + \beta_2 X_B + \beta_3 X_C + \beta_4 X_D + \beta_5 X_E + \beta_6 X_A X_B + \beta_7 X_A X_C + \beta_8 X_A X_D + \beta_9 X_A X_E + \beta_{10} X_B X_C + \beta_{11} X_B X_D + \beta_{12} X_B X_E + \beta_{13} X_C X_D + \beta_{14} X_C X_E + \beta_{15} X_D X_E + \beta_{16} X_A X_B X_C + \beta_{17} X_A X_B X_D + \beta_{18} X_A X_B X_E + \beta_{19} X_B X_C X_D + \beta_{20} X_B X_C X_E + \beta_{21} X_C X_D X_E + \beta_{22} X_A X_C X_D + \beta_{23} X_A X_C X_E + \beta_{24} X_B X_D X_E + \beta_{25} X_A X_D X_E + \beta_{26} X_A X_B X_C X_D + \beta_{27} X_B X_C X_D X_E + \beta_{28} X_A X_C X_D X_E + \beta_{29} X_A X_B X_D X_E + \beta_{30} X_A X_B X_C X_E + \beta_{31} X_A X_B X_C X_D X_E + \varepsilon \quad (3.3.1)$$

Where:

y is the response (i.e. Return Loss, VSWR, Input impedance, etc).

The β´s represent the regression model coefficients, particularly β_0 is the intercept.

ε, represents the error or residual of the model.

X_A, X_B, X_C, X_D, X_E are the five experiment codified factors.

These factors are codified in order to give an interpretation to the intercept. If the factors were not codified, the intercept could not be found because the levels of the factors do not include the zero. In addition, coding is important in order to make the scale of the factors levels comparable. Usually, this scale is not the same because it measures

different characteristics such as length (i.e. W, L_l, W_s, L_s); or the scale could be also dimensionless (i.e. ε_r).

The relation between the natural variables (factors in their original scale), and the codified variables is given by

$$\boxed{X_i = \frac{(\eta_i - \overline{\eta})}{\frac{range}{2}}} \qquad (3.3.2)$$

Where X_i is the codified variable, η_i is the natural variable and $\overline{\eta}$ is the average of the levels of the variable to be codified. When the natural variables only have two levels, as in 2^K factorial designs, the levels of the codified variables are 1 for high level and -1 for low level.

In order to simplify the model of equation (3.3.1), an initial approach supposes that the interactions of two, three, four and five factors do not influence the response significantly. Consequently, the simplified model is

$$y = \beta_0 + \beta_1 X_A + \beta_2 X_B + \beta_3 X_C + \beta_4 X_D + \beta_5 X_E + \varepsilon \qquad (3.3.3)$$

Using matrix notation

$$\mathbf{y = X\beta + \varepsilon} \qquad (3.3.4)$$

where

$$y = \begin{bmatrix} y_1 \\ y_2 \\ \vdots \\ \vdots \\ y_n \end{bmatrix} \quad X = \begin{bmatrix} 1 & x_{11} & x_{12} & .. & x_{1k} \\ 1 & x_{21} & x_{22} & .. & x_{2k} \\ \vdots & \vdots & \vdots & .. & \vdots \\ \vdots & \vdots & \vdots & .. & \vdots \\ 1 & x_{n1} & x_{n2} & .. & x_{nk} \end{bmatrix} \quad \beta = \begin{bmatrix} \beta_0 \\ \beta_1 \\ \vdots \\ \vdots \\ \beta_k \end{bmatrix} \quad \varepsilon = \begin{bmatrix} \varepsilon_1 \\ \varepsilon_2 \\ \vdots \\ \vdots \\ \varepsilon_n \end{bmatrix}$$

y is a vector (nx1) of the experiment observations, **X** is the design matrix (nxp) of the experiment factor levels, **β** is a vector (px1) of the regression model coefficient and **ε** is a vector (nx1) of errors or residuals.

The estimators for the coefficients that minimize the sum square error is

$$\boxed{\mathbf{b} = \left(X'X\right)^{-1}X'y} \tag{3.3.5}$$

For this 2^5 factorial design the Return Loss (dB) was chosen as the response, this response was divided in 2000 frequency points. For every point, a linear model as the equation (3.3.3) was estimated.

In order to validate the model and as an illustration of this approach, some simulation designs and their estimated model were compared for the RSRA Case1. To ease the calculations only the Designer replicate was used in order to calculate the estimated response. The estimated and simulated Return Loss for some designs is shown in Figure 3.3.1. According to the estimated plots, the model fails in some frequency ranges because it shows values of the return loss over zero dB. However in some points the estimated plots have a similar behavior than the simulated plots. In addition, the model adequacy checking is performed in the next section.

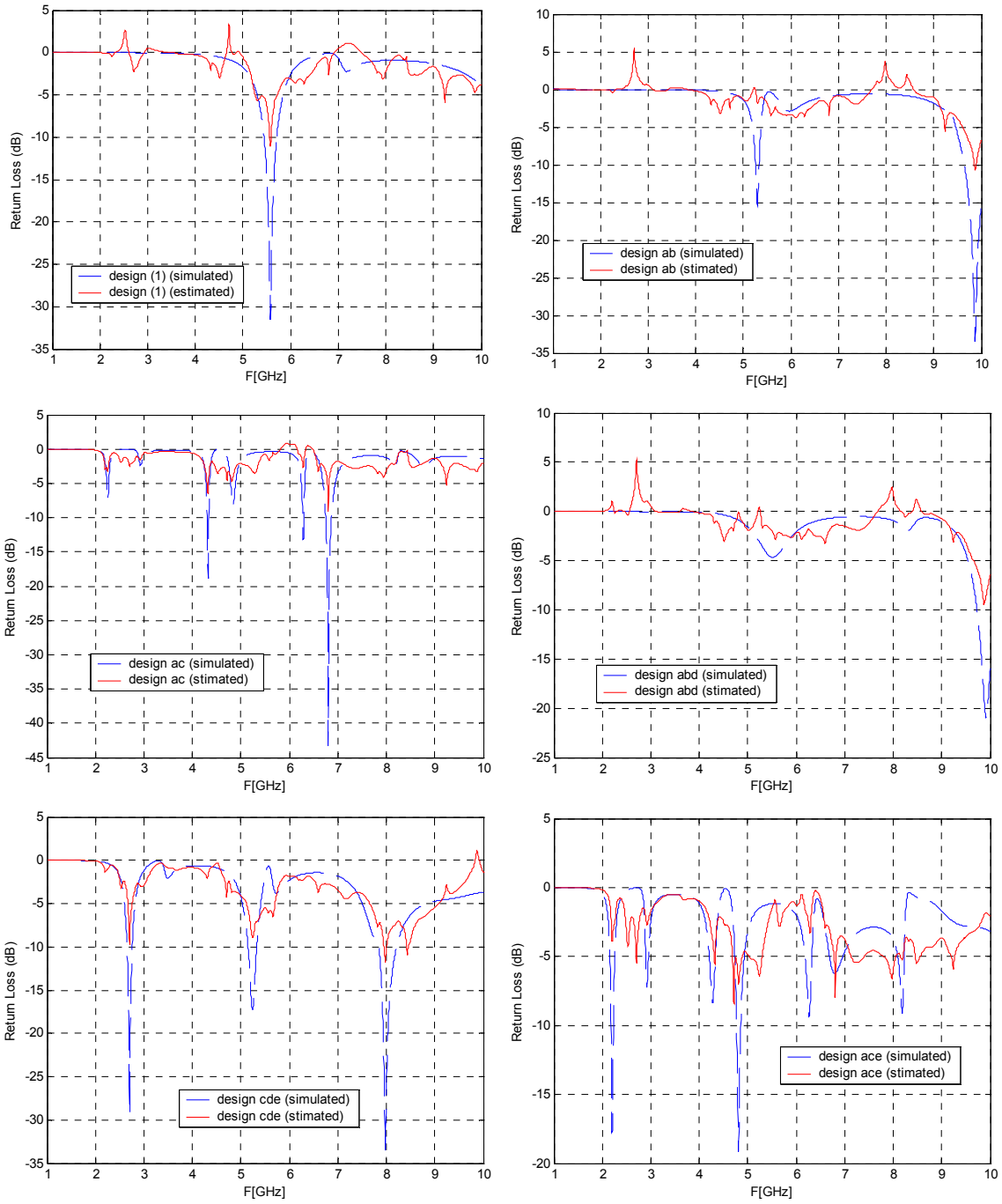

Figure 3.3.1. Simulated and estimated Return Loss for different designs.

3.3.1 Model Adequacy Checking

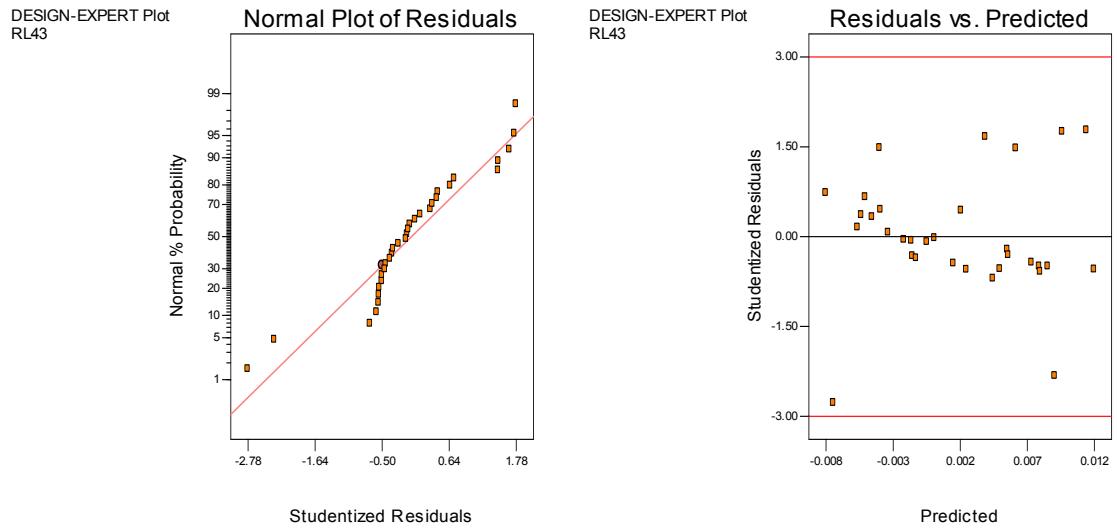

(a) (b)

Figure 3.3.2. Plot of residuals for the first frequency point. (a) Normal plot of residuals. (b) Residuals vs. predicted values

As an illustration, Figure 3.3.2 shows the residual distribution for the first frequency point. It is important that the residuals follow a normal probability distribution because is one of the assumptions for performing a linear regression; that is, the residual must follow a straight line as it is shown in Figure 3.3.2 (a). In general, moderate departures from normality are of little concern in the fixed effects analysis of variance. Figure 3.3.2 (b) shows the residuals vs. predicted values; if the model is correct and if the assumptions are satisfied, the residuals should be structureless and this plot should not reveal any obvious pattern. According to Figures 3.3.2 (a) and (b) there is no reason to suspect any violation of independence or constant variance assumptions.

Nevertheless, this procedure is not practical because it is necessary to run the adequacy checking of 2000 models. For this work the complete adequacy checking of the

model was not carried out, instead it was performed the adequacy checking in particular bands as it is shown in the final example in Section 3.3.3. In addition, some hypothesis testing was performed.

3.3.2 Hypothesis Testing in Linear Regression

In linear regression problems, there are some hypothesis tests [23] that measure the usefulness of the model. These tests require that the errors follow the assumptions of ANOVA.

3.3.2.1 Testing for Significance of Regression

Testing for Significance of Regression is a procedure to determine whether there is a linear relation between the response variable and the regression coefficients.

For this test the appropriate hypotheses are

$$H_0: \beta_1 = \beta_2 = \ldots = \beta_k = 0$$

$$H_1: \beta_i \neq 0 \text{ at least one i.}$$

Rejection of H_0 implies that at least one variable in the model contribute significantly to the fit. It was followed the procedure given in [23] for testing the significance of regression for the model of equation (3.3.3). Usually this procedure is performed in punctual responses but in this case the Return Loss response is sampled in 2000 frequency points; consequently it was necessary to calculate the F_0 value [23] for each frequency point. The F_0 value is the ratio between the mean square of the regression and the mean square of the error. Figure 3.3.3 shows the F_0 plot vs. frequency. Also it is

shown $F_{\alpha,k,n-k-1}$, where α is the significance level of the test; a common value used in this kind of test is α = 0.05. k is the degrees of freedom of the regression; for five regression coefficients, the degrees of freedom are 5. And n is the number of observations, in this case 32. The value of $F_{0.05,5,26}$ is easily found in the F distribution table in [23], this values is 2.59.

In order to check whether H_0 is rejected or not, it is necessary to compare F_0 and $F_{0.05,5,26}$. In the frequency points where $F_0 > F_{0.05,5,26}$, H_0 is rejected; which means that at least one of the five regressions coefficients contributes significantly to the regression. According to Figure 3.3.3, there only short intervals under the discontinue line, where $\beta_1 = \beta_2 = \beta_3 = \beta_4 = \beta_5 = 0$

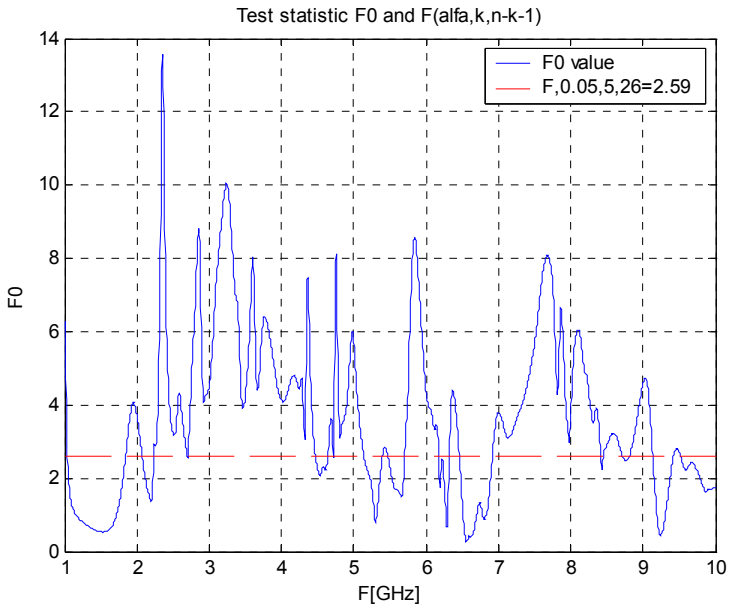

Figure 3.3.3. F_0 value and F statistic

3.3.2.2 Determination Coefficient and Adjusted Determination Coefficient

Determination Coefficient (DC) and Adjusted Determination Coefficient (ADC) measure the variability of the observations explained by the model and their values are between 0 and 1. The DC should be used with caution because it will always increase by adding more terms to the model, but this does not necessarily mean the new model is better. The ADC, instead, does not necessary increase as new regressors are adding to the model. In Figure 3.3.4 the DC and the ADC are shown. The DC is in reasonable agreement with the ADC. Roughly speaking, the model of Equation (3.3.3) explains about 10% to 30% of the observation variability. For a reliable model ADC should be at least from 50% to 60%.

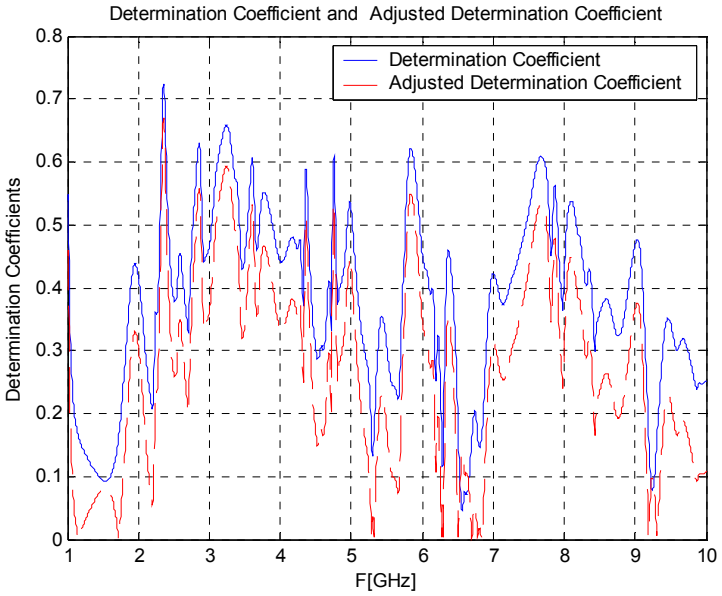

Figure 3.3.4. Determination Coefficient and Adjusted Determination Coefficient

3.3.2.3 Testing Hypotheses on Individual Regression Coefficients

Testing Hypotheses on individual Regression Coefficients is useful because it is possible to determine the value of each of the regressor variables in the model. For instance, the model might be more effective considering additional variables or deleting the less significant variables.

For this test the appropriate hypotheses are [23]

$$H_0: \beta_i = 0$$

$$H_1: \beta_i \neq 0$$

The test statistic is

$$\boxed{t_0 = \frac{\beta_i}{\sqrt{MS_E C_{ii}}}} \qquad (3.3.6)$$

where:

C_{ii} is the element in the diagonal in the variance-covariance matrix $(X'X)^{-1}$ that corresponds to the β_i coefficient.

$H_0: \beta_i = 0$ is rejected if $|t_0| > t_{\alpha/2,\, n-k-1}$. Again, $\alpha = 0.05$, $n = 32$, $k = 5$.

The value of $t_{0.025,26}$ is easily found in the t distribution table in [23], this values is 2.056.

In Figure 3.3.5 (a), (b), (c) are shown the t_0 values for β_0, β_1, β_2, β_3, β_4, β_5. Also, it is shown the value of $t_{0.025,26} = 2.056$ as a straight line. The values of t_0 over this line imply that the respective coefficient influence the model significantly. In addition, the level of the statistic t_0 of any coefficient is directly related with the absolute value of that coefficient; that is, if this level is very high, the coefficient will highly affect the response. According to Figure 3.3.5 (a), (b), (c), it is possible to deduct the significant

factors in the response; Table 3.3.1 summarizes this behavior in each frequency range. It is important to note that β_4 has the smallest influence interval in the model whereas β_0 has the longest one.

Table 3.3.1. Frequency Ranges Where the Model Coefficient is $\neq 0$ and its Location in the Model.

Coefficient	Location in the Model	Frequency ranges (in GHz) where the factor is significant or its coefficient is $\neq 0$
β_0	Intercept	1.5-10
β_1	Multiplies X_A	2.5-3, 4-5, 5.3-6, 7.8-9
β_2	Multiplies X_B	3-3.5, 4-4.5, 5.7-6.5, 9.3-10
β_3	Multiplies X_C	1.5-4, 5.8-6.5, 7.1-9
β_4	Multiplies X_D	3.5-3.8
β_5	Multiplies X_E	2.5-3.7, 3.8-4.2, 4.8-5.2, 5.6-6, 7-9.5

If the linear regression approach is going to be used to predict the Return Loss for a particular frequency, the codified values of β_0, β_1, β_2, β_3, β_4 and β_5 can be calculated using the curves shown in Figure 3.3.6.

General guidelines for this case are as follow. First of all, find out theβ's that are $\neq 0$ using the graphs shown in Figure 3.3.5 (a), (b) and (c) or Table 3.3.1 for the frequency of interest. Second, use the graphs shown in Figure 3.3.6 to calculate the β's. And finally, use Equation 3.3.3 to replace the β's and calculate the Return Loss for that frequency.

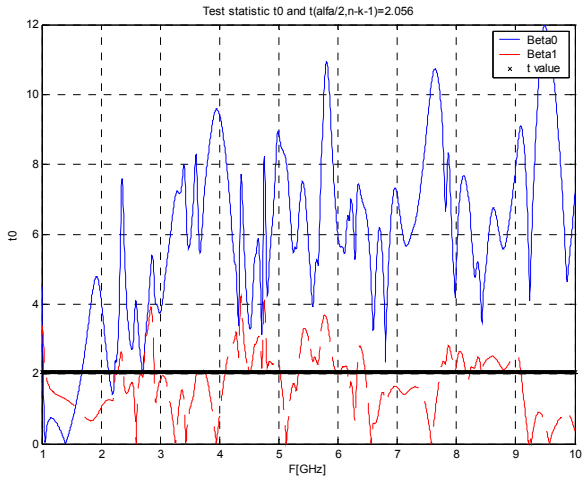

(a)

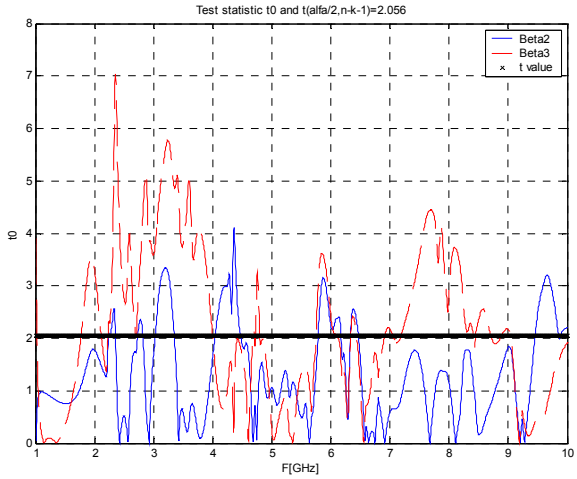

(b)

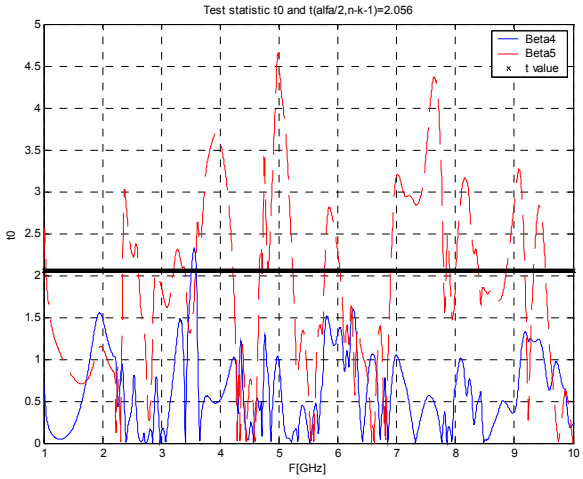

(c)

Figure 3.3.5. t_0 value and t statistic for Individual Regression Coefficients

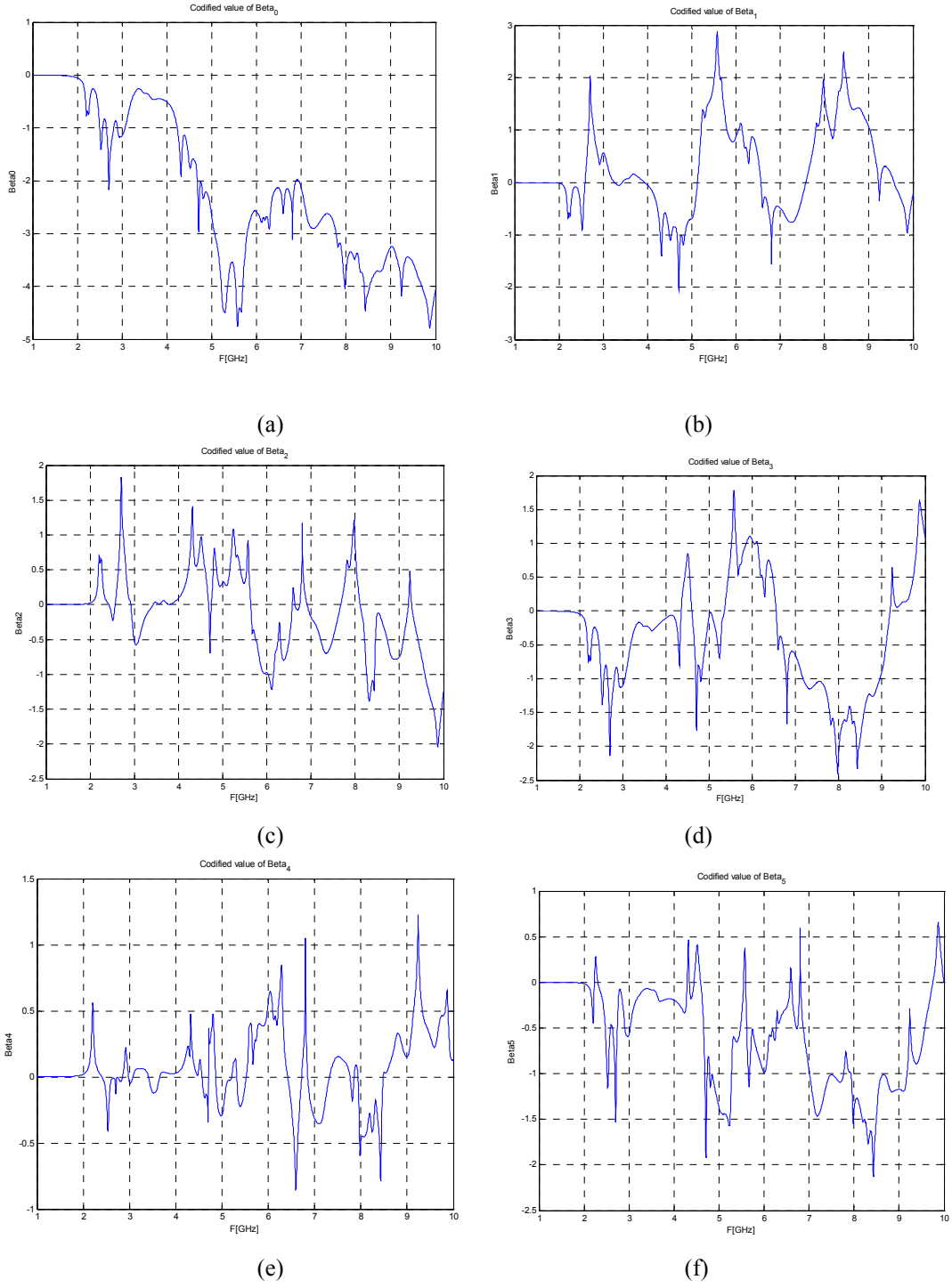

Figure 3.3.6. β's Codified Values. (a) β_0, (b) β_1, (c) β_2, (d) β_3, (e) β_4, (f) β_5.

3.3.3 Application Example

In addition, the plots shown in Figure 3.3.6 can be used to look for the point with the minimum Return Loss, that is to optimize the response. For instance, determine the substrate and the physical dimension of the RSRA in order to achieve the lower Return Loss in the frequency band from 5.5 to 6 GHz. According to the graphs shown in Figure 3.3.5 (a), (b) and (c) β_0, β_1, β_2, β_3 and β_5 are different from cero in this band. β_4 is not significant. Now, it is a good idea to take a zoom to the graphs shown in Figure 3.3.6 in the frequency band of interest and plot the six coefficients in a same graph. This graph is shown in Figure 3.3.7. From this figure β_1 has positive values in the frequency range of interest; consequently the factor that multiplies this coefficient should be set as (-1) or low level, because the factors are codified as -1 or 1. This same analysis is followed with the other coefficients and this information is summarized in Table 3.3.2.

Table 3.3.2. Behavior of the coefficients in the frequency band from 5.5 to 6 GHz

Coefficient	Sign of the coefficient in the freq range from 5.5 to 6 GHz	Level of the factor
β_0	Negative	N/A
β_1	Positive	-1
β_2	Negative	1
β_3	Positive	-1
β_4	Positive	Not significant
β_5	Negative	1

In the interest band, the Equation 3.3.3 is as follows

$$y = \beta_0 + \beta_1 (-1) + \beta_2 (1) + \beta_3 (-1) + \beta_5 (1) \qquad (3.3.7)$$

Therefore, the substrate and the physical dimensions of the antenna are

ε_r =3, W = 1 mm, L_1= 41.54 mm, W_s= 1mm or 2mm and L_s= 4mm. Because the distance between the parasitic ring and the feeding antenna (W_s) can be either in high or low level, there are two possible designs; they correspond to *bde* and b*e* in Table 3.2.3. These two designs were simulated and the results are shown in Figure 3.3.8 (a) and (b).

Now, it is important to find out how good the fitted linear regression model is. As it was mentioned before, it is not practical to plot the residuals for every frequency point as it is shown in Figure 3.3.2 because between 5.5 and 6 GHz there are almost 100 models. Instead, it is useful to deal with the determination coefficients. A zoom of the determination coefficients shown in Figure 3.3.4 is shown in Figure 3.3.9. This figure shows that the adjusted determination coefficient is lower than 0.6 which mean that the models described by Equation (3.3.3) are not very reliable. In the practice this coefficient should be over 0.6 in order that the models explain at least the 60% of the variability of the observations.

A practical recommendation to solve this problem is to consider interactions of two and three factors in order to improve the determination coefficients. This is considered in Chapter 4.

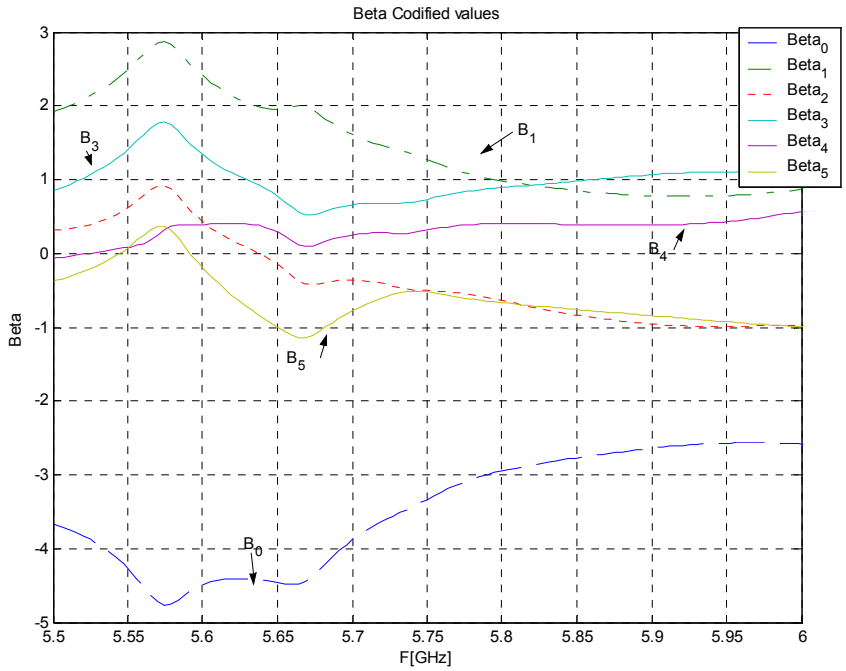

Figure 3.3.7. Beta Codified Values in the Interest Band

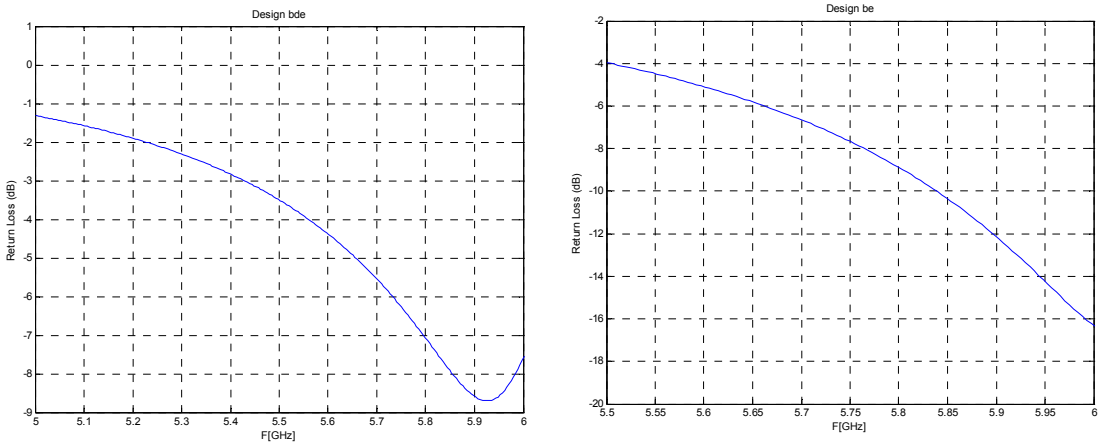

(a) (b)

Figure 3.3.8. Simulated Designs. (a) bde. (b) be.

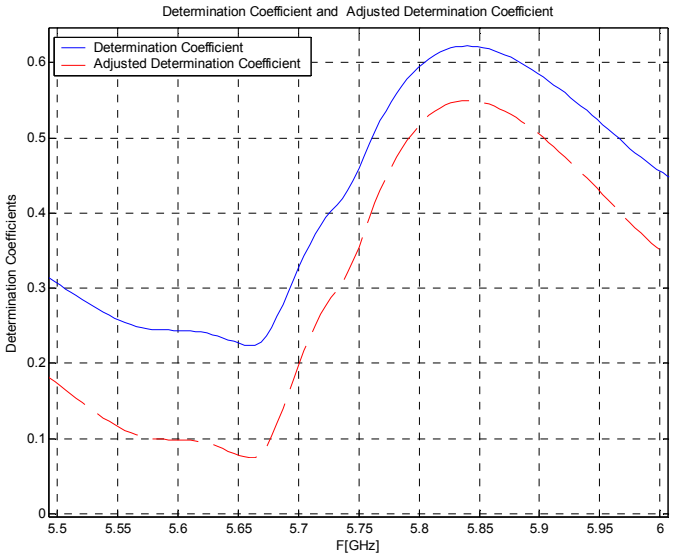

Figure 3.3.9. Determination Coefficients.

3.4 DOE Using Punctual Responses

The last approach that was used to analyze the antenna's response was to use punctual responses, such as the resonance frequency and the antenna's input impedance at resonance. This approach was applied for the RSRA Case 1 and the software Design Expert was used to perform the DOE analysis. The two simulation replicates and their DOE center points were used.

The data was collected from the simulations and from each design simulated three resonance points were taken. The design summary is shown in Table 3.4.1.

Table 3.4.1 RSRA Case 1 Design Summary

Response	Name	Units	Obs	Minimum	Maximum
Y1	1^{st} Fr	GHz	62	2.22	4.58
Y2	Zin_1	Normalized	62	0	1.68
Y3	2^{nd} Fr	GHz	57	4.27	8.25
Y4	Zin_2	Normalized	57	0	31.94
Y5	3^{rd} Fr	GHz	64	7.19	9.93
Y6	Zin_3	Normalized	64	0.12	24.08

The total number of runs performed was 68 but some resonances did not appear in some designs; this is the reason why the number of observations (Obs) was smaller.

1st Fr stands for first resonance frequency and Zin_1 stands for antenna input impedance at resonance. This applies for the other responses. In order to illustrate this approach, the 1st Fr was analyzed. The regression coefficients, as well as the residuals plots were presented. This same statistic analysis was performed to the other responses. The results and the analysis will be presented in Chapter 4.

In the Design Expert software there are a series of steps that must be followed to perform the analysis.

The first step is to select a response and chose a transformation that stabilizes the response variance. Some available transformations are square root, natural logarithm, base ten logarithm and inverse square root. In this case the response chosen was 1st Fr. Since the ratio of max to min of the observation is 2.0614, the transformation chosen was none. A ratio greater than 10 indicates a transformation is required.

The second step is to choose the significant effects from the normal probability plot. The non significant effects follow a normal distribution that means they form a straight line. This plot is shown in Figure 3.4.1. The significant effects are B and E which mean that the first resonance frequency response is influenced by the slot width (W) and the open circuit stub (L_s).

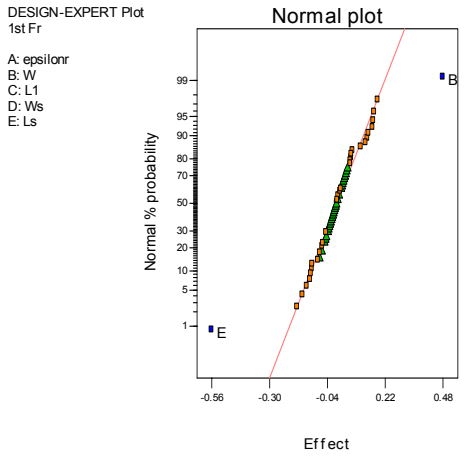

Figure 3.4.1. Normal Probability plot of the effects for the First Resonance frequency

The third step is the ANOVA. This ANOVA is shown in Table 3.4.2. According to this table the model and the effects B and E are significant. Also, the curvature that is measured by the difference between the average of the center points and the average of the factorial points is not significant.

Furthermore, the model lack of fit is bad; if a model shows lack of fit, it should not be used to predict the response. To overcome this lack of fit it is necessary to add more terms to the model, either interactions or quadratic terms.

Table 3.4.2. ANOVA for the First Resonance Frequency

Source	**Sum of Squares**	**DF**	**Mean Square**	**F value**	**Prob>F**	
Model	7.57	2	3.78	32.03	< 0.0001	Significant
B	3.34	1	3.34	28.26	< 0.0001	Significant
E	4.51	1	4.51	38.15	< 0.0001	Significant
Curvature	0.11	1	0.11	0.92	0.3417	Not significant
Residual	6.85	58	0.12			
Lack of Fit	4.58	29	0.16	2.02	0.0317	Significant
Pure Error	2.27	29	0.078			
Cor Total	14.53	61				

The final equation in terms of coded factors is

$$1^{st} F_r = 3.7 + 0.24B - 0.28E \qquad (3.4.1)$$

The final equation in terms of actual factors is

$$1^{st} F_r = 4.13361 + 0.04181W - 0.27895L_s \qquad (3.4.2)$$

The fourth step is to evaluate the model adequacy using the normal probability plot and the residuals vs. predicted values plot. These plots are shown in Figures 3.4.2 (a) and (b). According to these figures there is no reason to suspect any violation of independence or constant variance assumptions because the residuals follow a straight line (Figure 3.4.2 (a)) and they are structureless (Figure 3.4.2 (b)).

.

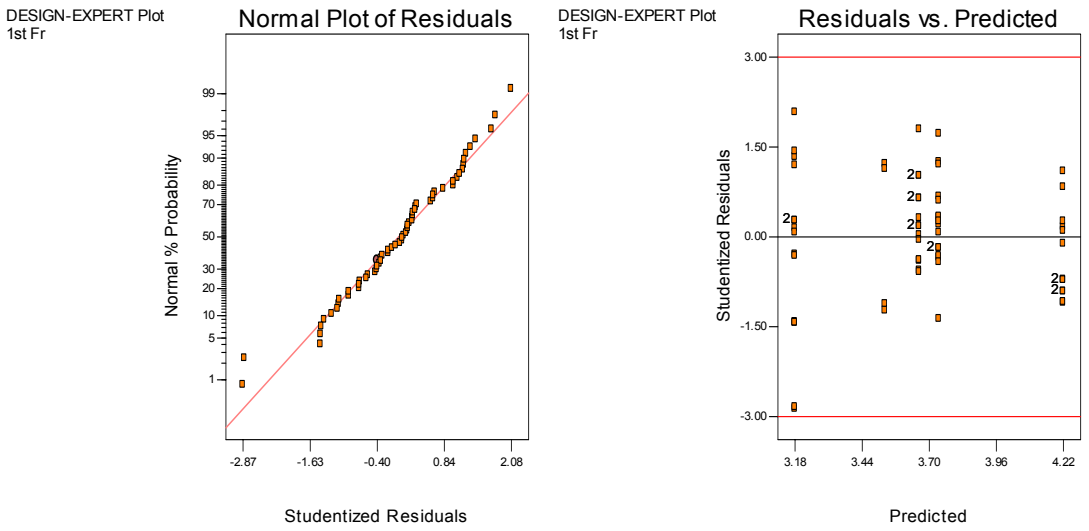

(a) (b)

Figure 3.4.2. Plot of residuals for First Resonance Frequency Response. (a) Normal plot of residuals. (b) Residuals vs. predicted values

The final step is to use the model graphs to interpret and evaluate the model. In addition, Design Expert has an optimization tool that will be used in the next chapter in order to optimize the models.

3.5 Antenna Fabrication and Testing

To validate the results obtained from the simulations, several antenna designs were fabricated using a milling machine and tested with the equipment available in the Radiation Laboratory at the University of Puerto Rico, Mayagüez.

It was important that the substrate used to build the antennas, had a constant relative permittivity (ε_r) over a wide range of frequencies and temperature. High frequency circuit material manufactures such as Rogers Corporation [27] has available substrates with the relative permittivity (ε_r) of 3 and 6.15 and the thickness (*H*) of 0.76 mm and 0.635 mm respectively. These substrates are of grade RO3003 with a relative permittivity of 3 and RO3006 with a relative permittivity of 6.15. Both grades are included in the RO3000 series that are ceramic filled PTFE composites and offer a stable dielectric constant versus temperature.

The measurements of Return Loss, VSWR, Input impedance, were performed with the Agilent 8719ES s-parameter network analyzer. Before each measurement the equipment was calibrated. The measurements and the results from the simulations are compared and analyzed in Chapter 4.

3.6 Summary

The methodology that explains the design, simulation and characterization of a RSRA is presented in this chapter. The three RSRA cases that are considered in this research as well as the factors in each antenna design are described. Base on particular cases the three approaches followed to analyze the different antenna responses were

illustrated. Finally, it is explained how the antennas were fabricated and the equipment that was used to measure the prototype antenna's return loss and VSWR is mentioned.

Chapter 4 Results and Discussions

4.1 First Approach: Intuitive Analysis

As mentioned in Chapter 3, the DOE intuitive analysis consists in organizing the responses according to the geometrical representation shown in Figure 3.2.2. Next, the effect in the responses is analyzed according to the changes in each factor or its interaction with other factors. In order to simplify this analysis only the main five factors effects (ε_r, L_1, W, W_s, L_s) were considered. In addition, the shift in the resonance frequency and the impedance bandwidth were analyzed.

4.1.1 RSRA with the Parasitic Ring outside the Feeding Antenna

The intuitive analysis was applied to the first case, RSRA with the parasitic ring outside the feeding antenna. The effects of changing each factor from low to high are as follow.

4.1.1.1 Effects of Changing the Substrate Permittivity on the Resonance Frequencies and Return Loss Response

When the factor ε_r was changed from 3 to 6.15, the resonances frequencies were shifted to lower frequencies as it is shown in Figures 4.1.1 (a) and (b). Each of these plots display two designs in which only the substrate permittivity was changed from low to high level. As it was established earlier design *(1)* means that all the five factors are in low level and design *a* means that only factor A or ε_r is in high. In Figures 4.1.1 (c) and

(d) it is shown that the operation points or frequencies of each resonance band with return loss better than -10 dB were also shifted in frequency. The effect of increasing the dielectric constant is that for the antenna to operate at the same frequency its dimensions need to decrease. In addition, a multiband operation was observed and the return loss increased when this change happened. In Figure 4.1.1 (c), design *(1)* presented a single band operation, whereas design *a* (discontinuous line) presented a dual band operation. In Figure 4.1.1 (d), design *ce* already had a three band operation but from experience it was known that this behavior was due to increase the antenna perimeter (factor L_1 or C). Design *ace* presented two operation bands plus three potential operation bands. An explanation to the shifting in frequency can be deduced from the expression in [19]

$$\text{For } 0.0015 \le W/\lambda_0 \le 0.075$$

$$2.22 \le \varepsilon_r \le 3.8$$

$$\lambda_g/\lambda_0 = 1.045 - 0.365 * \ln(\varepsilon_r) + \frac{(6.3*(W/H)*\varepsilon_r^{0.945})}{(238.64+100*(W/H)} - \left[0.148 - \frac{8.81(\varepsilon_r+0.95)}{100*\varepsilon_r}\right] * \ln(H/\lambda_0) \quad (4.1.1)$$

$$\text{For } 0.0015 \le W/\lambda_0 \le 0.075$$

$$3.8 \le \varepsilon_r \le 9.8$$

$$\lambda_g/\lambda_0 = 0.9217 - 0.27 * \ln\varepsilon_r + 0.0322*(W/H)*\left[\frac{\varepsilon_r}{W/H+0.435}\right]^{1/2} - 0.01*\ln(\frac{H}{\lambda_0})\left[4.6 - \frac{3.65}{\varepsilon_r^2\sqrt{W/\lambda_0}(9.06-100*W/\lambda_0)}\right] \quad (4.1.2)$$

Where λ_0 is the wavelength in free space, W is the slot width and H is the thickness of the substrate. It is important to mention that equations (4.1.1) and (4.1.2) are for slot lines, but they are a good initial approach for RSRAs.

Table 4.1.1. Values of λ_g according to expressions (4.1.1) and (4.1.2).

ε_r	H (mm)	W (mm)	λ_g (mm)
3	0.76	0.25	41.64
3	0.76	1	43.81
6.15	0.635	0.25	33.72
6.15	0.635	1	36.69

In Table 4.1.1, the possible values of λ_g for $\lambda_0 =$ 52 mm (or a resonance frequency of 5.77 GHz) are listed. If ε_r is changed from 3 to 6.15, then λ_g decreases, but the antenna physical perimeter remains constant. This means that the new antenna resonance point is in a lower frequency. This behavior agrees with the simulation results shown in Figure 4.1.1 (a) and (b). For instance, in design *(1)* the second resonance frequency occurs at 5.63 GHz, whereas, in design *a*, it occurs at 4.9 GHz. In design *ce* the second resonance frequency occurs at 5.19 GHz, whereas, in design *ace*, it occurs at 4.70 GHz. In addition, the antenna impedance bandwidth (VSWR $\leq$ 2) decreased when factor A or ε_r changed from low level to high level.

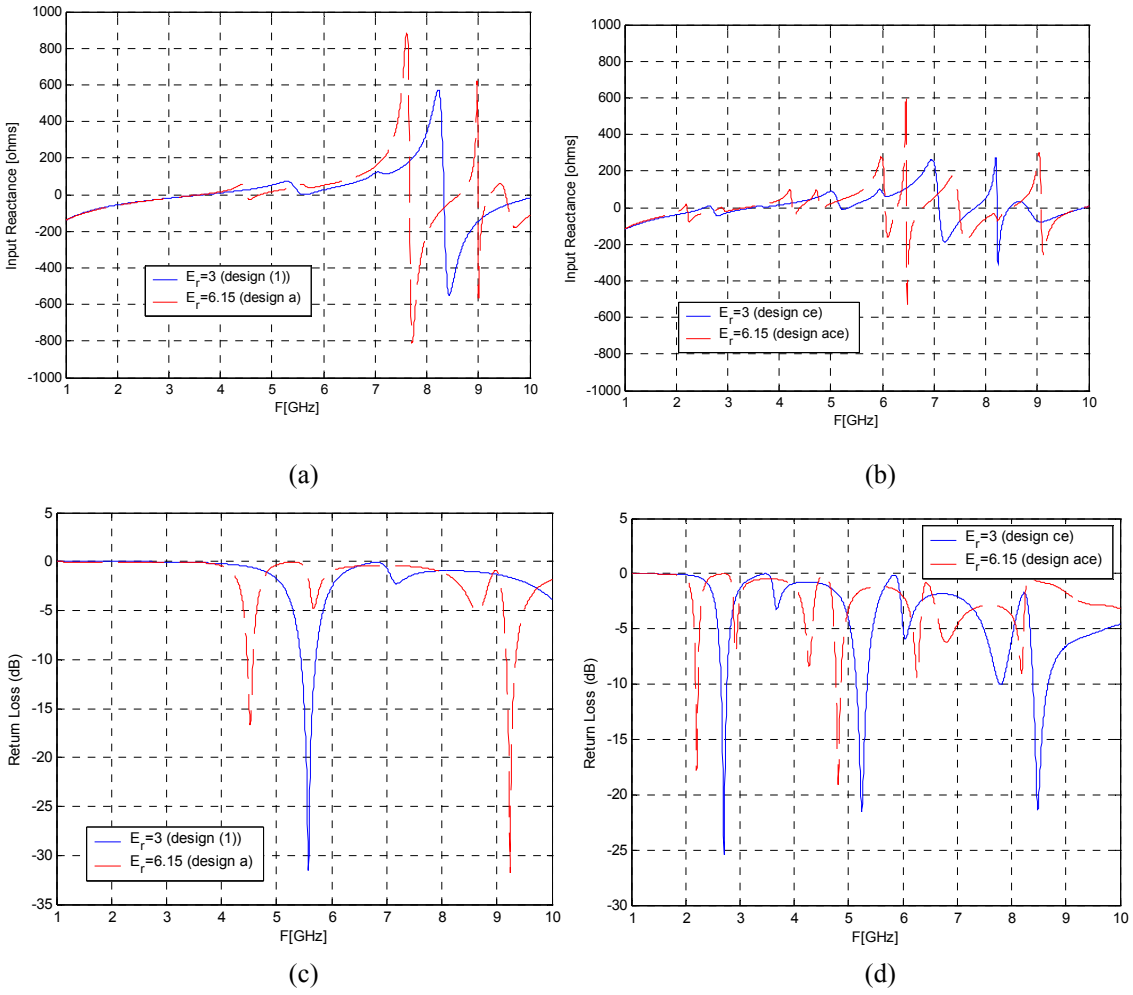

Figure 4.1.1 Input Reactance and Return Loss for two experiments. (a) Designs (*1*) and *a*. (b) Designs *ce* and *ace.* (c) Designs (*1*) and *a*. (d) Designs *ce* and *ace*

4.1.1.2 Effects of Changing the Slot Width (*W*) on the Resonance Frequencies and Return Loss Response

When the slot width was changed from 0.25 mm to 1mm the resonance frequencies were shifted to higher frequencies. This behavior is explained by equations (4.1.1) and (4.1.2) where λ_g increases but the antenna physical perimeter remains constant. This means that the new antenna operation points are in higher frequencies.

This behavior agrees with the simulation results shown in Figure 4.1.2 (a) and (b). It was also observed a decrease in the return loss and antenna impedance bandwidth (VSWR ≤ 2) as it is shown in Figure 4.1.2 (c) and (d).

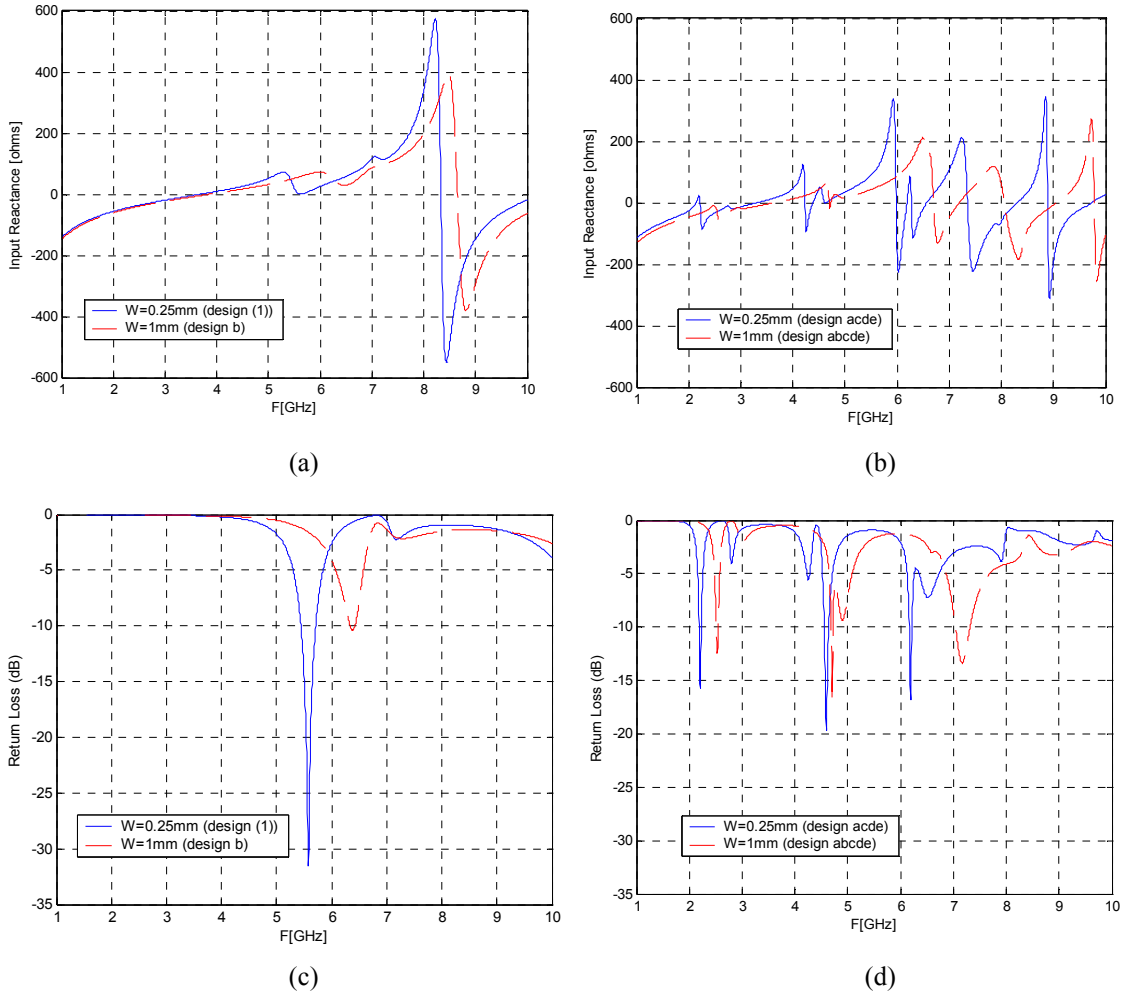

Figure 4.1.2. Input Reactance and Return Loss for two experiments. (a) Designs (*1*) and *b*. (b) Designs *acde* and *abcde*

4.1.1.3 Effects of Changing the Feeding Antenna Perimeter (L_1) on the Resonance Frequencies and Return Loss Response

When the perimeter of the feeding antenna was changed from 41.54 mm to 87.62 mm, new resonance frequencies appeared as it is shown in Figure 4.1.3 (a) and (b). In addition, in Figure 4.1.3 (c) and (d) the antenna changed from a single band operation to a three band operation. In design *(1)* and *e* only one operation point was presented; whereas, in designs *c* and *ce* multiple operation points were observed.

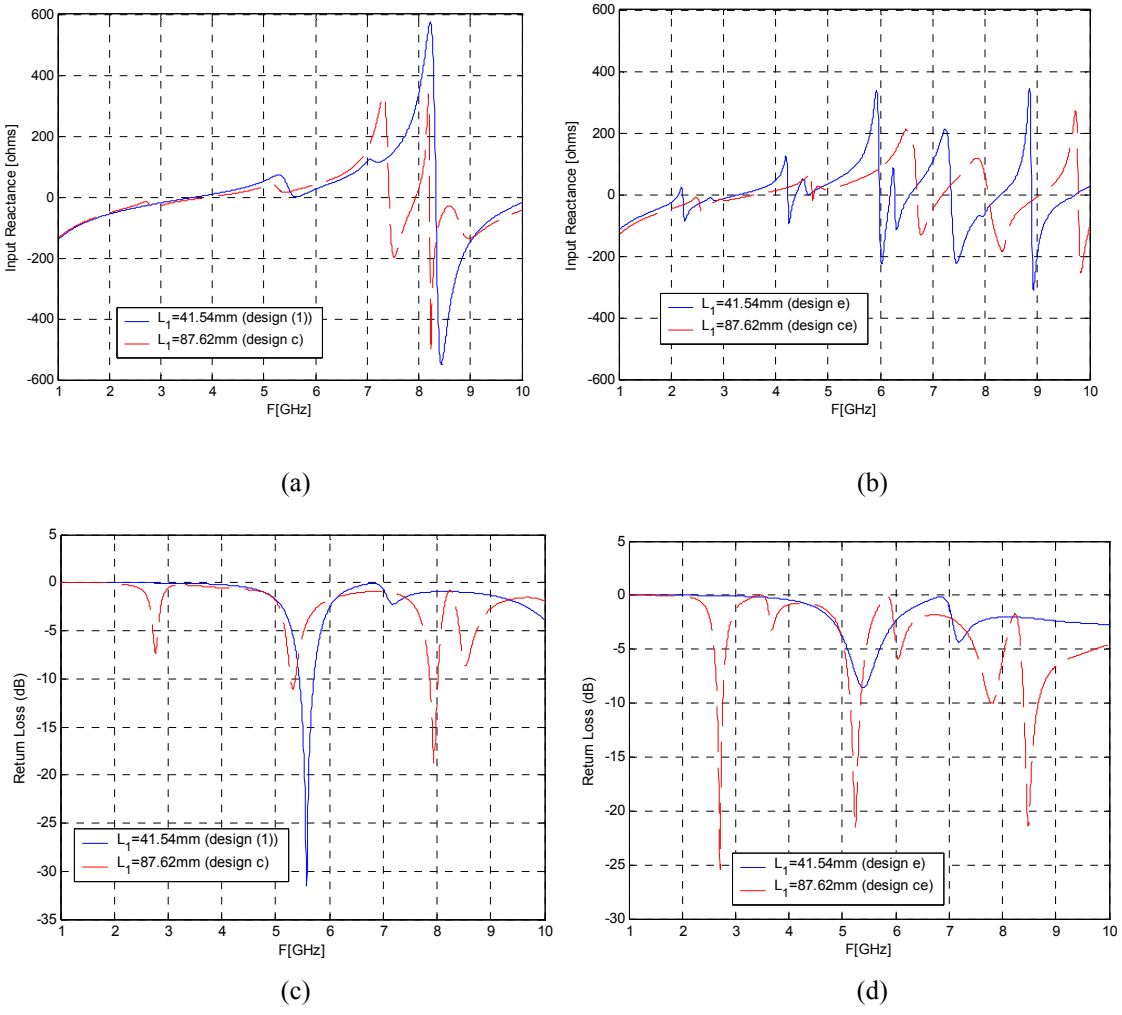

Figure 4.1.3. Input Reactance and Return Loss for two experiments. (a) Designs (*1*) and *c*. (b) Designs *e* and *ce*. (c) Designs (*1*) and *c*. (d) Designs *e* and *ce*

4.1.1.4 Effects of Changing the Distance (W_s) between the Parasitic Ring and the Feeding Antenna on the Resonance Frequencies and Return Loss Response

When the distance between the parasitic ring and the feeding antenna (W_s) was changed from 1 mm to 2 mm, the shift in the resonance frequencies was very subtle as it is shown in Figure 4.1.4 (a) and (b). Also, the return loss decreased in some operation points; this behavior is shown in Figure 4.1.4 (c) and (d).

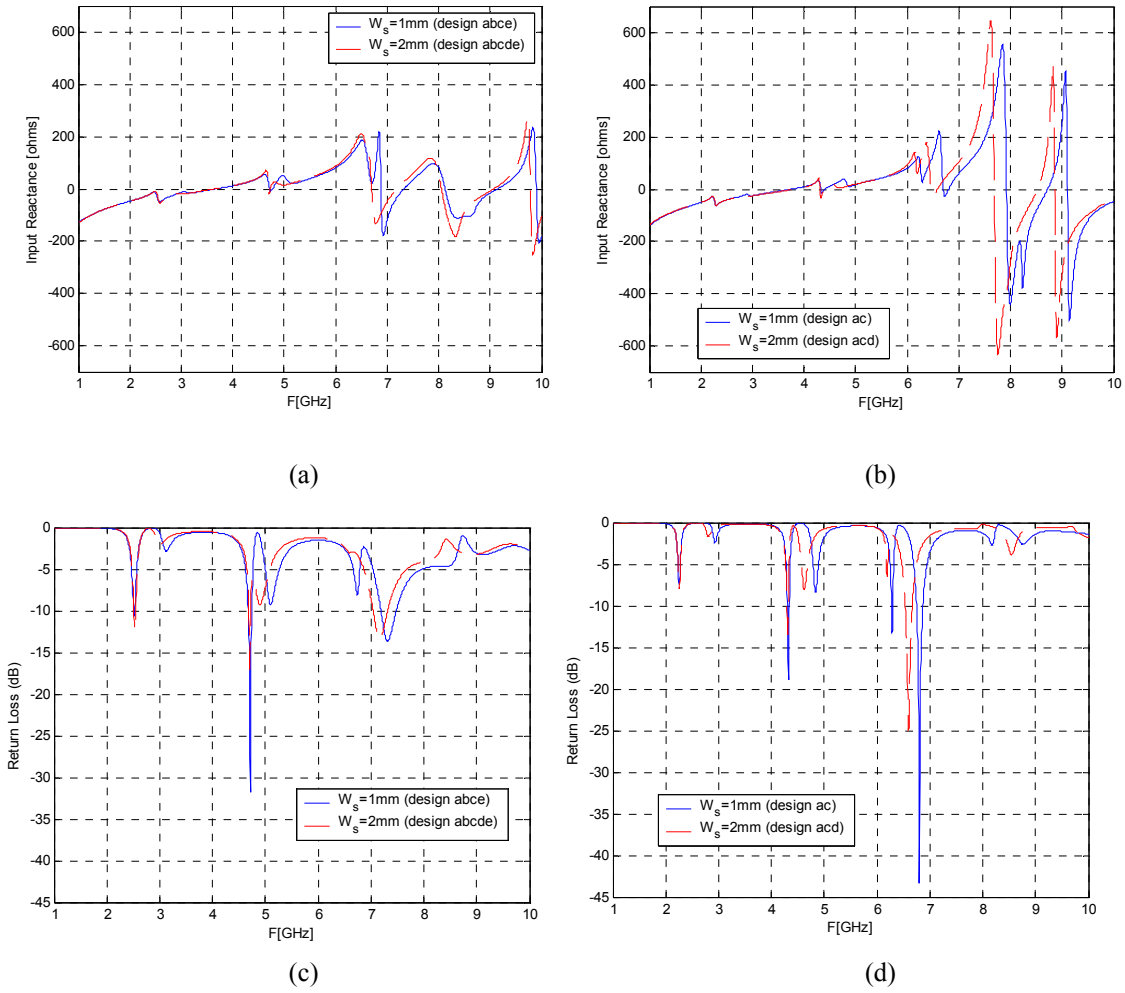

Figure 4.1.4. Input Reactance and Return Loss for two experiments. (a) Designs *abce* and *abcde*. (b) Designs *ac* and *acd.* (c) Designs *abce* and *abcde*. (d) Designs *ac* and *acd*

4.1.1.5 Effects of Changing the Length of the Open Circuit Stub (L_s) on the Resonance Frequencies ans Return Loss Response

When the length of the open circuit stub was changed from 2 mm to 4 mm, the resonance frequencies were shifted to lower frequencies as it is shown in Figure 4.1.5 (a) and (b). According to Figure 4.1.5 (c) and (d) the effect of this change in the return loss response was more complex than the former behavior because in some frequencies increased it and in others decreased it.

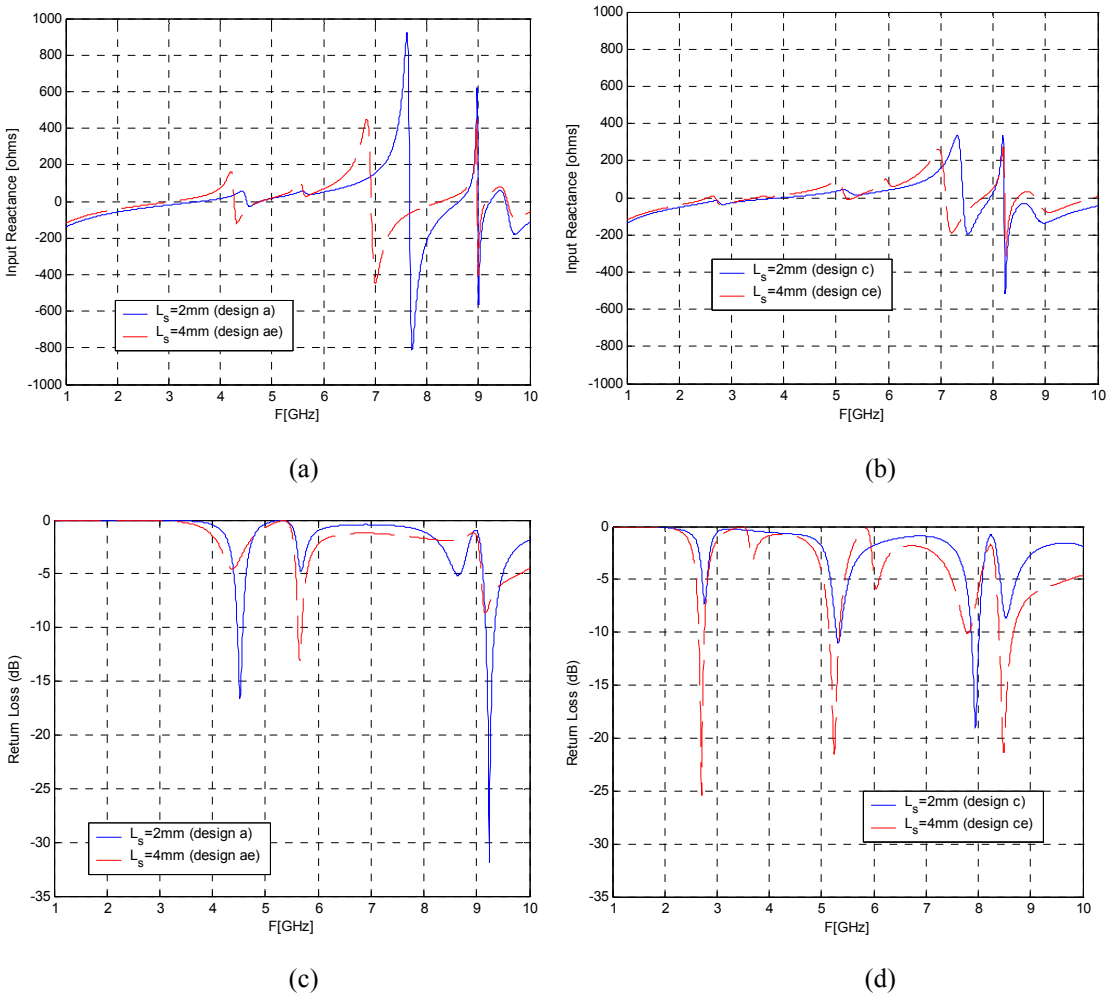

Figure 4.1.5. Input Reactance and Return Loss for two experiments. (a) Designs *a* and *ae*. (b) Designs *c* and *ce*. (c) Designs *a* and *ae*. (d) Designs *c* and *ce*

4.1.1.6 Summary of the Effects

According to the analysis performed above, the effects of the main factors are summarized in Table 4.1.2.

Table 4.1.2. Summarized Effects of the Main Factors when they were changed from Low to High Level

Factor	Resonance Frequency	Number of Operation Bands	Return Loss	Impedance Bandwidth (VSWR≤2)
ε_r	Shifted to lower frequencies	Increased	Increased	Decreased
W	Shifted to higher frequencies	Approximately the same	Increased	Decreased
L_1	Shifted to lower frequencies	Increased	Ambiguous behavior	Ambiguous behavior
W_s	Approximately the same	Approximately the same	Increased	Decreased
L_s	Shifted to lower frequencies	Approximately the same	Ambiguous behavior	Ambiguous behavior

4.1.2 RSRA with the Parasitic Ring inside the Feeding Antenna

The intuitive analysis was applied to the second case, RSRA with the parasitic ring inside the feeding antenna. The effects of changing each factor are as follow.

4.1.2.1 Effects of Changing the Substrate Permittivity on the Resonance Frequencies and Return Loss Response

The effect of changing the substrate permittivity (ε_r) from low level to high level was similar to the case of the RSRA with the parasitic ring outside the feeding antenna, the resonance frequencies were shifted to lower frequencies, the return loss and the impedance bandwidth decreased in some operation points. The simulation results are shown in Figure 4.1.6 (a), (b), (c) and (d).

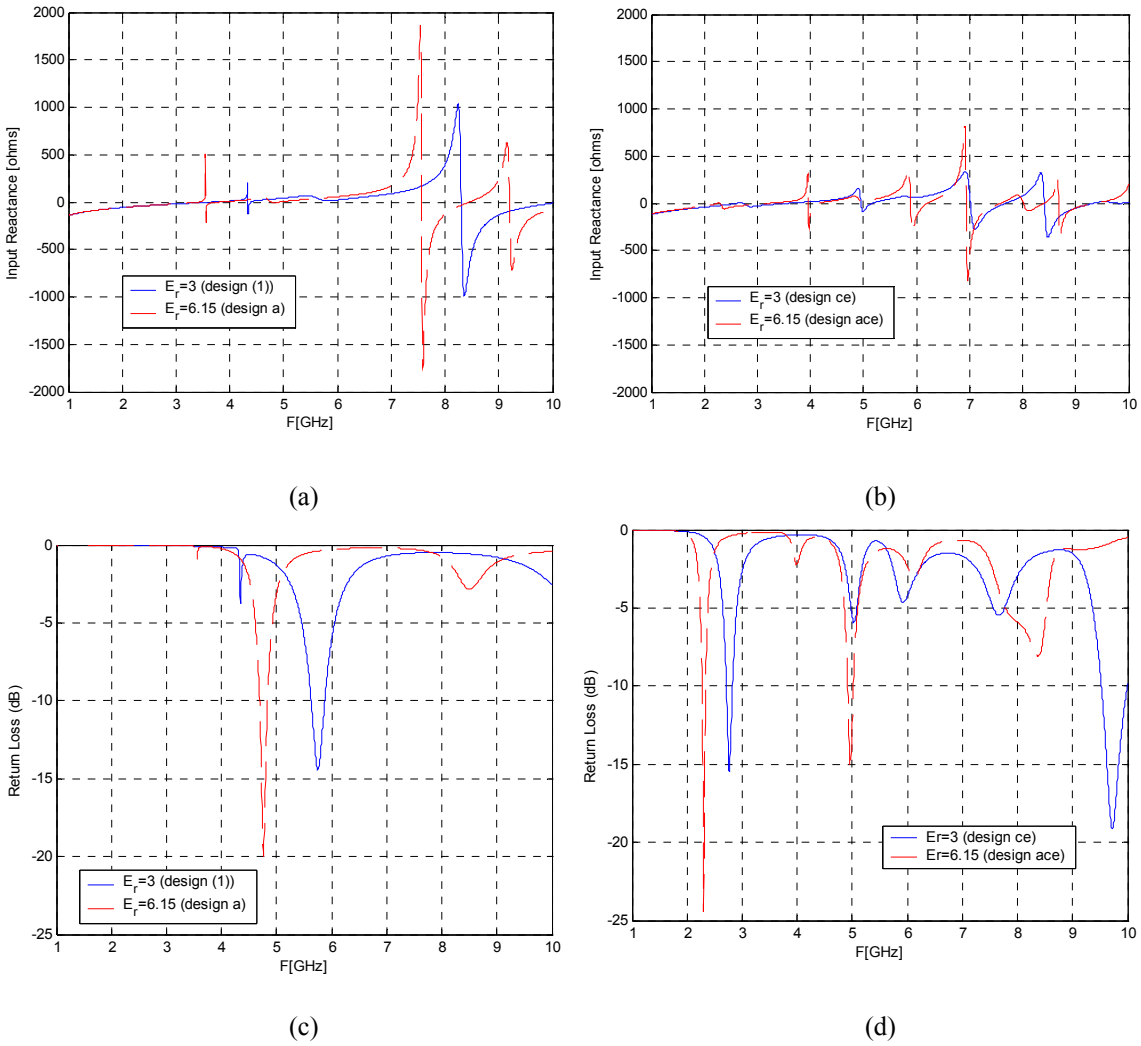

Figure 4.1.6. Input Reactance and Return Loss for two experiments. (a) Designs (*1*) and *a*. (b) Designs *ce* and *ace.* (c) Designs (*1*) and *a*. (d) Designs *ce* and *ace*

4.1.2.2 Effects of Changing the Slot Width (*W*) on the Resonance Frequencies and Return Loss Response

When *W* changed from low to high level, the resonance frequencies were shifted to higher frequencies, the return loss increased and the impedance bandwidth decreased. These behaviors are shown in Figure 4.1.7 (a), (b), (c) and (d).

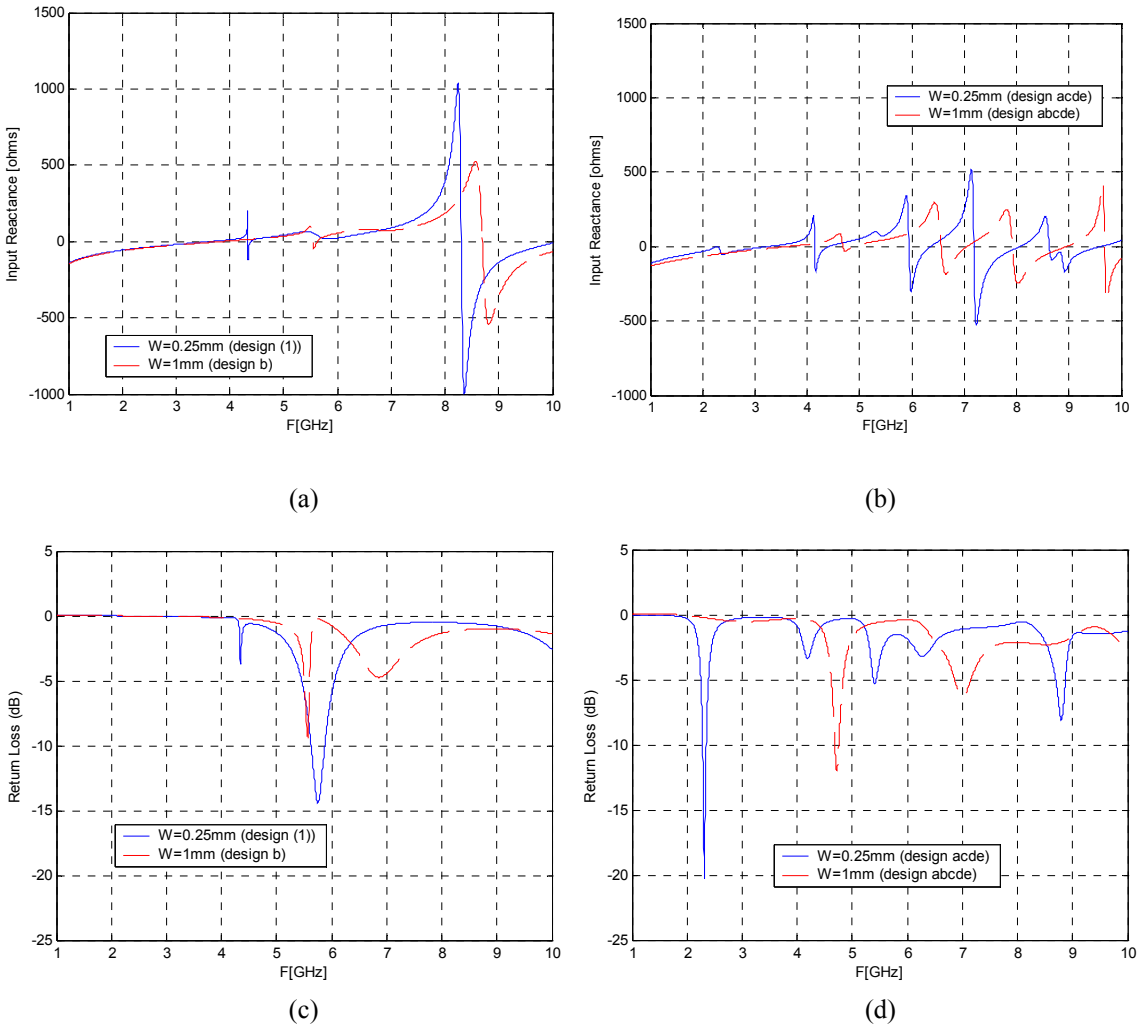

Figure 4.1.7. Input Reactance and Return Loss for two experiments. (a) Designs (*1*) and *b*. (b) Designs *acde* and *abcde.* . (c) Designs (*1*) and *b*. (d) Designs *acde* and *abcde*

4.1.2.3 Effects of Changing the Feeding Antenna Perimeter (L_1) on the Resonance Frequencies and Return Loss Response

When the perimeter of the feeding antenna was changed from low to high level, the resonance frequencies were shifted to lower frequencies. Also, the antenna changed from a single band operation to a dual band operation. The simulation results are shown

in Figure 4.1.8 (a), (b), (c) and (d); in design *(1)* and *e* only one operation point is observed; whereas, in designs *c* and *ce* two operation points are observed.

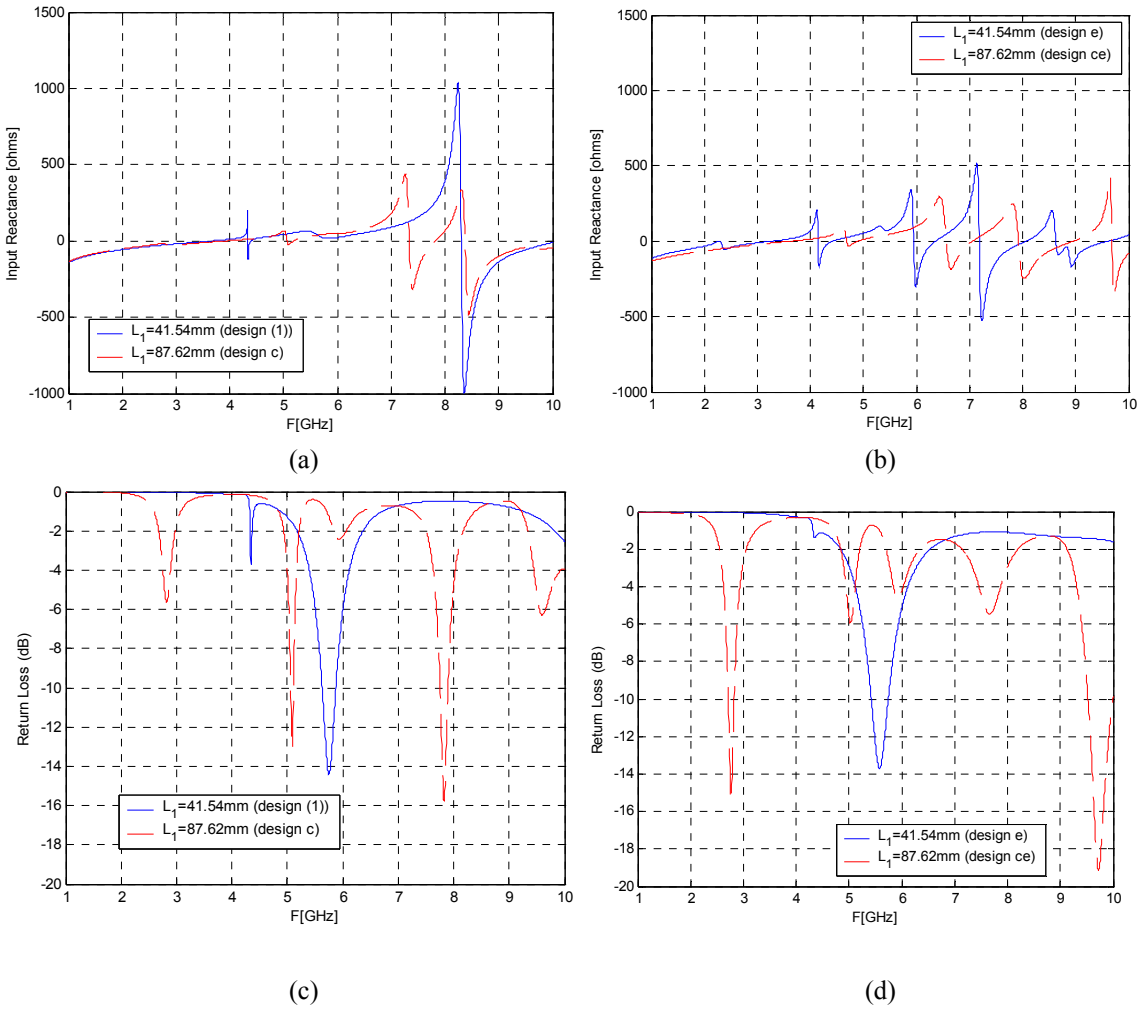

Figure 4.1.8. Input Reactance and Return Loss for two experiments. (a) Designs (*1*) and *c*. (b) Designs *e* and *ce.* (c) Designs (*1*) and *c*. (d) Designs *e* and *ce*

4.1.2.4 Effects of Changing the Distance (W_s) between the Parasitic Ring and the Feeding Antenna on the Return Loss Response

When the distance between the parasitic ring and the feeding antenna (W_s) was changed from 1 mm to 2 mm, the resonance frequencies were shifted to higher frequencies and the return loss decreased in some operation points. The simulation results are shown in Figure 4.1.9 (a), (b), (c) and (d).

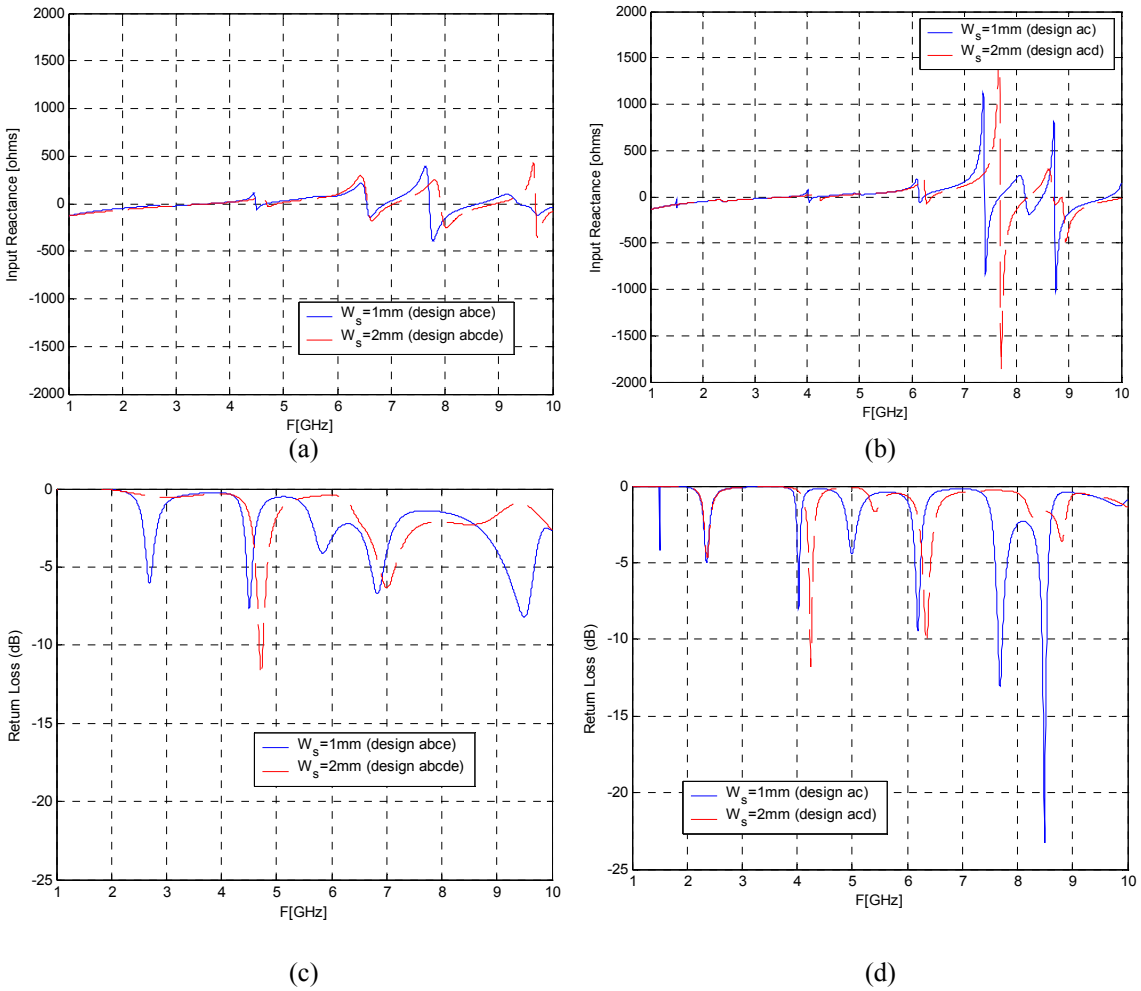

Figure 4.1.9. Input Reactance and Return Loss for two experiments. (a) Designs *abce* and *abcde*. (b) Designs *ac* and *acd,* (c) Designs *abce* and *abcde*. (d) Designs *ac* and *acd*

4.1.2.5 Effects of Changing the Length of the Open Circuit Stub (L_s) on the Return Loss Response

When the length of the open circuit stub was changed from 2 mm to 4 mm, the resonance frequencies were shifted to lower frequencies, the return loss increased in some operation points and in others decreased. The simulation results are shown in Figure 4.1.10.

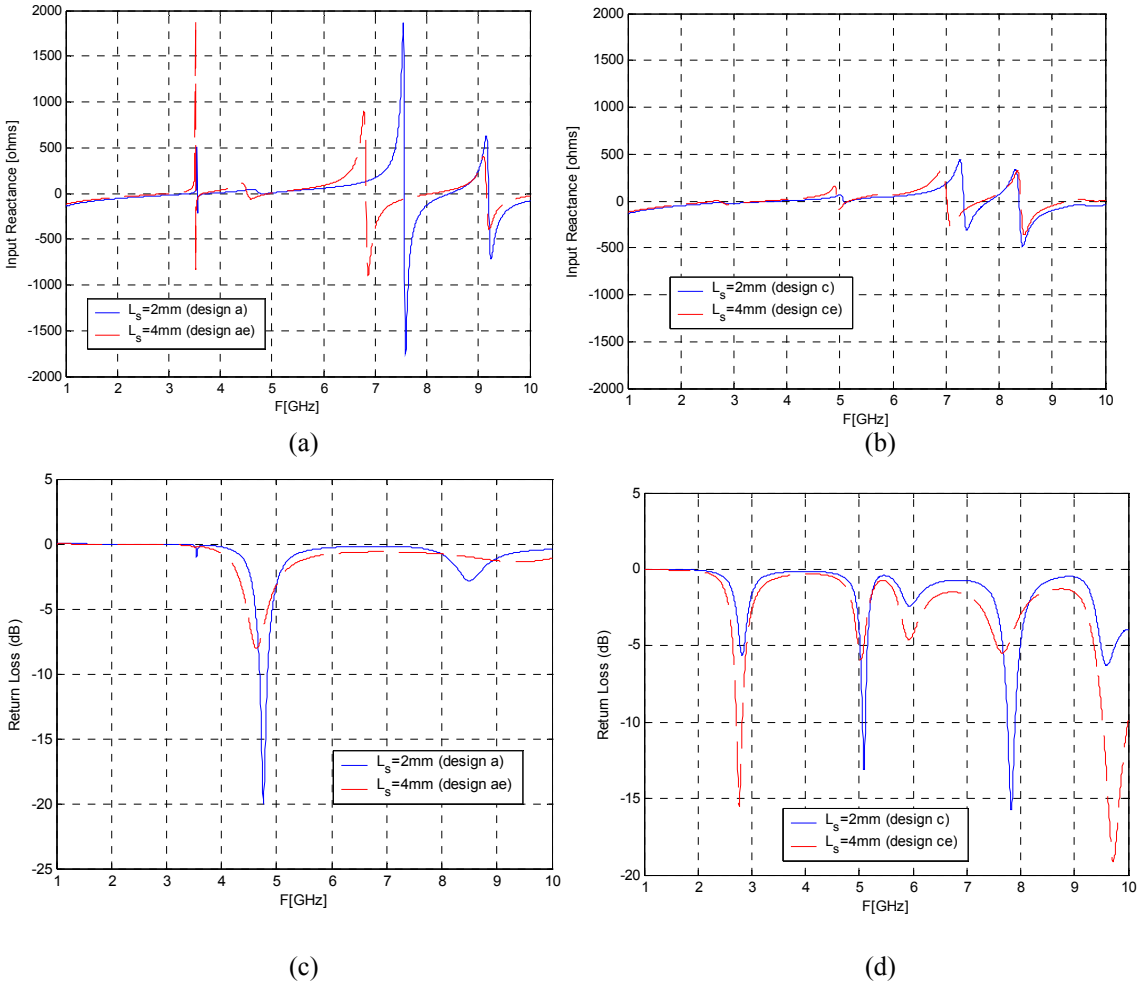

Figure 4.1.10. Input Reactance and Return Loss for two experiments. (a) Designs *a* and *ae*. (b) Designs *c* and *ce*. (c) Designs *a* and *ae*. (d) Designs *c* and *ce*

4.1.2.6 Summary of the Effects

According to the analysis performed for the RSRA with the parasitic ring inside the feeding antenna, the effects of the main factors are summarized in Table 4.1.3.

Table 4.1.3. Summarized Effects of the Main Factors when they were from Low to High Level

Factor	Resonance Frequency	Number of Operation Bands	Return Loss	Impedance Bandwidth (VSWR≤2)
ε_r	Shifted to lower frequencies	Approximately the same	Decreased	Decreased
W	Shifted to higher frequencies	Approximately the same	Increased	Decreased
L_1	Shifted to lower frequencies	Increased	Decreased	Decreased
W_s	Shifted to higher frequencies	Decreased	Decreased	Increased
L_s	Shifted to lower frequencies	Approximately the same	Ambiguous behavior	Ambiguous behavior

4.2 Second Approach: Linear Regression Analysis

This approach was applied to the RSRA Case 1 and 2. In this analysis, only the Designer replicate was considered because the simulations in momentum were adaptive and the number of points in both simulator results was not the same.

4.2.1 RSRA with the Parasitic Ring Outside the Feeding Antenna

In Chapter 3 Section 3.3.3 it was proved that the models with the form of Equation (3.3.3) had a poor reliability because according to the adjusted determination coefficient they do not explain at least the 60% of the variability of the data. In order to overcome this deficiency a new model form was proposed. This new model considered not only the main factors, but also the two factor interactions. The t tests of the interactions of three factors are plotted in the Appendix A. It is important to note that

most of these interactions have no effect in the response or the effect is significant in short frequency intervals. In addition, it was assumed that the interactions of four and five factors did not have effect in the response. Consequently, the new model form is

$$y = \beta_0 + \beta_1 X_A + \beta_2 X_B + \beta_3 X_C + \beta_4 X_D + \beta_5 X_E + \beta_6 X_A X_B + \beta_7 X_A X_C + \beta_8 X_A X_D +$$

$$\beta_9 X_A X_E + \beta_{10} X_B X_C + \beta_{11} X_B X_D + \beta_{12} X_B X_E + \beta_{13} X_C X_D + \beta_{14} X_C X_E + \beta_{15} X_D X_E \qquad (4.2.1)$$

To reduce the complexity of the problem the range of frequency from 1 to 10 GHz was divided in 4 bands using the criterion of an adjusted determination coefficient over 0.6. These bands were called as confidence bands; using this criterion, the inferences of the significant factors were more trusted.

The determination coefficients for 15 regressors was calculated and plotted in Figure 4.2.1. Also, the four confidence bands were plotted. The frequency range for each band is shown in Table 4.2.1.

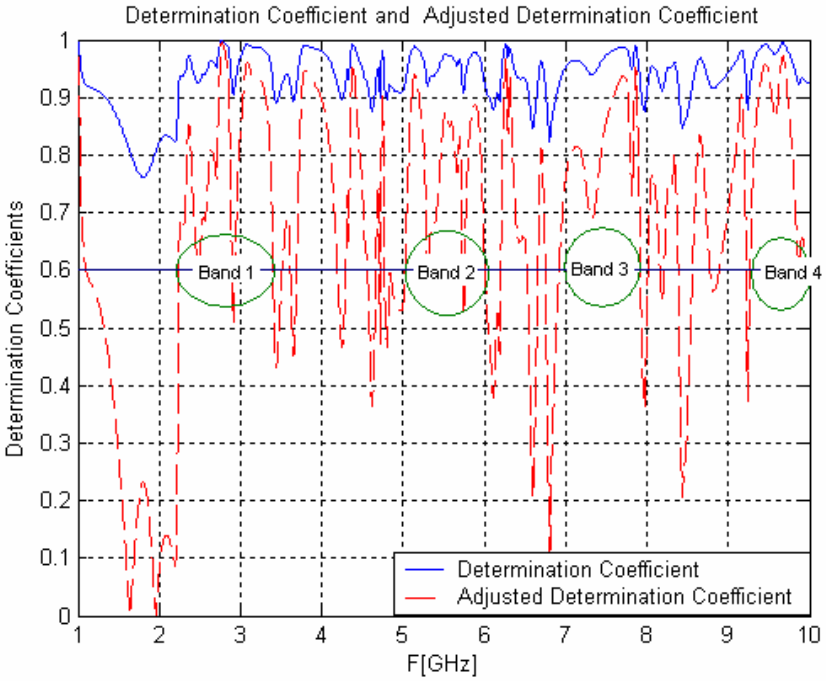

Figure 4.2.1. Determination Coefficients for 15 regressors and Confidence bands.

Table 4.2.1. Confidence Bands

Band 1 [GHz]	Band 2 [GHz]	Band 3 [GHz]	Band 4 [GHz]
2.2 - 3.4	5 - 6	6.9 - 7.9	9.3 - 10

Because the RSRA was designed to operate at 5.7 GHz; the t test and the codified regression coefficients will be plotted in Band 2. The t test are shown in Figure 4.2.2; it is important to notice that β_4, β_8, β_9 and β_{11} are approximately equal to cero which means that the factors and their interactions related to those coefficients have not effect in the response. In Table 4.2.2 it is shown the relation between the coefficients and the antenna factors.

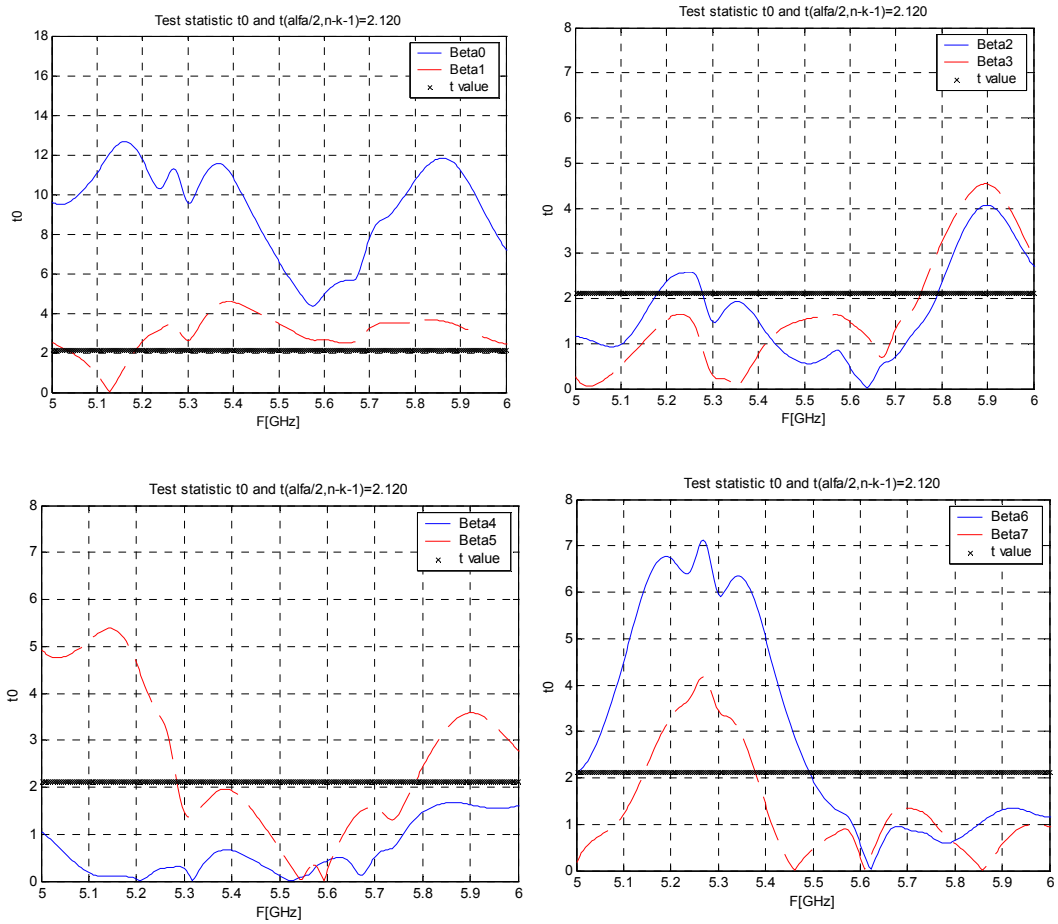

Figure 4.2.2. t_0 value and t statistic for Individual Regression Coefficients

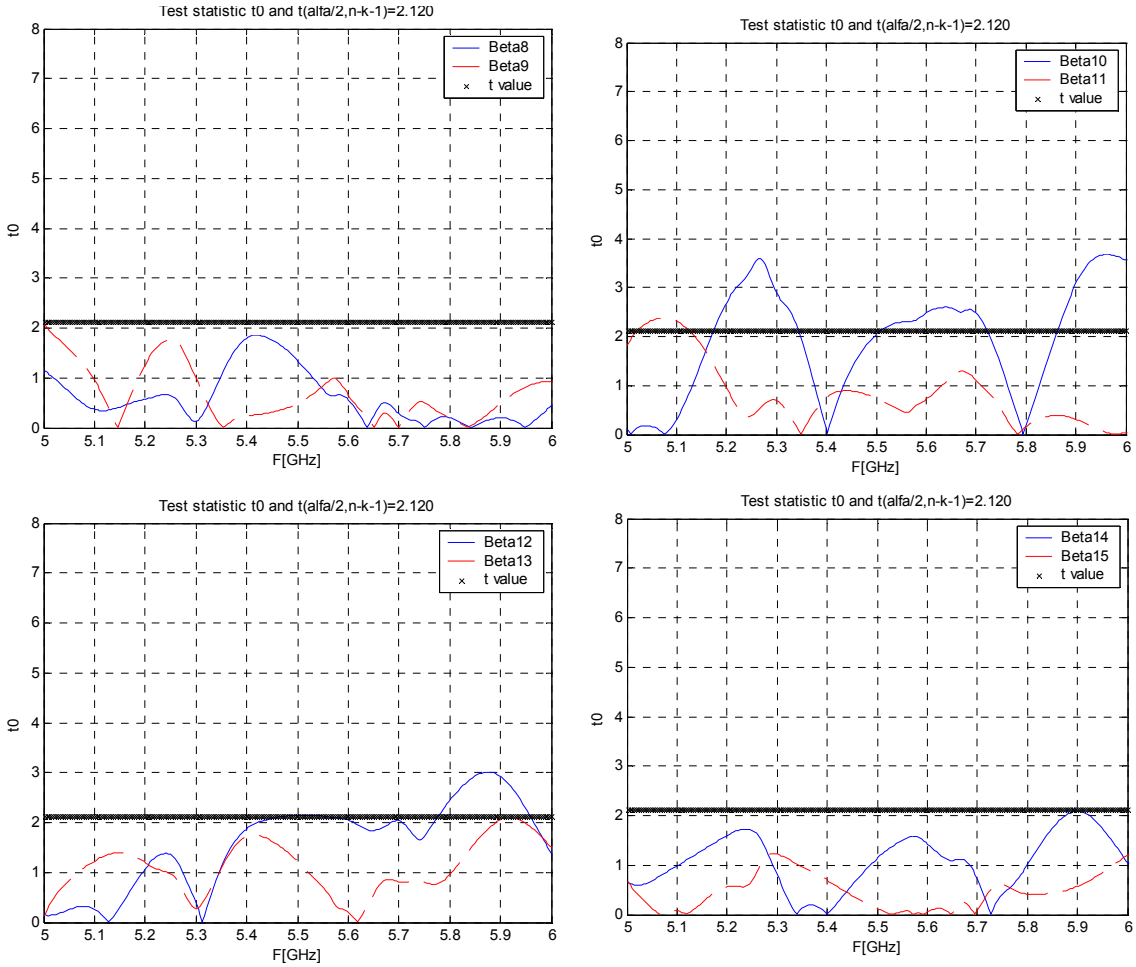

Figure 4.2.2. Continued

Table 4.2.2. Betas, Codified Factors and Natural Factors with low Impact in the Response.

Betas	Codified Factors	Natural Factors
β_4	X_D	W_s
β_8	$X_A X_D$	$\varepsilon_r * W_s$
β_9	$X_A X_E$	$\varepsilon_r * L_s$
β_{11}	$X_B X_E$	$W * W_s$

Finally the sixteen codified coefficient values are shown in Figure 4.2.3. As it was mentioned before, those plots can be used to predict or optimize the return loss response in dB using Equation (4.2.1).

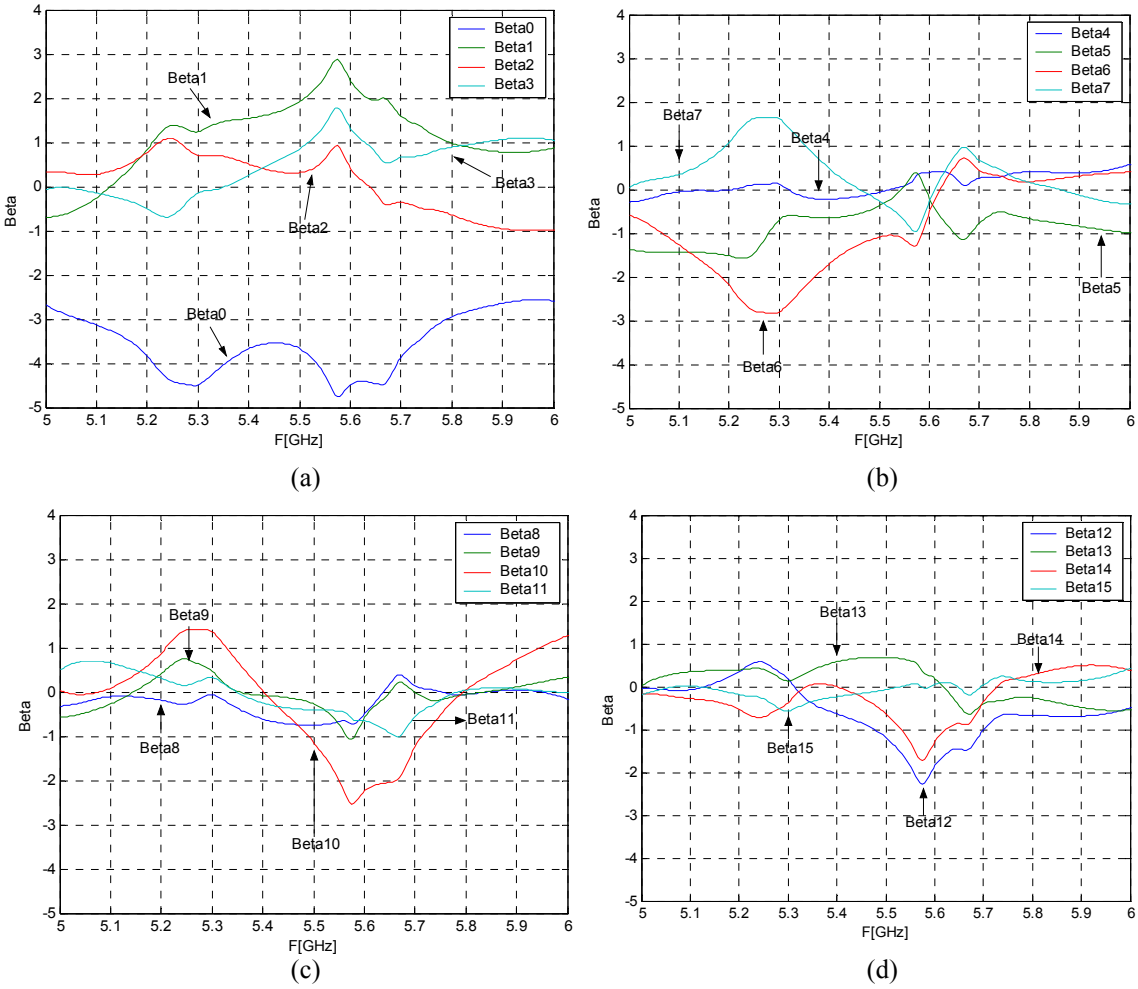

Figure 4.2.3. β's Codified Values. (a)β_0, β_1, β_2, β_3, (b)β_4, β_5, β_6, β_7, (c)β_8, β_9, β_{10}, β_{11}, (d)β_{12}, β_{13}, β_{14}, β_{15}

4.2.2 RSRA with the Parasitic Ring Inside the Feeding Antenna

A similar procedure was applied to the RSRA Case 2. The determination coefficients for 5 regressors have poor reliability in the whole frequency range; these coefficients are shown in the Appendix B. The determination coefficients for 15 are shown in Figure 4.2.4. According to this picture only two confidence bands are presented. Band 1 goes from 2.7 to 3.9 GHz and Band 2 goes from 7 to 7.9 GHz. For this case, the t test and the codified regression coefficients will be plotted in Band 1. The t

tests are shown in Figure 4.2.5; according to this figure the model of Equation (4.2.1) can be simplified. The sixteen codified coefficient values are shown in Figure 4.2.6.

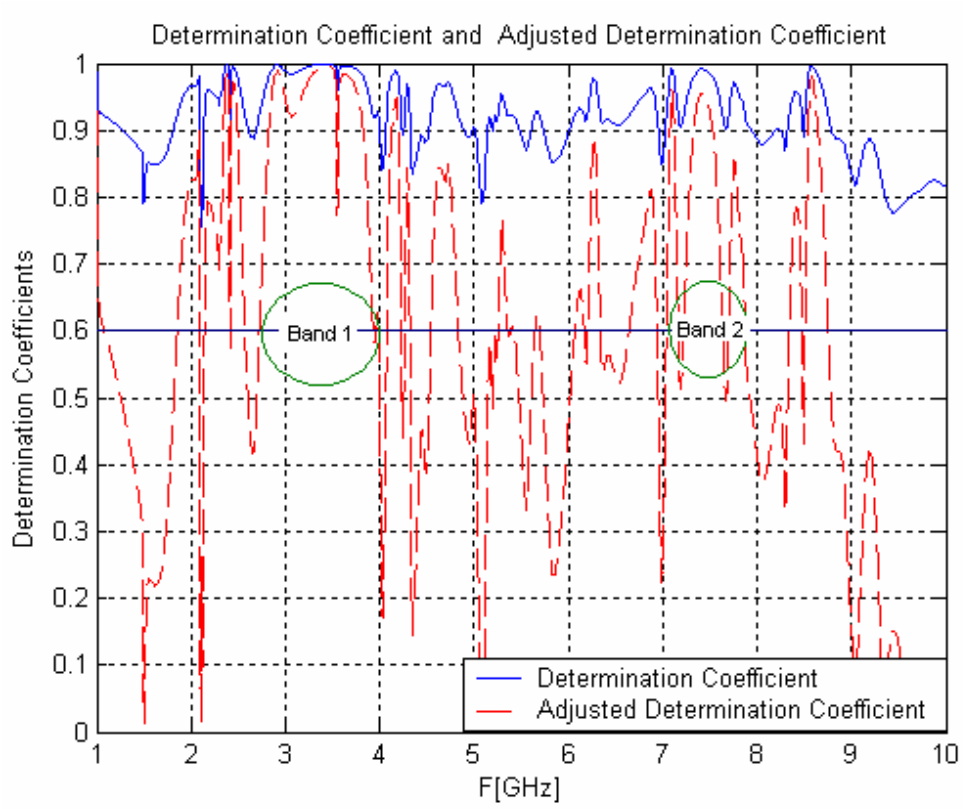

Figure 4.2.4. Determination Coefficients for 15 regressors and Confidence bands.

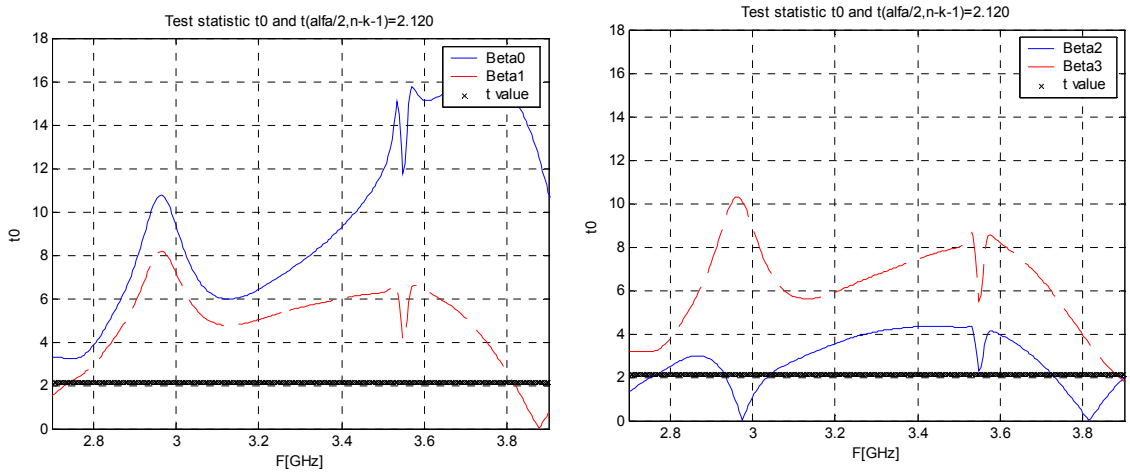

Figure 4.2.5. t_0 value and t statistic for Individual Regression Coefficients

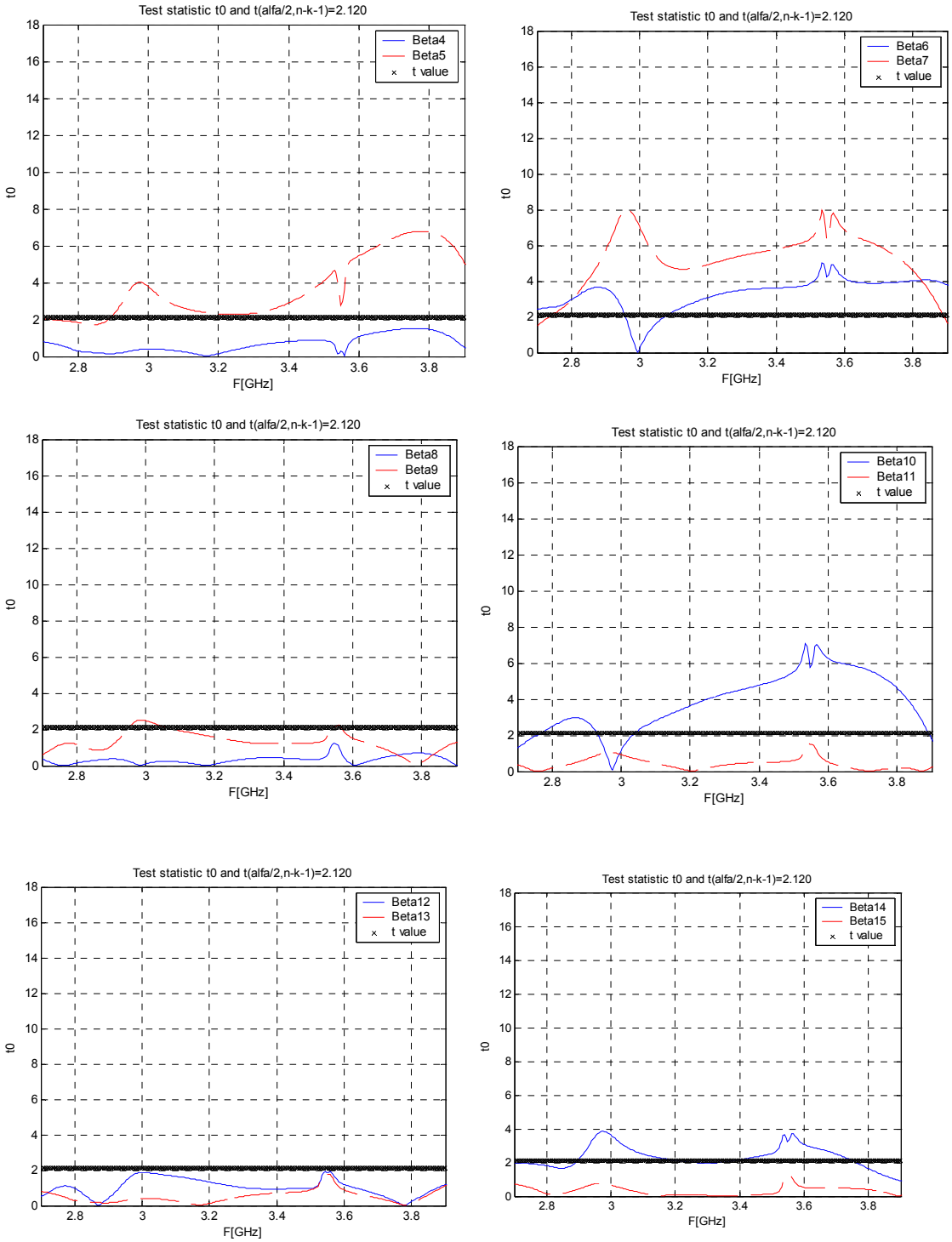

Figure 4.2.5. Continued.

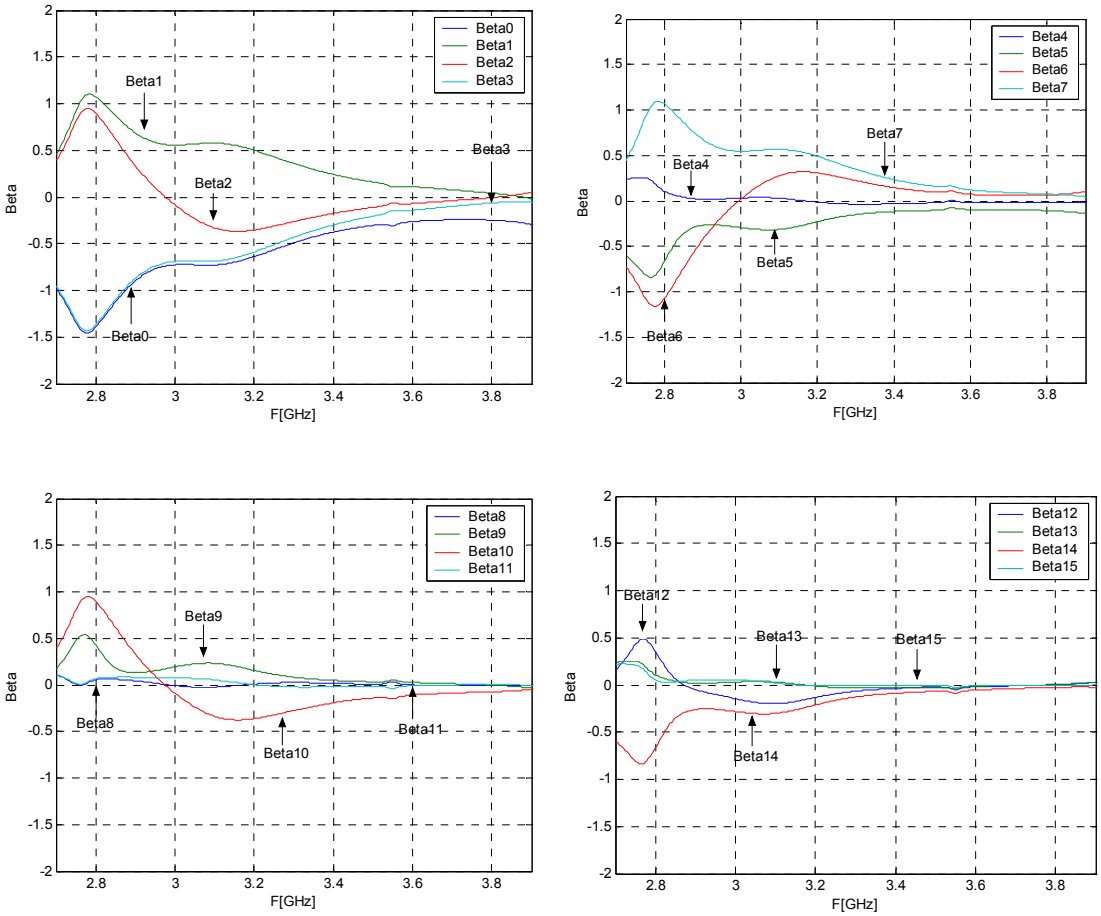

Figure 4.2.6. β's Codified Values. (a)β_0, β_1, β_2, β_3, (b)β_4, β_5, β_6, β_7, (c)β_8, β_9, β_{10}, β_{11}, (d)β_{12}, β_{13}, β_{14}, β_{15}

4.3 Third Approach: DOE Using Punctual Responses

The RSRA characterization followed in this approach evaluated how each factor affects the antenna resonance frequency and input impedance at resonance. In this analysis two replicates were considered one simulated in Ansoft's Designer and the other in Agilent's Momentum. Reasonable agreement was observed in both simulation results.

4.3.1 RSRA with the Parasitic Ring outside the Feeding Antenna

As it was established in Section 3.4, the RSRA Case1 was analyzed using this approach. The simulation results in Ansoft's Designer and Agilent's Momentum are shown in Table 4.3.1. NP stands for not present, which means that it was not available any resonance for that design. Norm stands for normalized values to 50 Ω. Roughly speaking, the first resonance is characterized for low input impedance however some designs such as *cde* and *ce* presented good matching to 50 Ω. In these designs the matching is achieved because of the feeding stub. The second resonance oscillated between 4.27 and 8.25 GHz; its input impedance varied between 0 and 31.94, some designs presented good matching to 50 Ω. The third resonance varied between 7.19 and 9.93 GHz and its input impedance varied between 0.12 and 24. The design summary is shown in Table 3.4.1. The responses were statistically analyzed in each of the following sections. According to this Table 4.3.1 the Designer and momentum replicate are pretty approximated. However, it is important to know whether there is significant difference between the simulator results. This suggests to block each replicate and to make an ANOVA for every response, i.e the first resonance frequency (1^{st} Fr). This ANOVA is shown in Table 4.3.2.

Table 4.3.1. First and Second Replicate. Designer and Momentum Results

Design	1st Fr [GHz] Designer	1st Fr [GHz] Momentum	Zin_1 (Norm) Designer	Zin_1 (Norm) Momentum	2nd Fr [GHz] Designer	2nd Fr [GHz] Momentum	Zin_2 (Norm) Designer	Zin_2 (Norm) Momentum
1	3.674	4.156	0	0	5.624	5.576	0.785	1.389
a	3.62	3.805	0	0	4.5	4.542	1.391	1.712
b	3.85	NP	0	NP	NP	4.492	NP	0
ab	3.913	4.273	0	0	5.34	5.45	0.467	0.461
c	3.962	3.277	0	0.062	7.429	6.25	10.8	8.781
ac	3.76	3.938	0	0	4.323	4.336	0.787	0.938
bc	3.98	NP	0	NP	NP	4.586	NP	0.02
abc	3.976	NP	0	NP	NP	4.313	NP	0.012
d	3.674	4.141	0	0.016	5.543	5.563	1.18	1.576
ad	3.629	3.844	0	0	4.489	4.521	1.783	2.246
bd	3.854	4.495	0	0.015	NP	NP	NP	NP
abd	3.913	4.25	0	0	NP	NP	NP	NP
cd	3.85	4.313	0	0.019	7.564	7.719	6.975	4.936
acd	3.823	3.594	0	0	7.686	7.164	25.744	31.936
bcd	3.976	4.583	0	0	NP	NP	NP	NP
abcd	4.179	4.304	0	0	NP	NP	NP	NP
e	3.269	3.625	0	0.012	5.714	5.935	0.271	0.247
ae	3.08	3.227	0	0	4.269	4.313	4.513	5.721
be	3.526	4	0	0.014	5.831	6	1.963	1.982
abe	3.472	3.719	0	0	5.331	5.453	0.126	0.122
ce	2.697	NP	0.878	NP	5.192	7.258	1.456	5.675
ace	2.216	2.226	1.484	1.684	4.782	4.786	1.559	2.25
bce	NP	NP	NP	NP	8.249	7.859	1.316	5.031
abce	3.67	3.875	0	0.037	7.326	7.328	0.656	4.426
de	3.269	3.578	0	0	5.142	5.195	3.33	4.205
ade	3.071	3.203	0	0	6.88	7	18.501	20.549
bde	3.53	4	0	0.014	6.079	6.18	0.317	0.501
abde	3.463	3.719	0	0	5.079	5.153	0.267	0.443
cde	2.702	2.698	0.939	0.964	5.174	5.194	1.662	2.07
acde	3.656	3.875	0	0	4.696	4.755	1.44	1.35
bcde	3.764	4.26	0	0	5.696	5.7	0.658	0.978
abcde	3.643	3.875	0	0	7.191	7.33	0.642	0.927
Centerpoint	3.89	3.865	0.612	0.618	7.06	7.33	0	1.483
Centerpoint	3.161	3.194	1.042	0.905	6.011	6.068	0.462	0.459

Table 4.3.1. Continued.

Design	3rd Fr [GHz] Designer	3rd Fr [GHz] Momentum	Zin_3 (Norm) Designer	Zin_3 (Norm) Momentum
1	8.34	8.719	18.224	24.082
a	9.235	9.288	0.943	1.387
b	8.649	9.29	12	16.76
ab	9.932	8.5	1.194	22.71
c	7.947	NP	1.254	NP
ac	8.717	8.8	0.137	0.138
bc	8.379	9.469	3.312	7.078
abc	9.658	9.875	0.389	0.629
d	8.303	8.75	19.61	21.467
ad	8.663	8.764	0.337	0.533
bd	8.636	9.219	11.489	12.531
abd	8.208	8.583	10.809	15.468
cd	7.816	7.833	1.366	1.867
acd	8.523	NP	0.212	NP
bcd	8.123	9.5	7.157	8.496
abcd	9.545	9.759	0.373	0.578
e	7.87	8.161	8.347	11.341
ae	9.145	9.195	0.452	0.64
be	8.343	8.75	5.841	7.026
abe	8.987	9.25	0.232	0.342
ce	8.465	NP	0.82	NP
ace	7.488	7.563	6	7.608
bce	8.388	8.336	0.679	1.431
abce	9.154	NP	0.186	NP
de	7.825	8.125	11.216	14.263
ade	8.276	8.438	0.116	0.179
bde	8.321	8.719	5.98	7
abde	8.996	9.234	0.18	0.292
cde	7.96	8.109	1	1.084
acde	7.186	7.33	0.644	0.927
bcde	8.429	8.664	1.01	1.569
abcde	9.073	9.315	0.179	0.212
Centerpoint	8.577	8.962	7.664	9.649
Centerpoint	8.397	8.84	0.172	0.297

Table 4.3.2. ANOVA for First Resonance Frequency and Block Analysis.

Source	Sum of Squares	DF	Mean Square	F value	Prob>F	
Block	0.036	1	0.036	0.163		Not significant
Model	1.79	3	0.60	2.65	0.0574	Not significant
C	0.034	1	0.034	0.15	0.7002	Not significant
D	0.23	1	0.23	1	0.3209	Not significant
CD	1.44	1	1.44	6.41	0.0142	Significant
Curvature	0.11	1	0.11	0.48	0.4929	Not significant
Residual	12.6	56	0.22			
Lack of Fit	10.74	53	0.20	0.33	0.9636	Not significant
Pure Error	1.85	3	0.62			
Cor Total	14.53	61				

From Table 4.3.2 the F_{value} for Block is 0.163; also from [23] $F_{0.05,1,56} = 4$. Because $F_{value} < F_{0.05,1,56}$ there are no significant difference between the simulator results for the first resonance frequency. The residuals for this ANOVA do not violate the independence or constant variance assumptions. It is necessary to perform this block analysis for every response; even though to simplify this document these analyses are not shown.

4.3.1.1 First Resonance Frequency

The analysis of variance and residuals for first Resonance (1^{st}Fr) was performed in Section 3.4, Table 3.4.2 and Figures 3.4.2 (a) and (b). The residuals did not violate the independence or constant variance assumptions; however the ANOVA, Table 3.4.2 showed a lack of fit. This lack of fit can be overcome adding more terms to the model either interactions or quadratic terms. It is not possible to add quadratic terms to the model because axial points were not considered in this project. If axial points had been considered, the number of simulations would be more than 100. The other alternative, to

improve the fit, is to add interactions to the model. The new ANOVA was applied and it is shown in Table 4.3.3. The new model equation in terms of coded factors is

$$1^{st} F_r = 3.69 + 0.24B + 0.079D - 0.27E + 0.060BCE + 0.063ACDE \quad (4.3.1)$$

Where the codified factors A, B, C, D and E represent the natural factors ε_r, W, L_1, W_s and L_s respectively. Even though, the new model has non-significant terms, the lack of fit is not significant any more in the ANOVA. The results obtained from the simulations and the results predicted by the regression model are shown in Table 4.3.4.

Table 4.3.3. ANOVA for the First Resonance Frequency

Source	Sum of Squares	DF	Mean Square	F value	Prob>F	
Model	8.40	5	1.68	15.32	< 0.0001	Significant
B	3.27	1	3.27	29.79	< 0.0001	Significant
D	0.35	1	0.35	3.21	0.0788	Not significant
E	4.36	1	4.36	39.77	< 0.0001	Significant
BCE	0.21	1	0.21	1.91	0.1728	Not significant
ACDE	0.23	1	0.23	2.08	0.1552	Not significant
Curvature	0.10	1	0.10	0.94	0.3354	Not significant
Residual	6.03	55	0.11			
Lack of Fit	3.76	26	0.14	1.85	0.0554	Not significant
Pure Error	2.27	29	0.078			
Cor Total	14.53	61				

Table 4.3.4. Values for the First Resonant Frequency simulated in Designer and Momentum and the Resonat Frequency obtained from the Model. Only some designs are shown.

Design	A	B	C	D	E	Fr (GHz) Designer	Fr (GHz) Momentum	Frmodel(GHz)
(1)	-1	-1	-1	-1	-1	3.674	4.156	3.6440
a	1	-1	-1	-1	-1	3.62	3.805	3.5180
b	-1	1	-1	-1	-1	3.85	Not present	4.2440
ab	1	1	-1	-1	-1	3.913	4.273	4.1180
c	-1	-1	1	-1	-1	3.962	3.277	3.6380
ac	1	-1	1	-1	-1	3.76	3.938	3.7640
bc	-1	1	1	-1	-1	3.98	Not present	3.9980
abc	1	1	1	-1	-1	3.976	Not present	4.1240
d	-1	-1	-1	1	-1	3.674	4.141	3.6760
ad	1	-1	-1	1	-1	3.629	3.844	3.8020
bd	-1	1	-1	1	-1	3.854	4.495	4.2760
abd	1	1	-1	1	-1	3.913	4.25	4.4020
cd	-1	-1	1	1	-1	3.85	4.313	3.9220
acd	1	-1	1	1	-1	3.823	3.594	3.7960
bcd	-1	1	1	1	-1	3.976	4.583	4.2820
abcd	1	1	1	1	-1	4.179	4.304	4.1560
e	-1	-1	-1	-1	1	3.269	3.625	3.0980

Even though there are differences between the predicted and the simulated values, the model follows the results simulations. It is important to notice, that the most significant factors in the model (Eq. 4.3.1) are B and E (W and L_s). Factor A has low importance in the model. In the intuitive analysis performed before (Section 4.1.1.1), it was concluded that factor A shifted the resonance frequencies to lower frequencies but a deeper analysis of Figures 4.1.1 (a) and (b) tell us that this shift is stronger in frequencies over 5 GHz. Consequently, it is reasonable that according to Equation 4.3.1, factor A has low impact in the first resonance frequency. On the other hand, in Section 4.1.1.2 it was concluded that factor B shifted the resonance frequencies to higher frequencies; therefore the model validates this conclusion with a positive impact of this factor in Equation 4.3.1. Also, factor E or L_s that shifted the resonance frequencies to lower frequencies has

negative impact in Equation 4.3.1. The analysis presented above show that both approaches agree with each other.

The residuals for this new ANOVA are shown in Figure 4.3.1. According to this figure the residuals do not violate the independence or constant variance assumptions because they follow a straight line (Figure 4.3.1. (a)) and they are structureless (Figure 4.3.1. (b)).

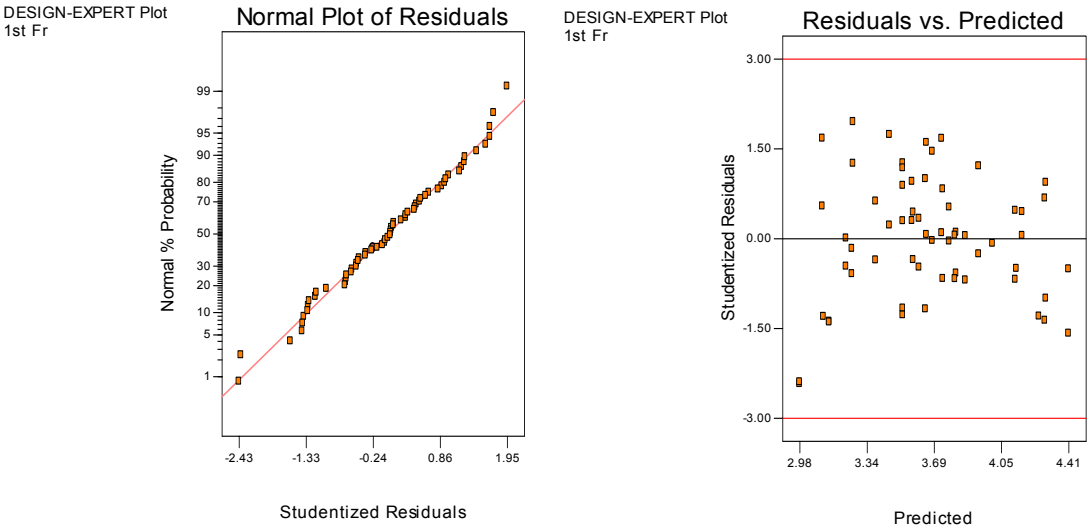

Figure 4.3.1. Plot of residuals for the First Resonance Frequency. (a) Normal plot of residuals. (b) Residuals vs. predicted values

4.3.1.2 Input Impedance at First Resonance Frequency

The Design Expert steps, given in Section 3.4 were followed for this response. First, it was necessary to choose a transformation that stabilized the response variance; this transformation was the inverse.

The second step was choosing the significant effects from the normal probability plot. This election was keeping in mind that the model should have no lack of fit. This plot is shown in Figure 4.3.2. The significant effects are represented by blue squares.

The third step was the ANOVA and it is shown in Table 4.3.5. The significant terms are A, B, C, E, BC, CD, CE, DE and ACDE. The curvature is significant which means that the second order model can be more appropriate. However this model can not be calculated because the axial points were not considered. The lack of fit is not significant.

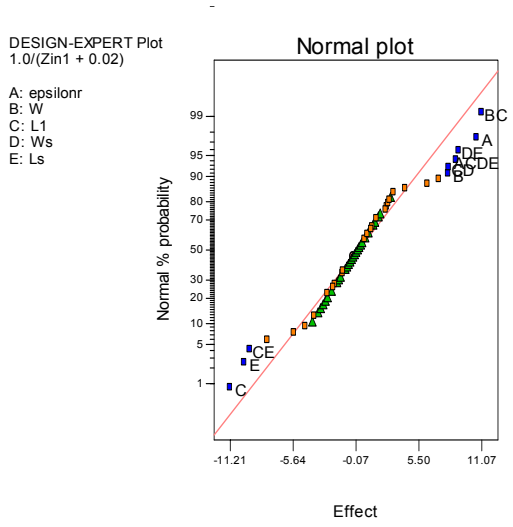

Figure 4.3.2. Normal Probability plot of the effects for the Input Impedance at First Resonance Frequency

Table 4.3.5. ANOVA for the Input Impedance at First Resonance Frequency

Source	Sum of Squares	DF	Mean Square	F value	Prob>F	
Model	12007.07	9	1334.12	7.89	< 0.0001	Significant
A	1555.93	1	1555.93	9.20	0.0038	Significant
B	1371.42	1	1371.42	8.11	0.0063	Significant
C	1796.34	1	1796.34	10.62	0.0020	Significant
E	2130.23	1	2130.23	12.60	0.0008	Significant
BC	1858.18	1	1858.18	10.99	0.0017	Significant
CD	747.16	1	747.16	4.42	0.0405	Significant
CE	1638.66	1	1638.66	9.69	0.0030	Significant
DE	1100.20	1	1100.20	6.51	0.0138	Significant
ACDE	763.33	1	763.33	4.51	0.0385	Significant
Curvature	8697.62	1	8697.62	51.44	< 0.0001	Significant
Residual	8623.74	51	169.09			
Lack of Fit	4363.07	22	198.32	1.35	0.2221	Not significant
Pure Error	4260.67	29	146.92			
Cor Total	29328.44	61				

$$\frac{1}{Z_{in1}+0.02} = 49.56 + 5.06A + 4.91B - 5.66C - 6.14E + 5.72BC + 3.65CD - 5.38CE + 4.41DE + 3.67ACDE \quad (4.3.2)$$

The model equation in terms of coded factors is represented by Equation (4.3.2). The results obtained from the simulations and the results predicted by the regression model are shown in Table 4.3.6. Agreement between the simulated and model values is observed.

Table 4.3.6. Values for the Input Impedance at the First Resonance Simulated in Designer and Momentum and the Input Impedance obtained from the Model. Only some design are shown.

Design	A	B	C	D	E	Zin_1 Designer	Zin_1 Momentum	Zin_1 model
(1)	-1	-1	-1	-1	-1	0	0	-0.0042
a	1	-1	-1	-1	-1	0	0	-0.0049
b	-1	1	-1	-1	-1	0	NP	-0.0038
ab	1	1	-1	-1	-1	0	0	-0.0045
c	-1	-1	1	-1	-1	0	0.062	0.0072
ac	1	-1	1	-1	-1	0	0	-0.0016
bc	-1	1	1	-1	-1	0	NP	-0.0028
abc	1	1	1	-1	-1	0	NP	-0.0068
d	-1	-1	-1	1	-1	0	0.016	0.0050
ad	1	-1	-1	1	-1	0	0	-0.0026
bd	-1	1	-1	1	-1	0	0.015	0.0061

The fourth step was to evaluate the model adequacy using the normal probability plot and the residuals vs. predicted values plot. These plots are shown in Figures 4.3.3 (a) and (b).

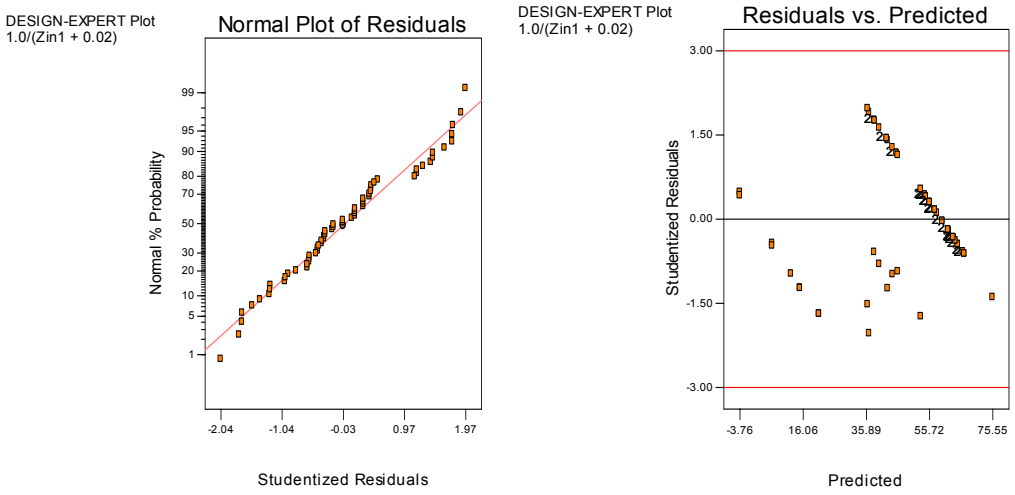

(a) (b)

Figure 4.3.3. Plot of residuals for Zin_1 at Resonance. (a) Normal plot of residuals. (b) Residuals vs. predicted values

4.3.1.3 Second Resonance Frequency

It was followed the same procedure for this response. The significant effects are shown in the normal probability plot in Figure 4.3.4.

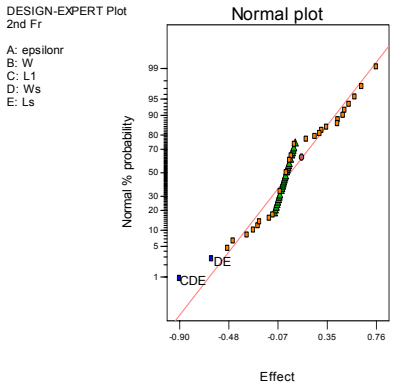

Figure 4.3.4. Normal Probability plot of the effects for the Second Resonance Frequency

The ANOVA is shown in Table 4.3.7. The significant terms are DE and CDE. The curvature is not significant and the lack of fit is significant. It was not possible to make the lack of fit not significant adding interactions to the model; consequently this model should not be used to predict the response. The model is expressed by Equation 4.3.3.

$$2^{nd} F_r = 5.78 - 0.30DE - 0.37CDE \tag{4.3.3}$$

The residuals are shown in Figure 4.3.5 and they do not violate the ANOVA assumptions.

Table 4.3.7. ANOVA for the Second Resonance Frequency

Source	Sum of Squares	DF	Mean Square	F value	Prob>F	
Model	12.02	2	6.01	5.52	0.0066	Significant
DE	4.74	1	4.74	4.36	0.0417	Significant
CDE	7.34	1	7.34	6.74	0.0121	Significant
Curvature	2.62	1	2.62	2.41	0.1267	Not significant
Residual	57.69	53	1.09			
Lack of Fit	53.21	26	2.05	12.32	<0.0001	Significant
Pure Error	4.48	27	0.17			
Cor Total	72.34	56				

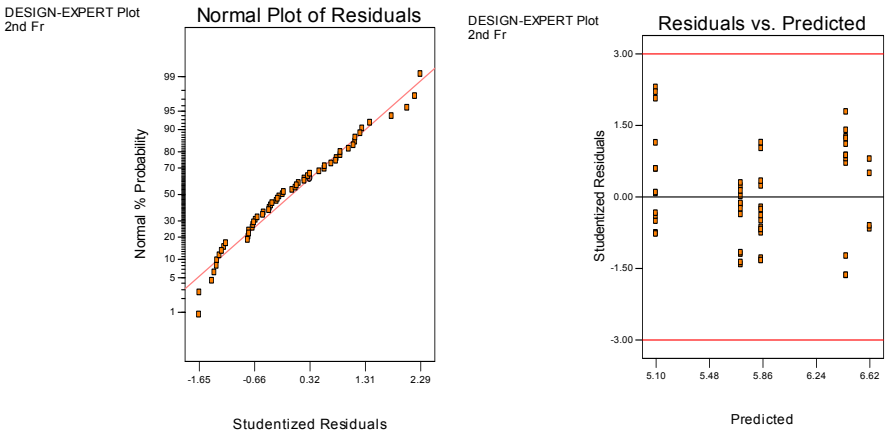

(a) (b)

Figure 4.3.5. Plot of residuals for Second Resonance Frequency. (a) Normal plot of residuals. (b) Residuals vs. predicted values

4.3.1.4 Input Impedance at Second Resonance Frequency

The significant factors for this response are shown in the normal probability plot in Figure 4.3.6. The ANOVA is shown in Table 4.3.8. The significant terms are B and ABE. The curvature is not significant and the lack of fit is significant. It was not possible to make the lack of fit not significant adding interactions to the model consequently this model should not be use to predict the response. The model is represented by Equation 4.3.4. The residuals follow the ANOVA assumptions and are shown in Figure 4.3.7.

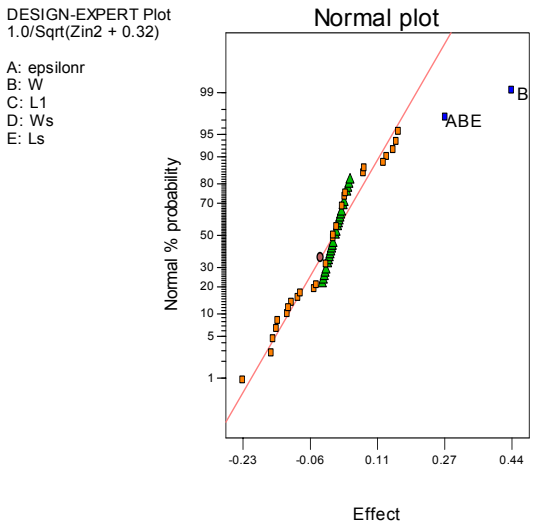

Figure 4.3.6. Normal Probability plot of the effects for the Input Impedance at Second Resonance Frequency

Table 4.3.8. ANOVA for the Input Impedance at Second Resonance Frequency

Source	Sum of Squares	DF	Mean Square	F value	Prob>F	
Model	3.45	2	1.72	15.92	<0.0001	Significant
B	2.91	1	2.91	26.87	<0.0001	Significant
ABE	0.45	1	0.45	4.18	0.0459	Significant
Curvature	0.40	1	0.40	3.72	0.0591	Not significant
Residual	5.74	53	0.11			
Lack of Fit	5.10	26	0.20	8.36	<0.0001	Significant
Pure Error	0.63	27	0.023			
Cor Total	9.58	56				

$$\frac{1}{\sqrt{Z_{in2}+0.32}} = 0.87 + 0.24B + 0.092ABE \tag{4.3.4}$$

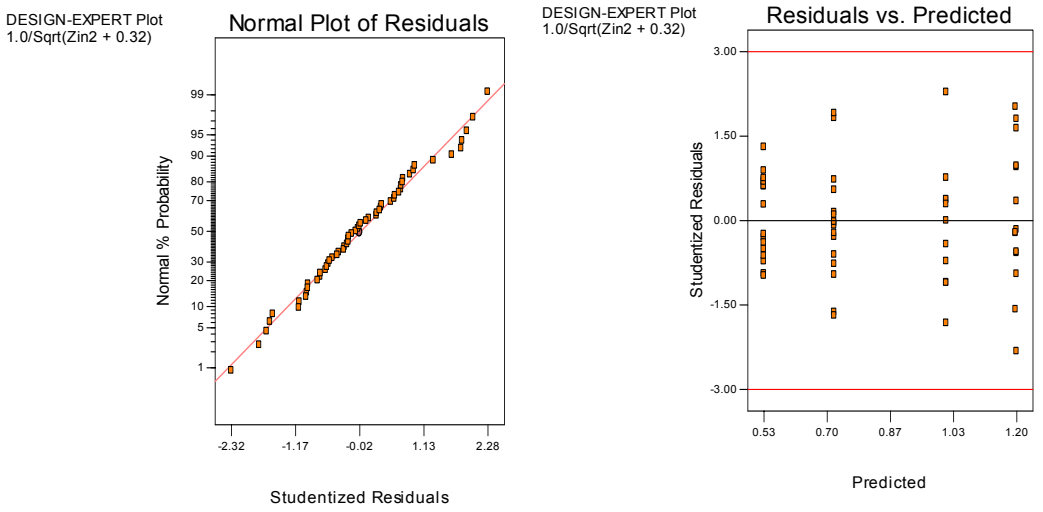

(a) (b)

Figure 4.3.7. Plot of residuals for the Input Impedance at Second Resonance Frequency. (a) Normal plot of residuals. (b) Residuals vs. predicted values

4.3.1.5 Third Resonance Frequency

The significant factors for this response are shown in the normal probability plot in Figure 4.3.8. The ANOVA is shown in Table 4.3.9. The significant terms are A, B, E, BC, ABC, ABE, ACE. The curvature and lack of fit are not significant. The model is expressed by Equation 4.3.5. The results obtained from the simulations and the results predicted by the regression model are shown in Table 4.3.10. Agreement between the simulated and model values is observed. The residuals follow the ANOVA assumptions and are shown in Figure 4.3.9.

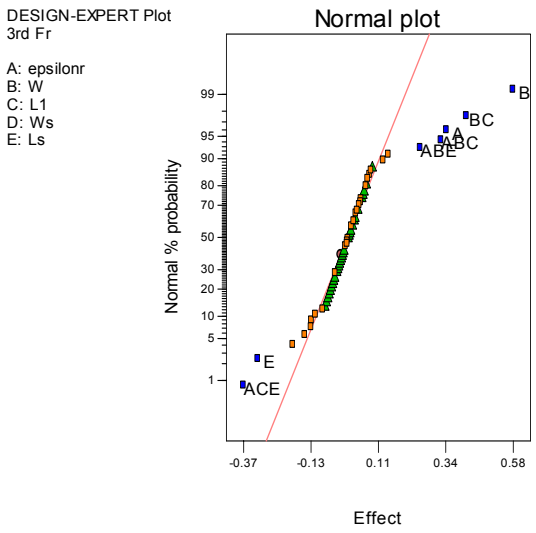

Figure 4.3.8. Normal Probability plot of the effects for the Third Resonance Frequency

Table 4.3.9. ANOVA for the Third Resonance Frequency

Source	Sum of Squares	DF	Mean Square	F value	Prob>F	
Model	16.88	7	2.41	24.68	<0.0001	Significant
A	2.10	1	2.10	21.44	<0.0001	Significant
B	5.55	1	5.55	56.74	<0.0001	Significant
E	1.30	1	1.30	13.26	0.0006	Significant
BC	2.60	1	2.60	26.55	<0.0001	Significant
ABC	1.78	1	1.78	18.23	<0.0001	Significant
ABE	1.21	1	1.21	12.36	0.0009	Significant
ACE	2.21	1	2.21	22.58	<0.0001	Significant
Curvature	0.030	1	0.030	0.31	0.5828	Not significant
Residual	5.38	55	0.098			
Lack of Fit	2.73	25	0.11	1.24	0.2878	Not significant
Pure Error	2.65	30	0.088			
Cor Total	22.29	63				

$$3^{rd}\,F_r = 8.6 + 0.18A + 0.31B - 0.15E + 0.21BC + 0.17ABC + 0.14ABE - 0.19ACE \qquad (4.3.5)$$

Table 4.3.10. Values for the Third Resonant Frequency simulated in Designer and Momentum and the Resonat Frequency obtained from the Model. Only some design are shown.

Design	A	B	C	D	E	Fr (GHz) Designer	Fr (GHz) Momentum	Frmodel(GHz)
(1)	-1	-1	-1	-1	-1	8.34	8.719	8.3500
a	1	-1	-1	-1	-1	9.235	9.288	8.9500
b	-1	1	-1	-1	-1	8.649	9.29	9.1700
ab	1	1	-1	-1	-1	9.932	8.5	8.5300
c	-1	-1	1	-1	-1	7.947	NP	7.8900
ac	1	-1	1	-1	-1	8.717	8.8	8.5700
bc	-1	1	1	-1	-1	8.379	9.469	8.8700
abc	1	1	1	-1	-1	9.658	9.875	9.6700
d	-1	-1	-1	1	-1	8.303	8.75	8.3500
ad	1	-1	-1	1	-1	8.663	8.764	8.9500
bd	-1	1	-1	1	-1	8.636	9.219	9.1700
abd	1	1	-1	1	-1	8.208	8.583	8.5300
cd	-1	-1	1	1	-1	7.816	7.833	7.8900
acd	1	-1	1	1	-1	8.523	NP	8.5700
bcd	-1	1	1	1	-1	8.123	9.5	8.8700
abcd	1	1	1	1	-1	9.545	9.759	9.6700
e	-1	-1	-1	-1	1	7.87	8.161	7.9500

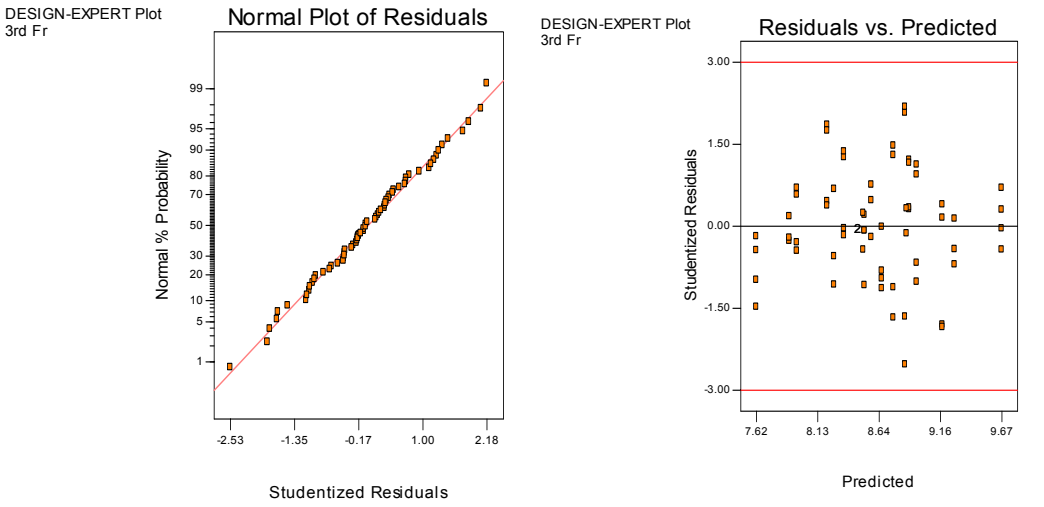

(a) (b)

Figure 4.3.9. Plot of residuals for the Third Resonance Frequency. (a) Normal plot of residuals. (b) Residuals vs. predicted values

4.3.1.6 Input Impedance at Third Resonance Frequency

The significant factors for this response are shown in the normal probability plot in Figure 4.3.10. The ANOVA is shown in Table 4.3.11. The significant terms are A, C, E, AC, BE, CE, ABC, ABE, ACE. The curvature and lack of fit are not significant. The model is expressed by Equation 4.3.6. The results obtained from the simulations and the results predicted by the regression model are shown in Table 4.3.12. Agreement between the simulated and model values is observed. Even though the residuals follow the ANOVA assumptions, two outliers are observed. These outliers correspond to the input impedances of 9.649 [Norm] and 0.172 [Norm] respectively. From experience it is known that they are reasonable values of the antenna input impedance and should be kept in the analysis. These experimental conditions correspond to the center points, that is, $\varepsilon_r = 3$, $W = 0.625$ mm, $L_1 = 64.63$ mm, $W_s = 1.5$ mm, $L_s = 3$ mm and $\varepsilon_r = 6.15$, $W = 0.625$ mm, $L_1 = 64.63$ mm, $W_s = 1.5$ mm, $L_s = 3$ mm. The residuals plots are shown in Figure 4.3.11.

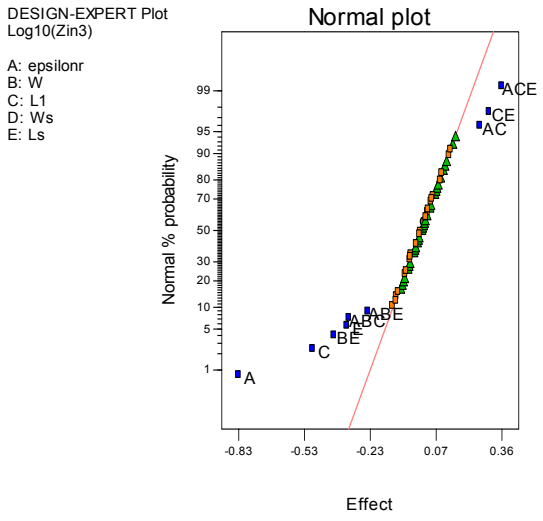

Figure 4.3.10. Normal Probability plot of the effects for the Input Resistance at Third Resonance Frequency

Table 4.3.11. ANOVA for the Input Resistance at Third Resonance Frequency

Source	Sum of Squares	DF	Mean Square	F value	Prob>F	
Model	26.78	9	2.98	23.09	<0.0001	Significant
A	10.72	1	10.72	83.19	<0.0001	Significant
C	4.40	1	4.40	34.11	<0.0001	Significant
E	1.70	1	1.70	13.21	0.0006	Significant
AC	1.22	1	1.22	9.45	0.0033	Significant
BE	2.35	1	2.35	18.22	<0.0001	Significant
CE	1.19	1	1.19	9.25	0.0037	Significant
ABC	1.82	1	1.82	14.11	0.0004	Significant
ABE	0.98	1	0.98	7.57	0.0081	Significant
ACE	2.12	1	2.12	16.48	0.0002	Significant
Curvature	0.019	1	0.019	0.14	0.7056	Not significant
Residual	6.83	53	0.13			
Lack of Fit	3.16	23	0.14	1.12	0.3771	Not significant
Pure Error	3.67	30	0.12			
Cor Total	33.63	63				

$$\log_{10} Z_{in3} = 0.21 - 0.4A - 0.27C - 0.17E + 0.14AC - 0.20BE + 0.14CE - 0.17ABC - 0.13ABE + 0.19ACE \quad (4.3.6)$$

Table 4.3.12. Values for the Input Impedance at Third Resonant Frequency simulated in Designer and Momentum and the Resonat Frequency obtained from the Model. Only some design are shown.

Design	A	B	C	D	E	Zin_3 Designer	Zin_3 Momentum	Zin_3 Model
(1)	-1	-1	-1	-1	-1	18.224	24.082	17.3780
a	1	-1	-1	-1	-1	0.943	1.387	0.8710
b	-1	1	-1	-1	-1	12	16.76	10.9648
ab	1	1	-1	-1	-1	1.194	22.71	8.7096
c	-1	-1	1	-1	-1	1.254	NP	1.5136
ac	1	-1	1	-1	-1	0.137	0.138	0.2291
bc	-1	1	1	-1	-1	3.312	7.078	4.5709
abc	1	1	1	-1	-1	0.389	0.629	0.4786
d	-1	-1	-1	1	-1	19.61	21.467	17.3780
ad	1	-1	-1	1	-1	0.337	0.533	0.8710
bd	-1	1	-1	1	-1	11.489	12.531	10.9648
abd	1	1	-1	1	-1	10.809	15.468	8.7096
cd	-1	-1	1	1	-1	1.366	1.867	1.5136
acd	1	-1	1	1	-1	0.212	NP	0.2291
bcd	-1	1	1	1	-1	7.157	8.496	4.5709
abcd	1	1	1	1	-1	0.373	0.578	0.4786
e	-1	-1	-1	-1	1	8.347	11.341	13.8038

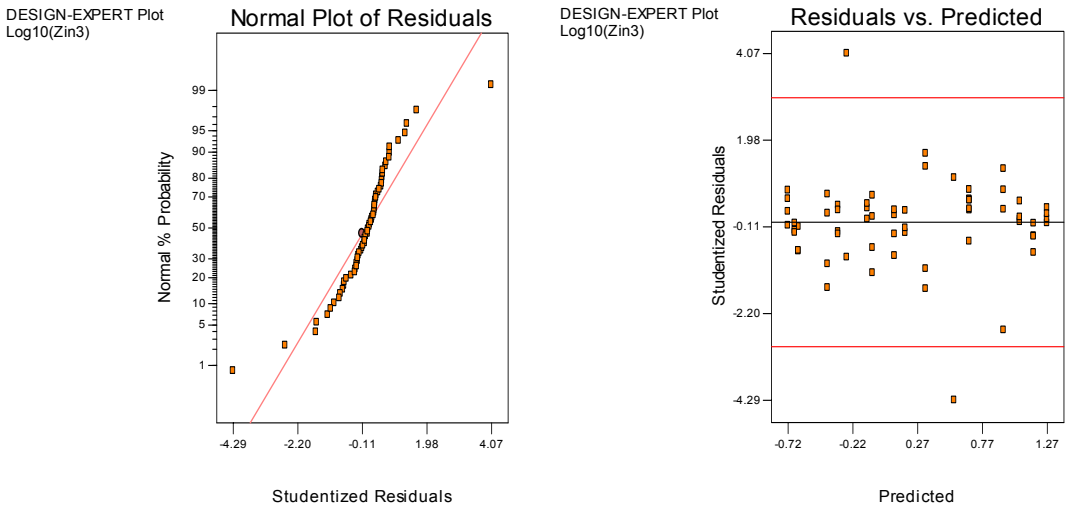

(a) (b)

Figure 4.3.11. Plot of residuals for the Input Impedance at Third Resonance Frequency. (a) Normal plot of residuals. (b) Residuals vs. predicted values

4.3.1.7 Model Optimization

Design Expert has an optimization tool that allows establishing goals in one or more models in order to find the optimum factors to achieve such criteria. The goals were set for the six models expressed by Equations 4.3.1 to 4.3.6. The frequencies 3.7, 5.7 and 8.7 GHz were chosen for the first, second and third resonance respectively. Also, the antenna input impedance at each resonance was set in 1 because it was normalized to 50 Ω. But each input impedance had a different transformation; for instance, the input impedance at first resonance frequency had the inverse transformation, $1/(Z_{in1}+0.02)$, Z_{in1} had to be equal to 1; consequently the transformation was set in 0.98. This applies for the other transformations. The goals are shown in Table 4.3.13. After the goals were set the program calculated 19 solutions. These solutions are shown in Table 4.3.14.

Table 4.3.13. Constraints for the Responses

Name	Goal	Lower limit	Upper limit
ε_r	Is in a range	3	6.15
W	Is in a range	0.25 mm	1 mm
L_1	Is in a range	41.54 mm	87.62
W_s	Is in a range	1 mm	2 mm
L_s	Is in a range	2 mm	4 mm
1^{st} F_r	Is target=3.7 GHz	2.216 GHz	4.583 GHz
$1/(Z_{in1}+0.02)$	Is target= 0.98	0.588	59.38
2^{nd} F_r	Is target=5.7 GHz	4.269 GHz	8.249 GHz
$1/\sqrt{(Z_{in2}+0.32)}$	Is target=0.87	0.176	1.769
3^{rd} F_r	8.7 GHz	7.186 GHz	9.875 GHz
$Log_{10}(Z_{in3})$	0	-0.936	1.382

Table 4.3.14. Solutions for the Optimization

ε_r	W [mm]	L_1 [mm]	W_s [mm]	L_s [mm]	1^{st} F_r [GHz]	$1/(Z_{in1}+0.02)$	2^{nd} F_r [GHz]	$1/\sqrt{(Z_{in2}+0.32)}$	3^{rd} F_r [GHz]	$Log_{10}(Z_{in3})$
3	0.64	87.62	1.56	4.00	3.43600	28.354	5.70001	0.873	8.47821	-0.000
3	0.64	87.55	1.56	4.00	3.43116	28.216	5.70002	0.870	8.47446	-0.000
3	0.64	86.92	1.56	4.00	3.43093	28.507	5.70000	0.870	8.46887	0.012
3	0.64	87.62	1.56	3.91	3.45599	29.240	5.70001	0.870	8.47076	0.018
3	0.64	87.59	1.24	3.99	3.42219	25.447	6.12726	0.870	8.47429	-0.000
3	0.47	87.62	1.58	3.74	3.37827	26.566	5.69999	0.795	8.35966	0.000
3	0.63	87.62	1.11	3.60	3.50555	29.086	6.08703	0.870	8.45683	0.085
3	0.64	87.62	1.00	3.83	3.44725	25.287	6.33612	0.870	8.46745	0.034
3	0.63	87.62	1.62	3.47	3.58198	34.603	5.70004	0.870	8.45144	0.112
6.15	0.63	87.59	1.28	4.00	3.36201	32.515	6.06978	0.870	8.45871	-0.171
6.15	0.63	87.62	1.24	4.00	3.35068	31.568	6.12328	0.870	8.45843	-0.171
6.15	0.63	87.56	1.27	4.00	3.35763	32.169	6.09085	0.870	8.45931	-0.172
6.15	0.63	87.62	1.20	3.93	3.36057	31.702	6.15446	0.870	8.48311	-0.183
6.15	0.63	87.29	1.31	4.00	3.36929	33.275	6.03456	0.870	8.46108	-0.174
6.15	0.63	87.62	1.40	4.00	3.39389	35.139	5.91839	0.870	8.45841	-0.171
6.15	0.62	87.62	1.28	4.00	3.35418	32.222	6.06993	0.861	8.43694	-0.158
6.15	0.63	87.62	1.03	3.78	3.36218	30.672	6.27631	0.870	8.53295	-0.206
6.15	0.63	87.62	1.51	4.00	3.42543	37.746	5.76886	0.870	8.45845	-0.171
6.15	0.50	87.62	1.94	3.13	3.65488	48.169	5.69999	0.783	8.51177	-0.233

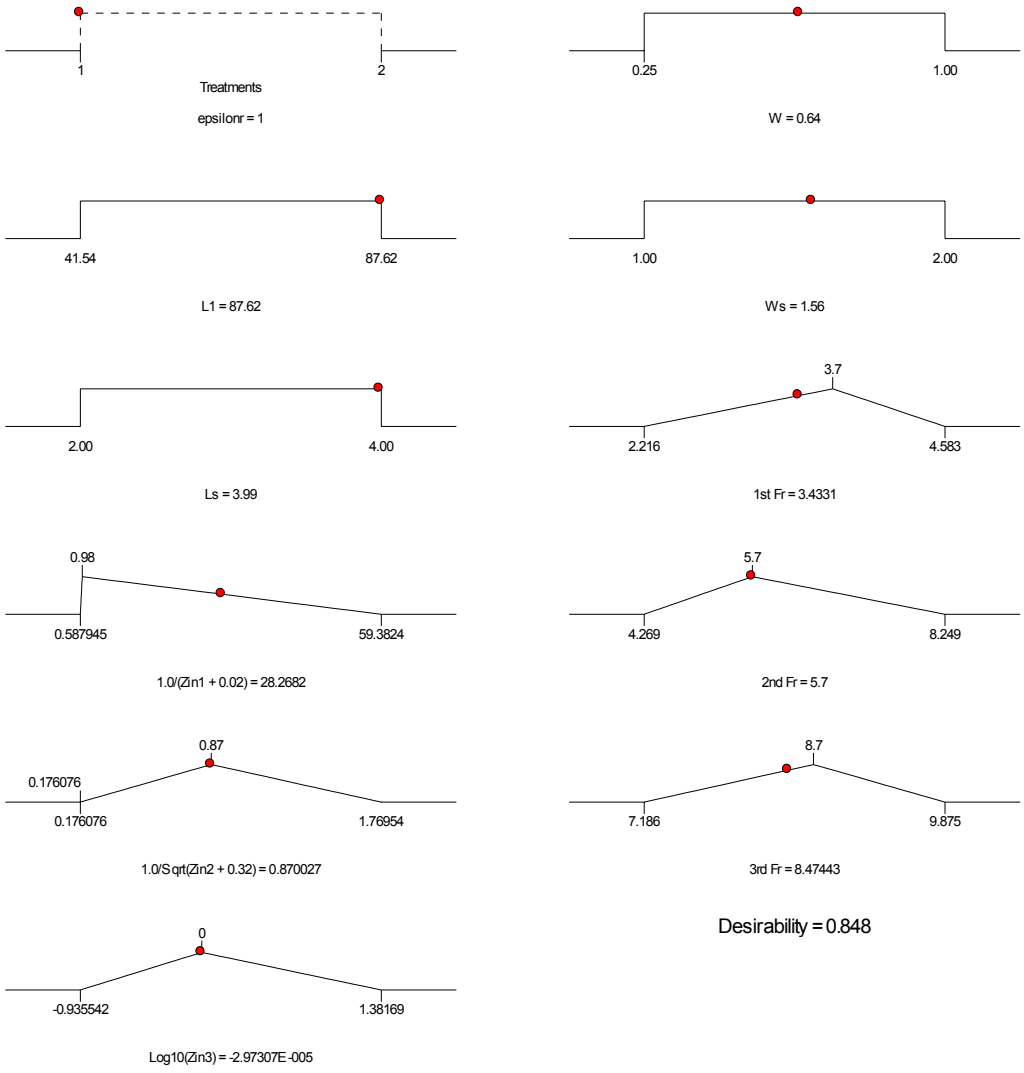

Figure 4.3.12. Graphical Representation of Factors and Responses for the first Row of Table 4.3.14

As an interpretation of the first optimization solution given in the first row of Table 4.3.14, a graphical representation of the constraints values are shown in Figure 4.3.12. In this figure the antenna five factors are shown with their low and high levels. Also, the goals are presented. The values of the input factors and responses calculated by the optimization are represented by the red point on each graph. For some responses such

as 2^{nd} F_r, Z_{in2} and Z_{in3} the goal was achieved. In the other responses it was not possible. This design has a desirability of 0.848. A desirability of 1 is the ideal case.

4.3.2 RSRA with the Parasitic Ring inside the Feeding Antenna

The RSRA Case2 was analyzed using the punctual response approach. The simulation results in Ansoft's Designer and Agilent's Momentum are shown in Table 4.3.15 and Table 4.3.16. As before NP stands for not present and Norm stands for Normalized values to 50 Ω. The first resonance in this case is characterized for a low input impedance 0 Ω. The second resonance oscillated between 4 and 6 GHz; its input impedance varied between 0 and 15.24, some designs presented good matching to 50 Ω. The third resonance varied between 7.66 and 9.95 GHz and its input impedance varied between 0 and 74.27. The design summary is shown in Table 4.3.17. The responses were statistically analyzed in each of the following sections.

Table 4.3.15. First and Second Replicate. Designer and Momentum Results

Design	1st Fr [GHz] Designer	1st Fr [GHz] Momentum	Zin_1 (Norm) Designer	Zin_1 (Norm) Momentum	2nd Fr [GHz] Designer	2nd Fr [GHz] Momentum	Zin_2 (Norm) Designer	Zin_2 (Norm) Momentum
1	3.652	4.042	0	0	4.336	4.339	4.4	6.6
a	3.809	3.961	0	0	4.786	4.823	0.744	0.958
b	3.841	4.456	0	0	5.538	5.58	2.278	2.549
ab	3.881	4.208	0	0	4.746	4.819	1.679	1.852
c	3.904	3.25	0	0	5.066	5.111	1.766	0.719
ac	3.67	3.797	0	0	4.024	4.034	2.354	2.792
bc	3.971	4.563	0	0	NP	NP	NP	NP
abc	3.958	4.281	0	0	NP	NP	NP	NP
d	3.665	4.098	0	0	5.282	5.313	2.117	2.693
ad	3.611	3.766	0	0	4.35	4.378	2.21	2.809
bd	3.845	4.492	0	0	NP	NP	NP	NP
abd	3.913	4.25	0	0	NP	NP	NP	NP
cd	3.827	4.292	0	0	5.291	5.266	0.591	1
acd	3.688	3.847	0	0	4.242	4.263	1.729	2.051
bcd	3.958	4.586	0	0	NP	NP	NP	NP
abcd	3.967	4.305	0	0	NP	NP	NP	NP
e	3.251	3.578	0	0	5.372	5.438	2.181	2.657
ae	3.013	3.125	0	0	4.521	4.563	2.831	3.618
be	3.517	4	0	0	5.313	5.383	4.728	5.283
abe	3.445	3.672	0	0	4.548	4.638	4.896	5.63
ce	3.584	3.875	0	0	5.178	5.25	0.138	0.124
ace	3.247	3.375	0	0	4.174	4.222	0	0
bce	3.975	2.111	0	0	5.375	5.453	2.542	0.952
abce	3.598	3.813	0	0	4.48	4.532	2.695	2.941
de	3.26	3.578	0	0	5.48	5.617	0	0
ade	3	3.188	0	0	4.152	4.188	6.49	8.545
bde	3.535	4	0	0	5.867	6.089	1.963	1.851
abde	3.472	3.719	0	0	5.435	5.594	0.245	0.302
cde	2.095	2.096	0	0	5.342	5.444	0.257	0.236
acde	3.265	3.344	0	0	4.142	4.167	6	7.377
bcde	3.816	4.281	0	0	NP	NP	NP	NP
abcde	3.615	3.859	0	0	4.684	4.764	1.921	1.866
Centerpoint	3.043	3.07	0	0	NP	NP	NP	NP
Centerpoint	2.825	2.469	0	0	5.543	5.681	15.241	10.291

Table 4.3.16. First and Second Replicate. Designer and Momentum Results

Design	3rd Fr [GHz] Designer	3rd Fr [GHz] Momentum	Zin_3 (Norm) Designer	Zin_3 (Norm) Momentum
1	8.316	8.719	31	47.314
a	8.456	8.531	0.159	0.245
b	8.69	9.292	17.388	26.643
ab	9.712	9.948	0.427	0.905
c	7.825	7.764	0.72	0.624
ac	8.492	8.545	0.872	1
bc	8.456	8.438	1.616	3.206
abc	9.235	9.313	2.722	2.797
d	8.321	8.729	29.428	42
ad	8.64	8.734	0.22	0.345
bd	8.699	9.271	27	41
abd	8.24	8.531	60	74.272
cd	7.893	7.656	0.81	7.155
acd	8.24	8.311	0.1	0.168
bcd	8.613	8.539	1.759	3.659
abcd	8.316	8.938	36.939	10.528
e	7.825	8.167	15.979	17.778
ae	9.163	9.25	12.756	13.941
be	8.397	8.813	7.821	9.782
abe	8.924	9.188	0.121	0.193
ce	7.686	7.813	0.305	0.39
ace	8.411	8.484	0.429	0.518
bce	8.287	8.289	0.966	2.052
abce	8.64	8.854	0.136	0.223
de	9.568	8.125	0	17.243
ade	8.253	8.398	0	0.104
bde	8.397	8.875	9.5	11.22
abde	9.023	9.281	0.136	0.218
cde	7.76	7.91	0.334	0.451
acde	8.628	8.693	4.912	5.56
bcde	8.335	8.547	0.585	0.917
abcde	7.927	8.099	8.136	10.104
Centerpoint	8.606	8.979	18.074	27.866
Centerpoint	8.278	8.635	0.142	0.191

Table 4.3.17 RSRA Case 2 Design Summary

Response	Name	Units	Obs	Minimum	Maximum
Y1	1^{st} Fr	GHz	68	2.10	4.59
Y2	Zin_1	Normalized	68	0	0
Y3	2^{nd} Fr	GHz	52	4.02	6.09
Y4	Zin_2	Normalized	52	0	15.24
Y5	3^{rd} Fr	GHz	68	7.66	9.95
Y6	Zin_3	Normalized	68	0	74.27

4.3.2.1 First Resonance Frequency

The analysis of variance and residuals for first Resonance (1^{st}Fr) was performed. The significant effects are shown in the normal probability plot in Figure 4.3.13. The ANOVA is shown in Table 4.3.18. The significant terms are B and E. The curvature is significant, this means that the second order model should be more appropriated but it is not possible to calculate such model because of lack of axial points. The lack of fit is not significant. The model is expressed by Equation 4.3.7.

$$1^{st} F_r = 3.70 + 0.21B - 0.28E \tag{4.3.7}$$

It is reasonable that factor B (W) influences the model positively because in Section 4.1.2.2 it was concluded that this factor shifted the resonance frequencies to higher frequencies; therefore the model validates this conclusion. Also, factor E or L_s that shifted the resonances frequencies to lower frequencies has negative impact in Equation 4.3.7. The results obtained from the simulations and the results predicted by the regression model are shown in Table 4.3.19. Even though the model of Equation 4.3.7 is very simple the predicted values follow the simulated results. The residuals are shown in Figure 4.3.14 (a) and (b). The precency of two unusual observations give us reasons to suspect of the model. These observations are the resonance frequency of 2.111 and 2.095 GHz. From experience it is known that they are valid observations of the resonance

frequency and should be kept in the analysis. These responses correspond to the experimental coditions *bce* and *cde* respectively.

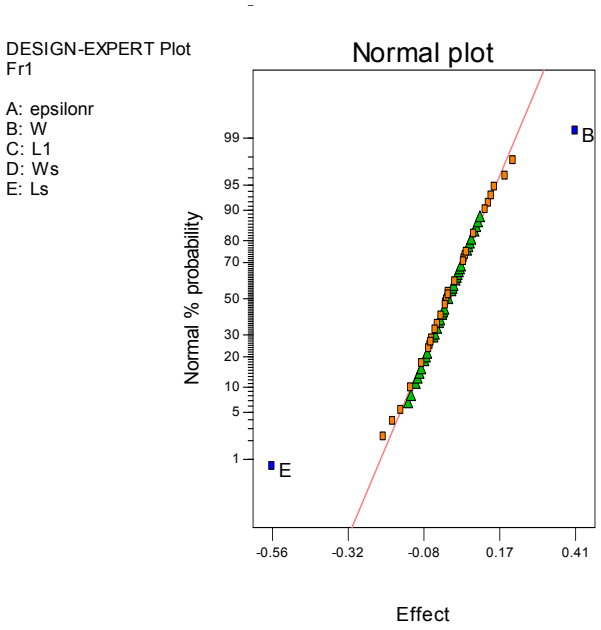

Figure 4.3.13. Normal Probability plot of the effects for the First Resonance Frequency

Table 4.3.18. ANOVA for the First Resonance Frequency

Source	Sum of Squares	DF	Mean Square	F value	Prob>F	
Model	7.79	2	3.9	27.69	< 0.0001	Significant
B	2.7	1	2.7	19.20	< 0.0001	Significant
E	5.09	1	5.09	36.18	< 0.0001	Significant
Curvature	2.69	1	2.69	19.15	< 0.0001	Significant
Residual	9.01	64	0.14			
Lack of Fit	4.91	30	0.16	1.36	0.1915	Not significant
Pure Error	4.09	34	0.12			
Cor Total	19.49	67				

Table 4.3.19. Values for the First Resonant Frequency simulated in Designer and Momentum and the Resonat Frequency obtained from the Model. Only some design are shown.

Design	A	B	C	D	E	Fr (GHz) Designer	Fr (GHz) Momentum	Frmodel(GHz)
(1)	-1	-1	-1	-1	-1	3.652	4.042	3.7700
a	1	-1	-1	-1	-1	3.809	3.961	3.7700
b	-1	1	-1	-1	-1	3.841	4.456	4.1900
ab	1	1	-1	-1	-1	3.881	4.208	4.1900
c	-1	-1	1	-1	-1	3.904	3.25	3.7700
ac	1	-1	1	-1	-1	3.67	3.797	3.7700
bc	-1	1	1	-1	-1	3.971	4.563	4.1900
abc	1	1	1	-1	-1	3.958	4.281	4.1900
d	-1	-1	-1	1	-1	3.665	4.098	3.7700
ad	1	-1	-1	1	-1	3.611	3.766	3.7700
bd	-1	1	-1	1	-1	3.845	4.492	4.1900
abd	1	1	-1	1	-1	3.913	4.25	4.1900
cd	-1	-1	1	1	-1	3.827	4.292	3.7700
acd	1	-1	1	1	-1	3.688	3.847	3.7700
bcd	-1	1	1	1	-1	3.958	4.586	4.1900
abcd	1	1	1	1	-1	3.967	4.305	4.1900
e	-1	-1	-1	-1	1	3.251	3.578	3.2100

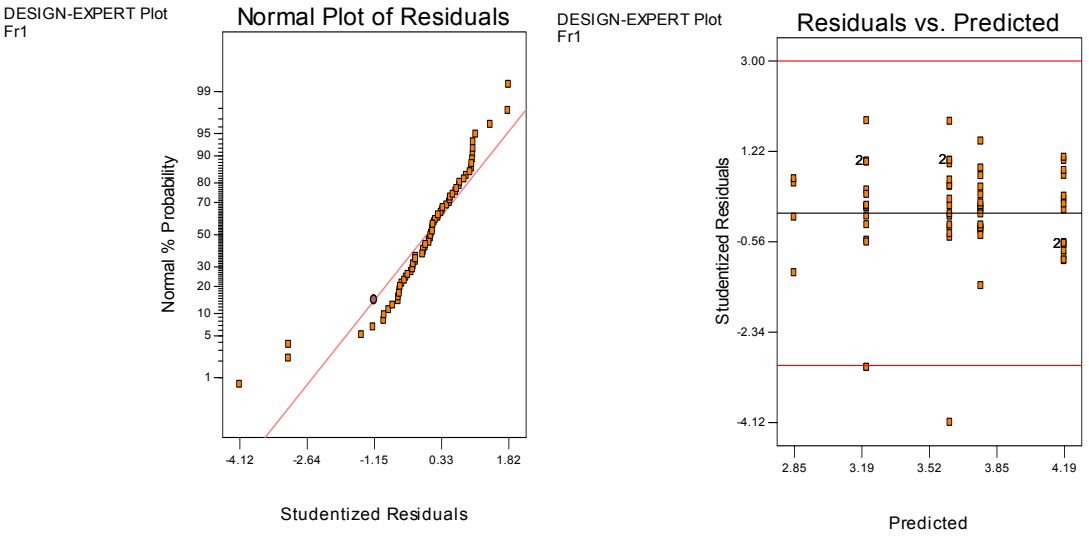

(a) (b)

Figure 4.3.14. Plot of residuals for the First Resonance Frequency. (a) Normal plot of residuals. (b) Residuals vs. predicted values

4.3.2.2 Input impedance at First Resonance Frequency

As it is shown in Table 4.3.15 and 4.3.16, all the observations in both replicates for the input impedance at first resonance frequency were cero or approximately cero. It has no sense to calculate a model to predict these observations. The response is always cero despite the factors levels.

4.3.2.3 Second Resonance Frequency

The significant effects for this response are shown in the normal probability plot in Figure 4.3.15. The ANOVA is shown in Table 4.3.20. The significant terms are A and B. The curvature is significant and the lack of fit is significant. It was not possible to make the lack of fit not significant adding interactions to the model consequently this model should not be use to predict the response. Also the second order model should be the appropriate; it was not possible to calculate it because of the lack of axial points. The model is expressed by Equation 4.3.8.

$$2^{nd} F_r = 4.98 - 0.40A + 0.22B \tag{4.3.8}$$

The fact that factor A influences the model negatively and B influences it positively agrees the intuitive analysis in Section 4.1.2.1 and Section 4.1.2.2 respectively. The residuals follow the ANOVA assumptions and are shown in Figure 4.3.16.

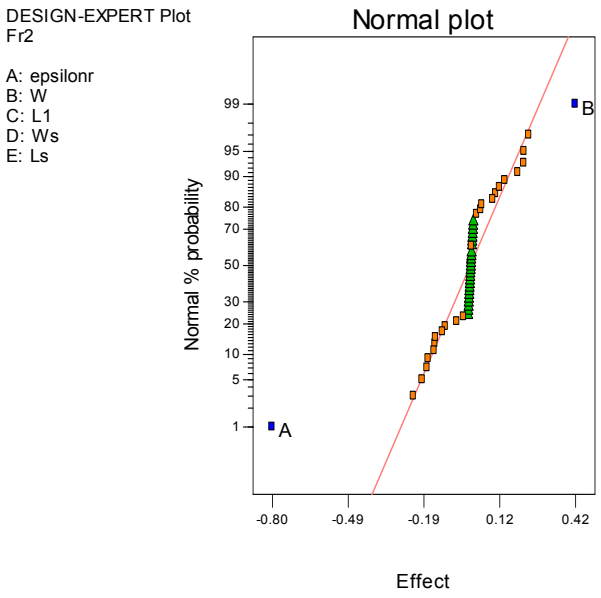

Figure 4.3.15. Normal Probability plot of the effects for the Second Resonance Frequency

Table 4.3.20. ANOVA for the Second Resonance Frequency

Source	Sum of Squares	DF	Mean Square	F value	Prob>F	
Model	10.30	2	5.15	47.75	<0.0001	Significant
A	8.22	1	8.22	76.26	<0.0001	Significant
B	2.30	1	2.30	21.31	<0.0001	Significant
Curvature	0.77	1	0.77	7.14	0.0103	Significant
Residual	5.17	48	0.11			
Lack of Fit	5.09	23	0.22	68.84	<0.0001	Significant
Pure Error	0.080	25	3.217E-3			
Cor Total	16.24	51				

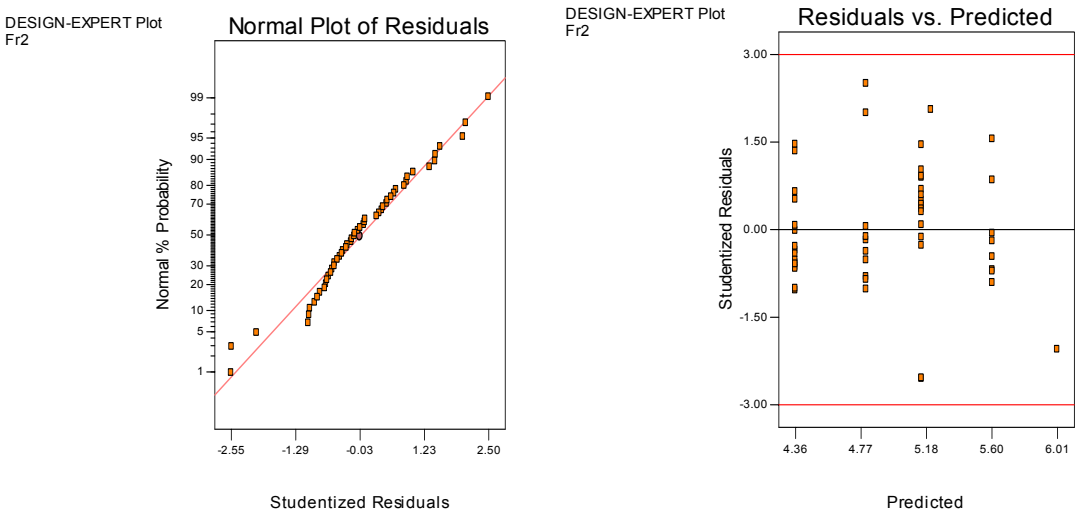

(a) (b)

Figure 4.3.16. Plot of residuals for Second Resonance Frequency. (a) Normal plot of residuals. (b) Residuals vs. predicted values

4.3.2.4 Input Impedance at Second Resonance Frequency

The significant factors for this response are shown in the normal probability plot in Figure 4.3.17. The ANOVA is shown in Table 4.3.21. The significant terms are AE and BD. The curvature and the lack of fit are significant. The curvature tells us that the second order model is more appropriated. It can not be calculated because of the lack of axial points in the DOE. It was not possible to make the lack of fit not significant adding interactions to the model; therefore, this model should not be use to predict the response. The model is expressed by Equation 4.3.9.

$$\sqrt{Z_{in2}+0.15} = 1.44 + 0.19AE - 0.18BD \tag{4.3.9}$$

The residuals follow the ANOVA assumptions and are shown in Figure 4.3.18.

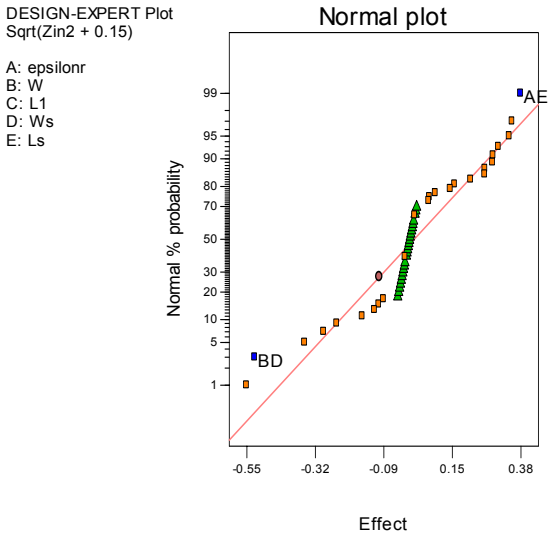

Figure 4.3.17. Normal Probability plot of the effects for the Input Impedance at Second Resonance Frequency

Table 4.3.21. ANOVA for the Input Impedance at Second Resonance Frequency

Source	Sum of Squares	DF	Mean Square	F value	Prob>F	
Model	3.09	2	1.55	3.94	0.0260	Significant
AE	1.89	1	1.89	4.81	0.0331	Significant
BD	1.59	1	1.59	4.05	0.0497	Significant
Curvature	8.79	1	8.79	22.41	<0.0001	Significant
Residual	18.82	48	0.39			
Lack of Fit	18.19	23	0.79	31.44	<0.0001	Significant
Pure Error	0.63	25	0.025			
Cor Total	30.69	51				

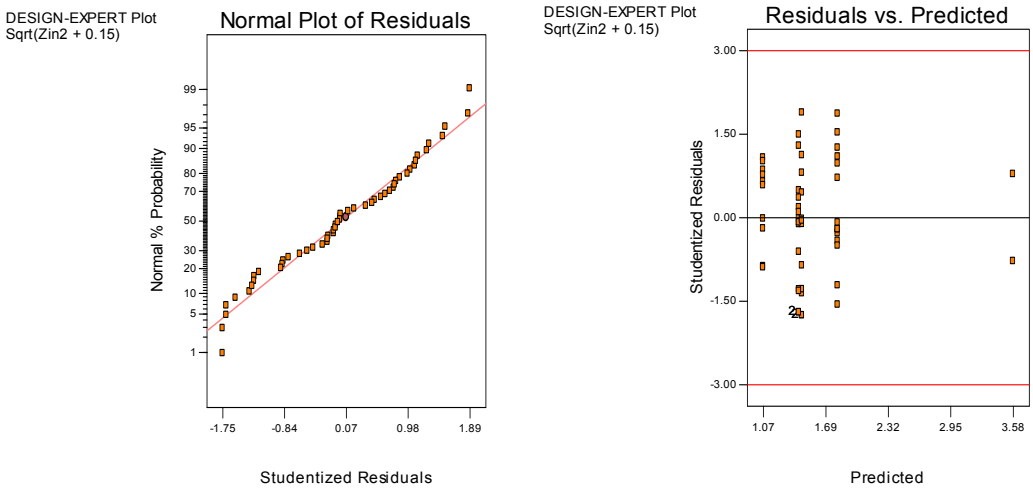

(a) (b)

Figure 4.3.18. Plot of residuals for the Input Impedance at Second Resonance Frequency. (a) Normal plot of residuals. (b) Residuals vs. predicted values

4.3.2.5 Third Resonance Frequency

The significant factors for this response are shown in the normal probability plot in Figure 4.3.19. The ANOVA is shown in Table 4.3.22. The significant terms are A, B, C, AD, BD, BE, ABDE, ABCDE. The curvature and lack of fit are not significant. The model is expressed by Equation 4.3.10.

$$3^{rd}F_r = 8.55 + 0.18A + 0.20B - 0.21C - 0.15AD - 0.082BD - 0.083BE + 0.092ABDE - 0.12ABCDE \quad (4.3.10)$$

The results obtained from the simulations and the results predicted by the regression model are shown in Table 4.3.23. Agreement between the simulated and model values is observed. The residuals follow the ANOVA assumptions and are shown in Figure 4.3.20.

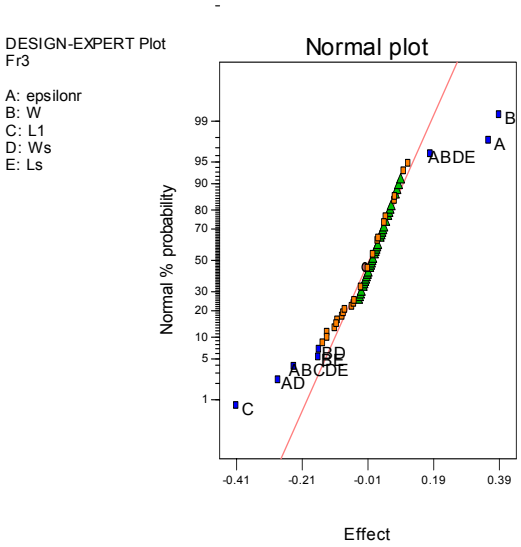

Figure 4.3.19. Normal Probability plot of the effects for the Third Resonance Frequency

Table 4.3.22. ANOVA for the Third Resonance Frequency

Source	Sum of Squares	DF	Mean Square	F value	Prob>F	
Model	11.31	8	1.41	16.02	<0.0001	Significant
A	2.16	1	2.16	24.44	<0.0001	Significant
B	2.56	1	2.56	29.00	<0.0001	Significant
C	2.86	1	2.86	32.44	<0.0001	Significant
AD	1.37	1	1.37	15.49	0.0002	Significant
BD	0.43	1	0.43	4.89	0.0309	Significant
BE	0.44	1	0.44	5.00	0.0292	Significant
ABDE	0.55	1	0.55	6.20	0.0157	Significant
ABCDE	0.94	1	0.94	10.67	0.0018	Significant
Curvature	0.019	1	0.019	0.22	0.6438	Not significant
Residual	5.12	58	0.088			
Lack of Fit	2.72	24	0.11	1.61	0.1006	Not significant
Pure Error	2.40	34	0.071			
Cor Total	16.45	67				

Table 4.3.23. Values for the Third Resonant Frequency simulated in Designer and Momentum and the Resonat Frequency obtained from the Model. Only some design are shown.

Design	A	B	C	D	E	Fr (GHz) Designer	Fr (GHz) Momentum	Frmodel(GHz)
(1)	-1	-1	-1	-1	-1	8.316	8.719	8.0930
a	1	-1	-1	-1	-1	8.456	8.531	8.5130
b	-1	1	-1	-1	-1	8.69	9.292	8.7670
ab	1	1	-1	-1	-1	9.712	9.948	9.6670
c	-1	-1	1	-1	-1	7.825	7.764	7.4330
ac	1	-1	1	-1	-1	8.492	8.545	8.3330
bc	-1	1	1	-1	-1	8.456	8.438	8.5870
abc	1	1	1	-1	-1	9.235	9.313	9.0070
d	-1	-1	-1	1	-1	8.321	8.729	8.5010
ad	1	-1	-1	1	-1	8.64	8.734	8.8010
bd	-1	1	-1	1	-1	8.699	9.271	8.9590
abd	1	1	-1	1	-1	8.24	8.531	8.7790
cd	-1	-1	1	1	-1	7.893	7.656	8.3210
acd	1	-1	1	1	-1	8.24	8.311	8.1410
bcd	-1	1	1	1	-1	8.613	8.539	8.2990
abcd	1	1	1	1	-1	8.316	8.938	8.5990
e	-1	-1	-1	-1	1	7.825	8.167	8.2030

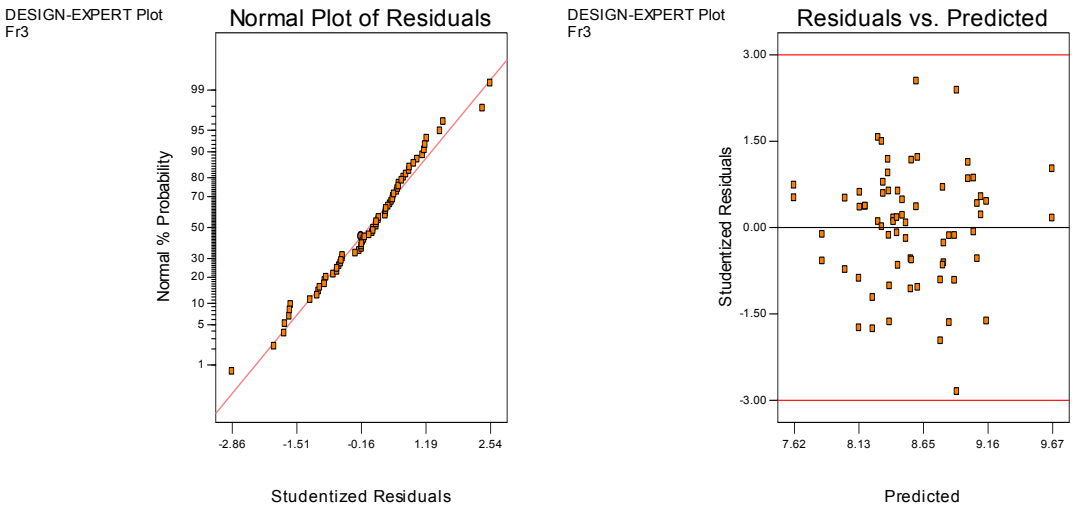

(a) (b)

Figure 4.3.20. Plot of residuals for the Third Resonance Frequency. (a) Normal plot of residuals. (b) Residuals vs. predicted values

4.3.2.6 Input Impedance at Third Resonance Frequency

The significant factors for this response are shown in the normal probability plot in Figure 4.3.21. The ANOVA is shown in Table 4.3.24. The significant terms are A, B, C, E, AC, BD, BE, DE, ABD, ABE, BCD, CDE, ACDE. The curvature and lack of fit are not significant. The model is expressed by Equation 4.3.11.

$$\log_{10}(Z_{in3}+0.74) = 0.59 - 0.16A + 0.10B - 0.21C - 0.14E + 0.26AC + 0.15BD - 0.13BE - 0.096DE + 0.12ABD - 0.17ABE - 0.095BCD + 0.14CDE + 0.13ACDE \quad (4.3.11)$$

The results obtained from the simulations and the results predicted by the regression model are shown in Table 4.3.25. Agreement between the simulated and model values is observed. Even though the residuals follow the ANOVA assumptions one outlier is presented. This outlier is the observation 66 that corresponds to the input impedance of 27.866 (normalized to 50 Ω). From experience it is known that this response is a validate observation of the antenna input impedance and should be kept in the analysis. These plots are shown in Figure 4.3.22.

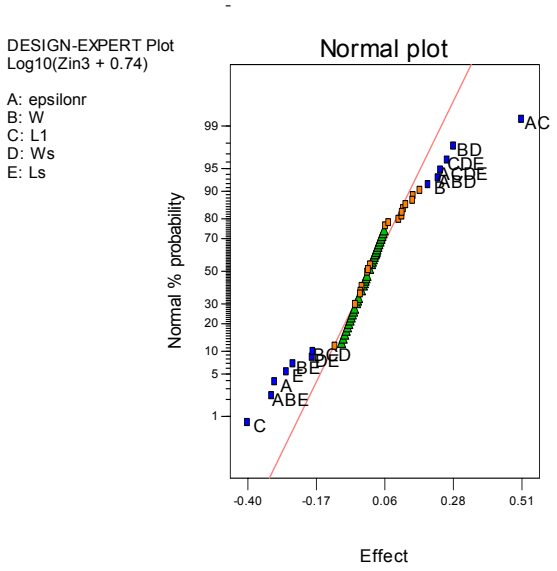

Figure 4.3.21. Normal Probability plot of the effects for the Input Resistance at Third Resonance Frequency

Table 4.3.24. ANOVA for the Input Resistance at Third Resonance Frequency

Source	Sum of Squares	DF	Mean Square	F value	Prob>F	
Model	19.36	13	1.49	12.08	<0.0001	Significant
A	1.65	1	1.65	13.37	0.0006	Significant
B	0.69	1	0.69	5.59	0.0218	Significant
C	2.75	1	2.75	22.31	<0.0001	Significant
E	1.26	1	1.26	10.25	0.0023	Significant
AC	4.49	1	4.49	36.43	<0.0001	Significant
BD	1.40	1	1.40	11.33	0.0014	Significant
BE	1.06	1	1.06	8.63	0.0049	Significant
DE	0.59	1	0.59	4.80	0.0330	Significant
ABD	0.94	1	0.94	7.60	0.0080	Significant
ABE	1.76	1	1.76	14.26	0.0004	Significant
BCD	0.58	1	0.58	4.67	0.0352	Significant
CDE	1.20	1	1.20	9.71	0.0030	Significant
ACDE	1.01	1	1.01	8.16	0.0061	Significant
Curvature	0.019	1	0.019	0.15	0.6977	Not significant
Residual	6.53	53	0.12			
Lack of Fit	3.02	19	0.16	1.54	0.1333	Not significant
Pure Error	3.51	34	0.10			
Cor Total	25.91	67				

Table 4.3.25. Values for the Input Impedance at Third Resonant Frequency simulated in Designer and Momentum and the Resonat Frequency obtained from the Model. Only some design are shown.

Design	A	B	C	D	E	Zin_3 Designer	Zin_3 Momentum	Zin_3 Model
(1)	-1	-1	-1	-1	-1	31	47.314	20.1049
a	1	-1	-1	-1	-1	0.159	0.245	0.5752
b	-1	1	-1	-1	-1	17.388	26.643	14.7125
ab	1	1	-1	-1	-1	0.427	0.905	0.8053
c	-1	-1	1	-1	-1	0.72	0.624	0.8781
ac	1	-1	1	-1	-1	0.872	1	2.9668
bc	-1	1	1	-1	-1	1.616	3.206	2.1374
abc	1	1	1	-1	-1	2.722	2.797	9.7072
d	-1	-1	-1	1	-1	29.428	42	18.3585
ad	1	-1	-1	1	-1	0.22	0.345	0.5813
bd	-1	1	-1	1	-1	27	41	44.0313
abd	1	1	-1	1	-1	60	74.272	44.0313
cd	-1	-1	1	1	-1	0.81	7.155	2.5034
acd	1	-1	1	1	-1	0.1	0.168	0.0030
bcd	-1	1	1	1	-1	1.759	3.659	2.4296
abcd	1	1	1	1	-1	36.939	10.528	9.7554
e	-1	-1	-1	-1	1	15.979	17.778	14.0852

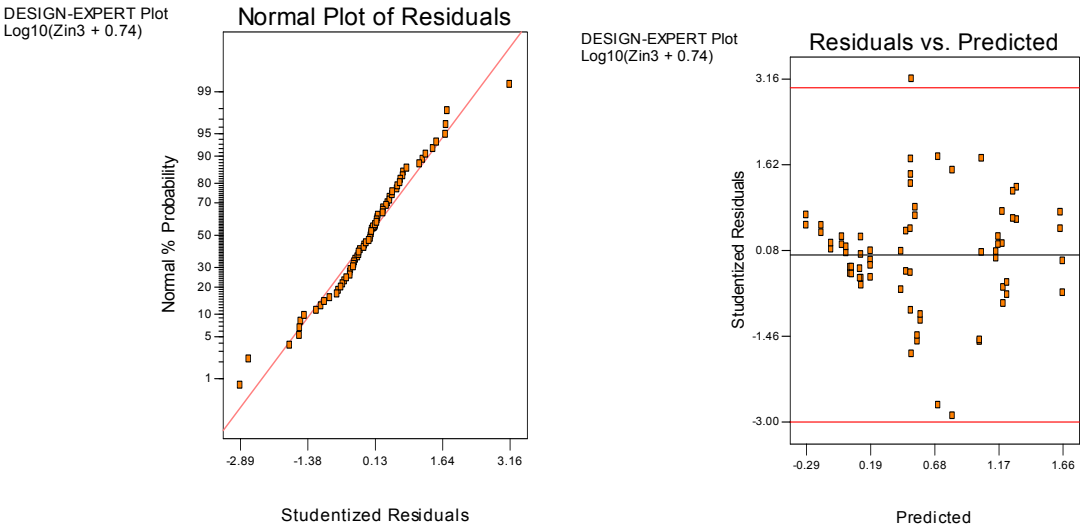

(a) (b)

Figure 4.3.22. Plot of residuals for the Third Resonance Frequency. (a) Normal plot of residuals. (b) Residuals vs. predicted values

4.3.2.7 Model Optimization

The goals were set for the some models expressed by Equations 4.3.7 to 4.3.11. The frequency 5.7 GHz was chosen for the second resonance response. The antenna input impedance at second resonance was set to 1. But this impedance was transformed as $\sqrt{(Z_{in2}+0.15)}$; consequently the transformation was set to 1.0724. Table 4.3.25 summarizes the constraints for the optimization. After the goals were set the program calculated 20 solutions. These solutions are shown in Table 4.3.26.

Table 4.3.26. Constraints for the Responses

Name	Goal	Lower limit	Upper limit
ε_r	Is in a range	3	6.15
W	Is in a range	0.25 mm	1 mm
L_1	Is in a range	41.54 mm	87.62
W_s	Is in a range	1 mm	2 mm
L_s	Is in a range	2 mm	4 mm
2^{nd} F_r	Is target=5.7 GHz	4.024 GHz	6.089 GHz
$\sqrt{(Z_{in2}+0.15)}$	Is target=1.0724	0.390	3.923

Table 4.3.27. Solutions for the Optimization

ε_r	W [mm]	L_1 [mm]	W_s [mm]	L_s [mm]	2^{nd} F_r [GHz]	$\sqrt{(Z_{in2}+0.15)}$	Desirability
3	1.00	61.45	2.00	3.98	5.6004	1.070	0.969831
3	1.00	48.41	1.99	3.99	5.60039	1.070	0.96983
3	1.00	75.40	1.99	4.00	5.60028	1.070	0.969792
3	1.00	41.54	2.00	3.98	5.5997	1.071	0.969414
3	0.99	87.62	2.00	4.00	5.59174	1.073	0.966737
3	1.00	41.55	1.57	4.00	5.6004	1.221	0.943798
3	1.00	86.42	1.55	4.00	5.60039	1.228	0.942531
3	1.00	41.56	1.44	4.00	5.6004	1.268	0.9356
3	1.00	41.55	2.00	2.66	5.6004	1.325	0.925443
3	1.00	42.34	1.13	4.00	5.6004	1.380	0.915689
6.15	1.00	76.96	1.99	2.01	4.80348	1.070	0.68197
6.15	1.00	51.41	1.99	2.01	4.80348	1.070	0.68197
6.15	1.00	50.81	1.99	2.00	4.80348	1.070	0.68197
6.15	1.00	78.42	1.98	2.01	4.80348	1.072	0.681726
6.15	1.00	82.98	2.00	2.02	4.80173	1.070	0.681205
6.15	1.00	41.54	1.98	2.00	4.80224	1.075	0.680857
6.15	1.00	64.78	1.90	2.00	4.80348	1.102	0.678115
6.15	0.98	41.54	2.00	2.27	4.79346	1.126	0.670834

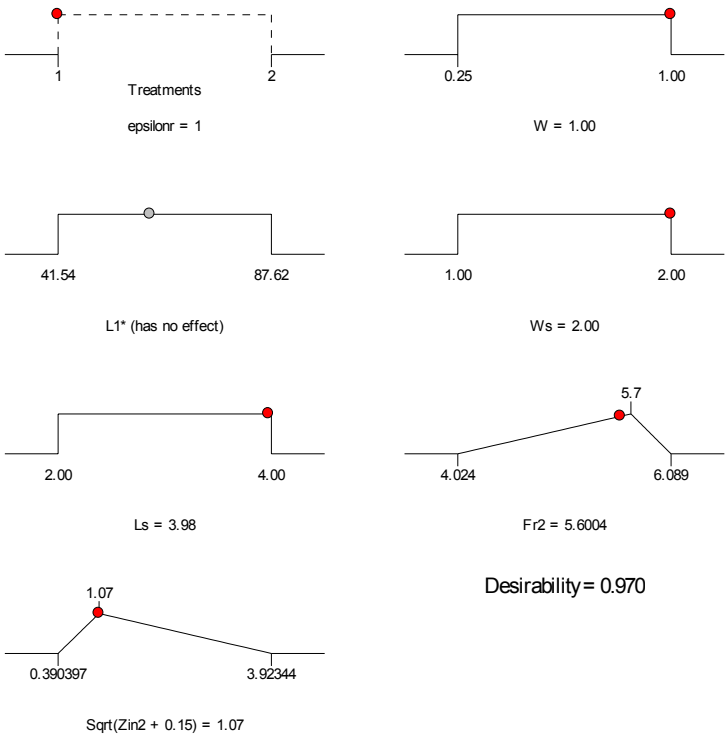

Figure 4.3.23 Graphical Representation of Factors and Responses for the first Row of Table 4.3.26

As an interpretation of the first optimization solution given in the first row of Table 4.3.26, a graphical representation of the constraints values are shown in Figure 4.3.23. In this figure the antenna five factors are shown with their low and high levels. Also, the goals are presented. The values of the input factors and responses calculated by the optimization are represented by the red point on each graph. For Z_{in2} response the goal was achieved. This design has a desirability of 0.97.

4.3.3 Characterization Summary

In Sections 4.1 to 4.3 some techniques to characterize RSRA are described; these techniques are summarized in Figure 4.3.24.

Figure 4.3.24 Characterization Summary

It is possible to apply any approach shown in Figure 4.3.24 to design a RSRA. In fact, a recommended procedure is as follows. First of all, to choose a RSRA case (Case 1 or 2). Second, to set the initial factors A, B, C, D and E. Third, calculate the resonance frequency using the appropriate linear model according to the third approach. From Tables 4.3.1 and 4.3.15 the first, second and third resonance frequency oscillate from 2.1 to 4.5 GHz, 4.6 to 8.1 GHz and 8.2 to 9.9 GHz respectively. Fourth, according to Tables 4.1.2 and 4.1.3, the resonance frequency can be shifted, adjusting ε_r , W and L_1 (or codified factors A, B and C). Consequently, if the desired resonance frequency is not achieved, adjust A, B or C. Fifth, Calculate the antenna input impedance using the appropriate linear model according to third approach. Finally adjust D or E to achieve the

desired input impedance. This procedure is shown in Figure 4.3.25. The natural values of ε_r, W, L_1, W_s and L_s can be calculated using the Equation 3.3.2.

A more sophisticated solution for an antenna design with multiple operation points is to use an optimization software such as Design expert [26]. This procedure is followed in Sections 4.3.1.7 and 4.3.2.7. In addition, the scaling principle can be used in order to design a RSRA in any frequency. This principle states that if all antenna geometries are decreased by a scale factor, the operating frequency will increase by this scale factor. It is recommended to define the antenna dimensions in terms of λ_{eff} or effective wave length as in [22]; after calculating each antenna factor in term of λ_{eff} new linear models can be calculated changing the former factors by the new factors in term or λ_{eff}. The advantage of these new models is that they are independent of the substrate permitivitty.

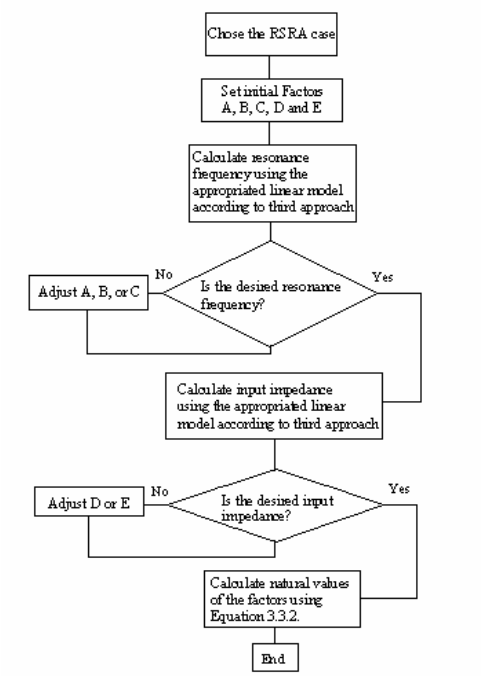

Figure 4.3.25 Flow Chart Design Guide.

4.4 Matching Technique

The equation models deduced in Sections 4.3.1 and 4.3.2 can be used to have a quick initial approach of the antenna resonance frequency and input impedance. In [9] it is suggested some geometric changes in the RSRA to match it at the first or second resonance. In that work the first resonance was matched by feeding the antenna with an inset open circuited CPW stub. The second resonance was matched by increasing the width of the top slot. This technique can be applied in the RSRA under research. In Figure 4.4.1 (a), it is shown a RSRA Case 2 with a new variable W_t that denotes the top slot width. This slot width was varied from 0.25 mm to 1.5 mm; this effect is shown in Figure 4.4.1 (b). According to this plot, if W_t increases a second operation point with a return loss less than -10 dB is achieved.

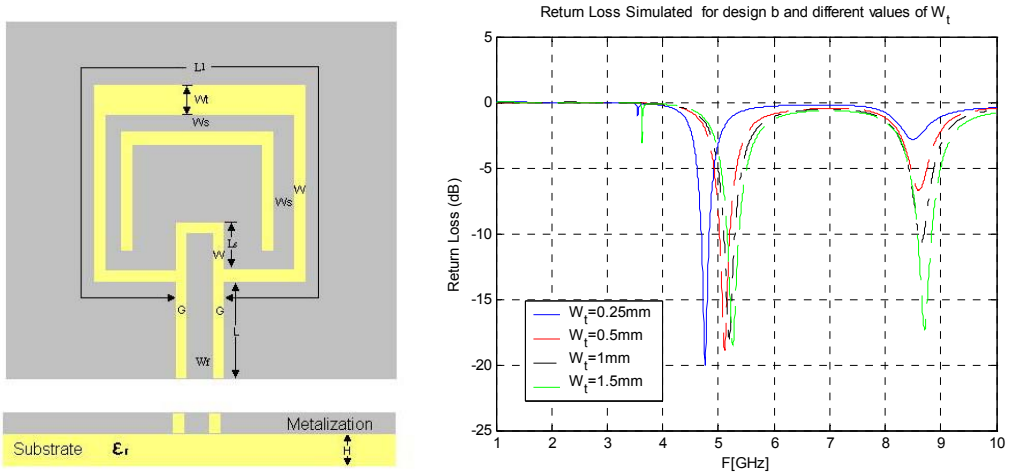

(a) (b)

Figure 4.4.1. (a) RSRA Case 2. (b) Effects of increasing W_t for design b.

4.5 RSRA Case 3

The equation models deduced in Sections 4.3.1 and 4.3.2 can be extended to the RSRA Case 3 that is shown in Figure 3.2.4. In addition this antenna presents some properties that are described in the following sections.

4.5.1 Superposition of Responses

This property is the superposition of the RSRA Case 1 response and RSRA Case 2 response. In Figure 4.5.1 it is shown the Return Loss for the RSRA Case1 with ε_r = 6.15, W = 0.25 mm, L_1 = 41.54 mm, W_s = 1mm and L_s = 2 mm. Also, it is shown the RSRA Case 2 with the same values for ε_r, W, L1, W_s and L_s. The union of these two structures is the RSRA Case 3 with $W_{s1} = W_{s2}$ = 1mm. The Return Loss response for this case is the superposition of both responses.

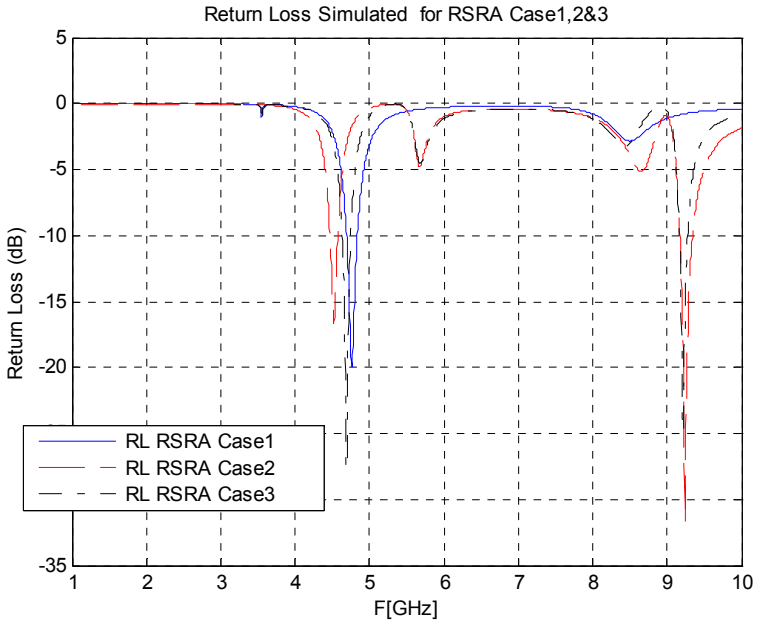

Figure 4.5.1. Illustration of the Superposition Property.

4.5.2 Impedance Scaling Varying W_{s2} in the RSRA Case 3

The effect of varying the distance between the outside parasitic ring and the feeding antenna, W_{s2}, is shown in Figure 4.5.2. The antenna input impedance that was scaled is at the second resonance frequency. The RSRA Case 3 design that presented this behavior is $\varepsilon_r = 3$, W = 0.25 mm, $L_1 = 41.54$ mm, $L_s = 2$ mm and $W_{s1} = 1$mm. W_{s2} was varied from 1 to 3 mm in steps of 1 mm. This effect is analogous to the multiple slot scaling described in [5] and suggests that by adding multiple parasitic rings, it would be possible to scale the antenna input impedance.

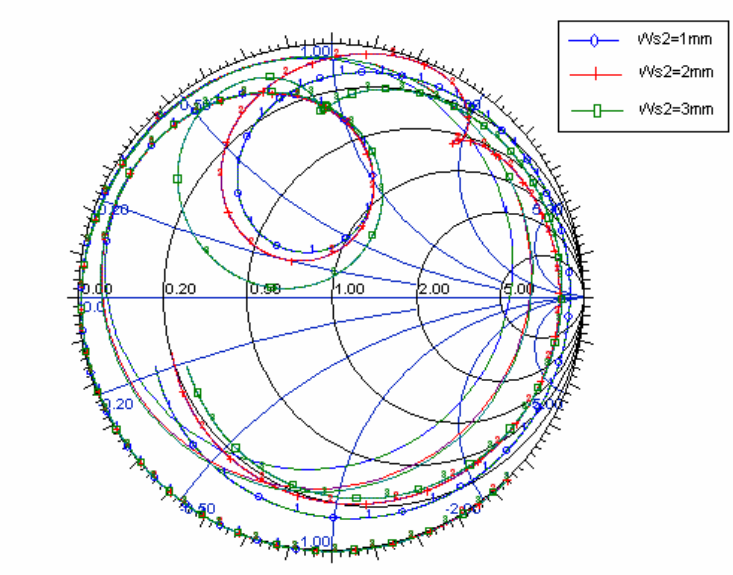

Figure 4.5.2. Impedance Scaling Varying W_{s2} for the RSRA Case 3.

4.5.3 Impedance Scaling Adding Multiple Parasitic Rings in the RSRA Case 3

A similar scaling effect was presented adding multiple parasitic rings. Initially the design had a parasitic ring inside the feeding antenna and its parameters were $\varepsilon_r = 3$, W =

0.25 mm, L_1 = 41.54 mm, L_s = 2 mm and W_s = 1mm. Then, a second exterior ring was added with W_{s2} = 1 mm. In addition, a third exterior ring was added with W_{s2} = 2mm. The three designs results are shown in Figure 4.5.3 (a) and (b).

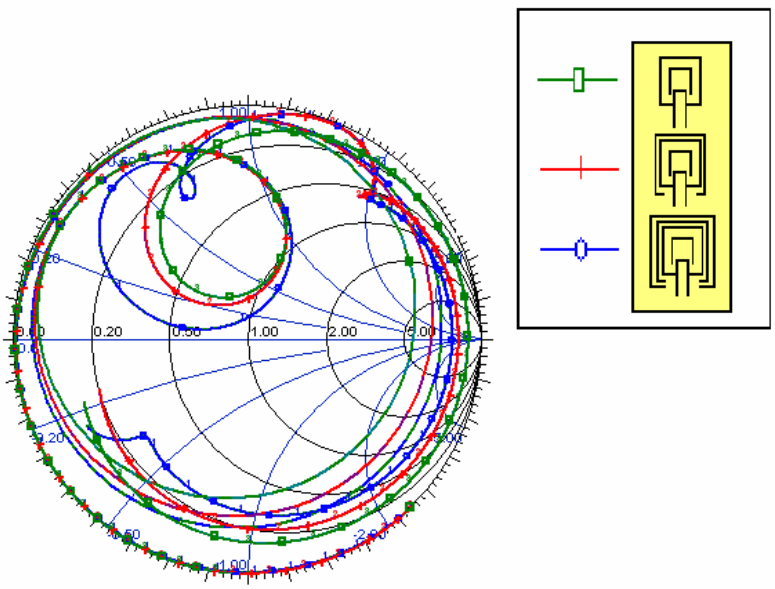

(a)

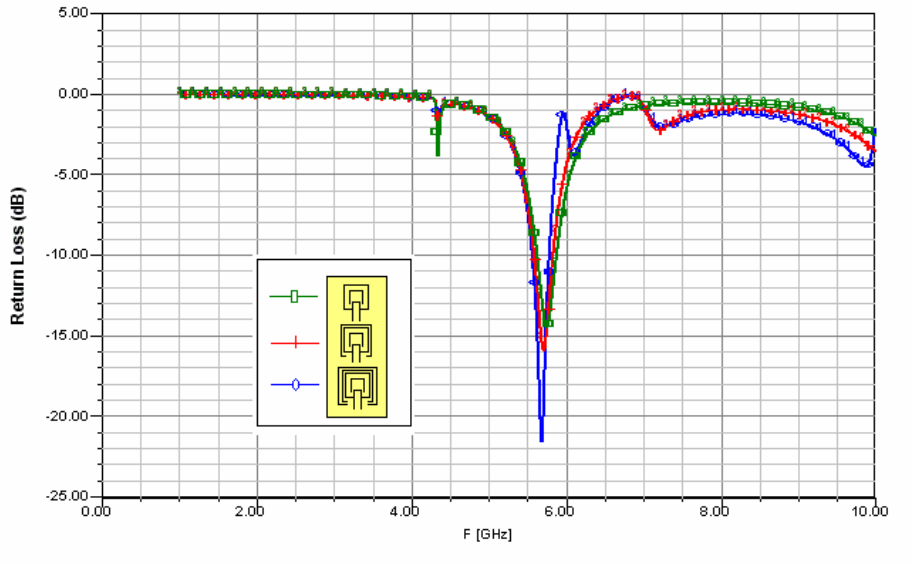

(b)

Figure 4.5.3. Impedance Scaling Adding Multiple Exterior Rings. (a) Smith Chart. (b) Return Loss.

4.6 RSRA Electric Field Distribution, Radiation Pattern and Gain

The electric field distribution, radiation pattern and gain for the RSRA were studied using Ansoft's Designer simulator. Figure 4.6.1 shows the simulated electric field distribution on the substrate side at the resonance frequency of 5.6 GHz. This is the design with the five factors in low level or design *(1)*. According to this figure, the major electric field is along the Y axis, which means that the antenna is linearly polarized.

The radiation pattern in a RSRA is bidirectional as it is shown in Figure 4.6.2. It depends on the antenna operation frequency but this figure is a representative radiation pattern in the frequency range from 1 to 10 GHz. The antenna gain for design *(1)* is about 2.36 dBi at $\theta = 0$ deg.

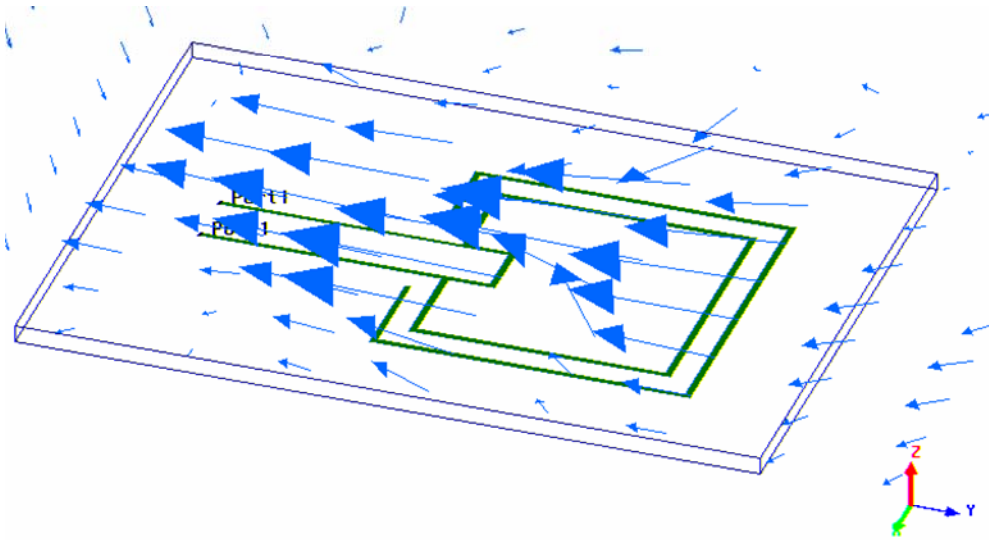

Figure 4.6.1. Electric Field Distribution on the Substrate Side for the RSRA design *(1)* at 5.6 GHz.

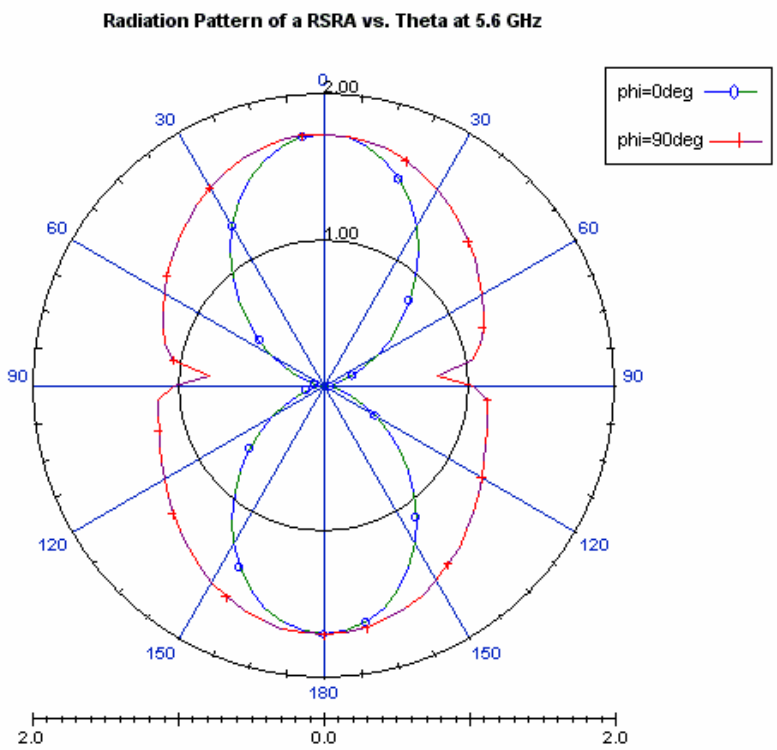

Figure 4.6.2. Radiation Pattern for Design *(1)* at 5.6 GHz. φ =0 deg or xz plane and φ =90 deg or yz plane

Design *(1)* with the parasitic ring inside the feeding antenna was also analyzed. The effect of the parasitic ring in the radiation pattern is shown in Figure 4.6.3. The simulated gain is about 2.22 dBi at 5.6 GHz.

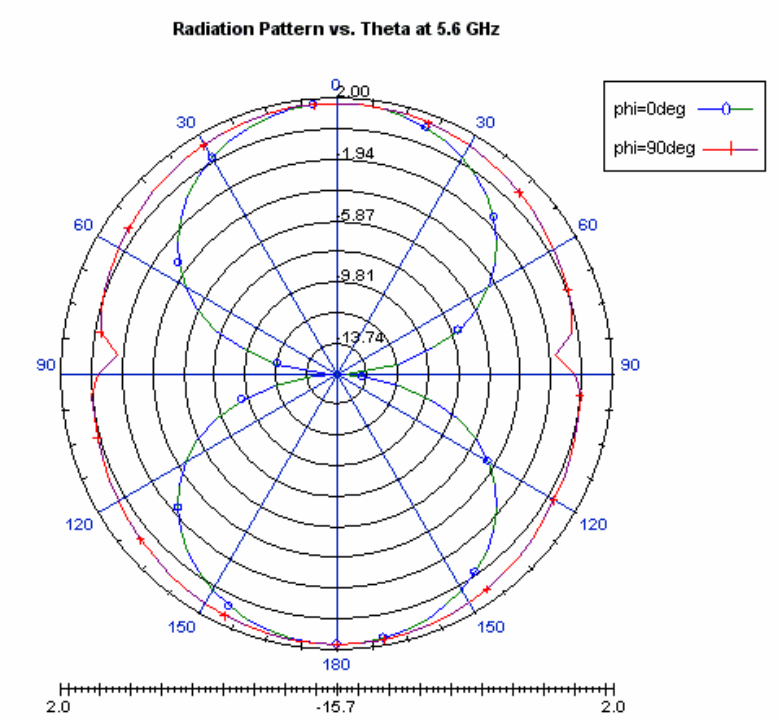

Figure 4.6.3. Radiation Pattern for Design *(1)* (Case 2) at 5.6 GHz. φ =0 deg or xz plane and φ =90 deg or yz plane

Finally, the radiation pattern and gain for the RSRA Case 3 is very similar to Case 1 and Case 2 at the frequency of 5.6 GHz. The radiation pattern is shown in Figure 4.6.4 and the simulated gain is about 2 dBi at θ = 0 deg.

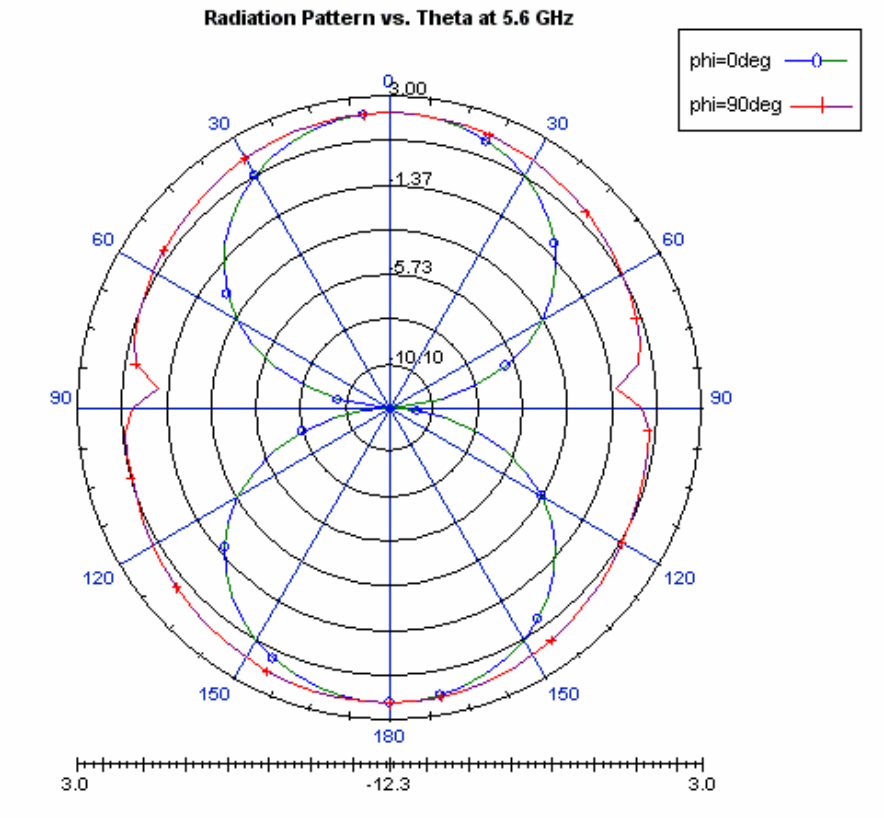

Figure 4.6.4. Radiation Pattern for Design *(1)* (Case 3) at 5.6 GHz. φ =0 deg or xz plane and φ =90 deg or yz plane

4.7 Antenna Testing

In order to validate the simulation results some antennas were fabricated using a milling machine. The Return Loss measurements were performed with the Agilent 8719ES s-parameter network analyzer. Both RSRA Case 1 and Case 2 were testing and the comparison between simulations and measurements are shown in Figure 4.7.1 and 4.7.2. Reasonable agreement between the simulations and the measured Return Loss is observed.

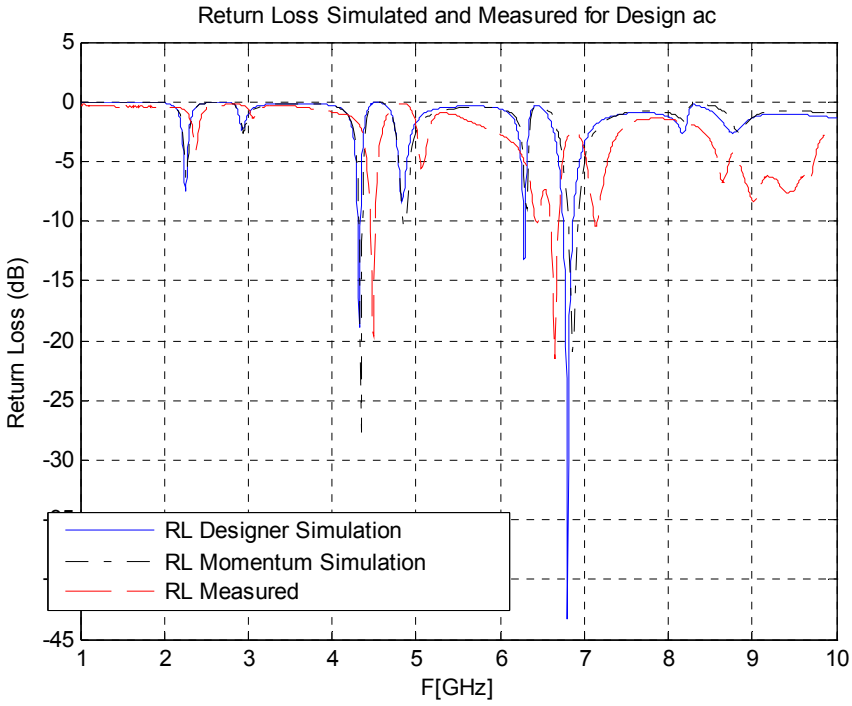

(a)

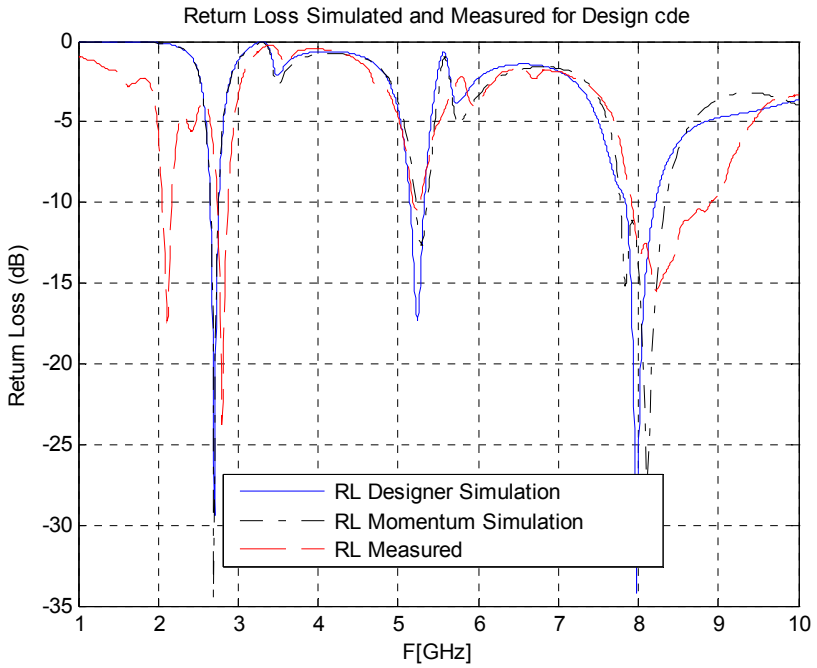

(b)

Figure 4.7.1. Simulated and measured Return Loss for the RSRA Case 1. (a) Design ac. (b) Design cde. (c) Design (1).

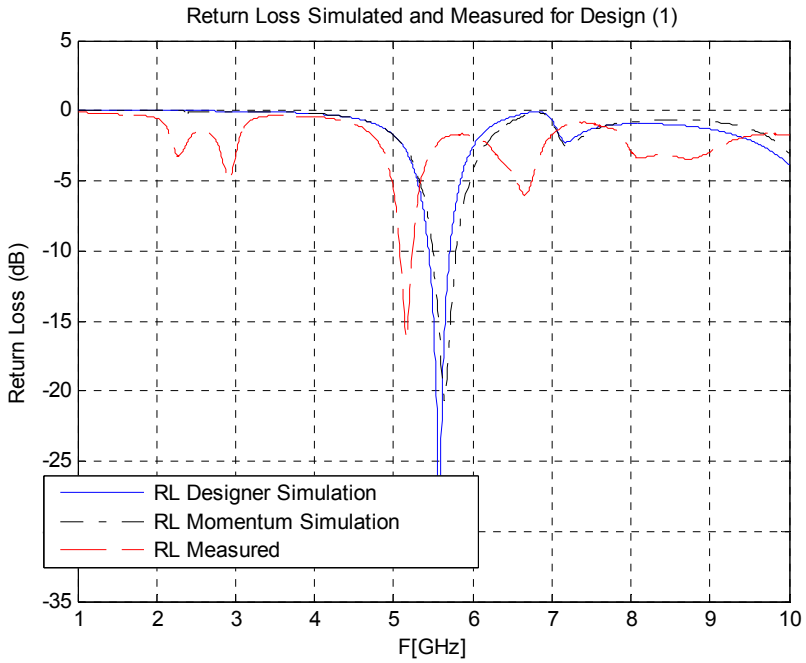

(c)

Figure 4.7.1. Continued

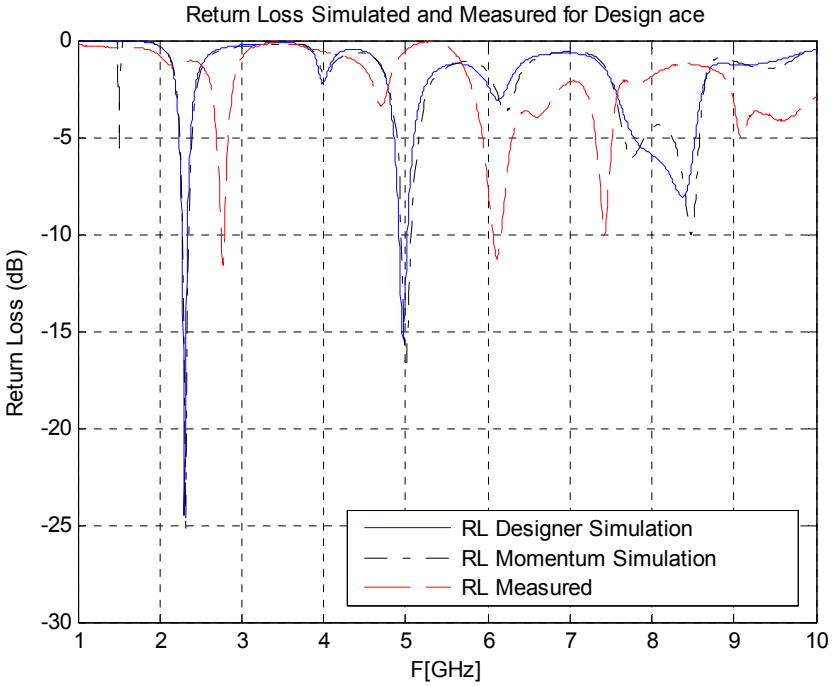

(a)

Figure 4.7.2. Simulated and measured Return Loss for the RSRA Case 2. (a) Design ace. (b) Design cd. (c) Design bcde

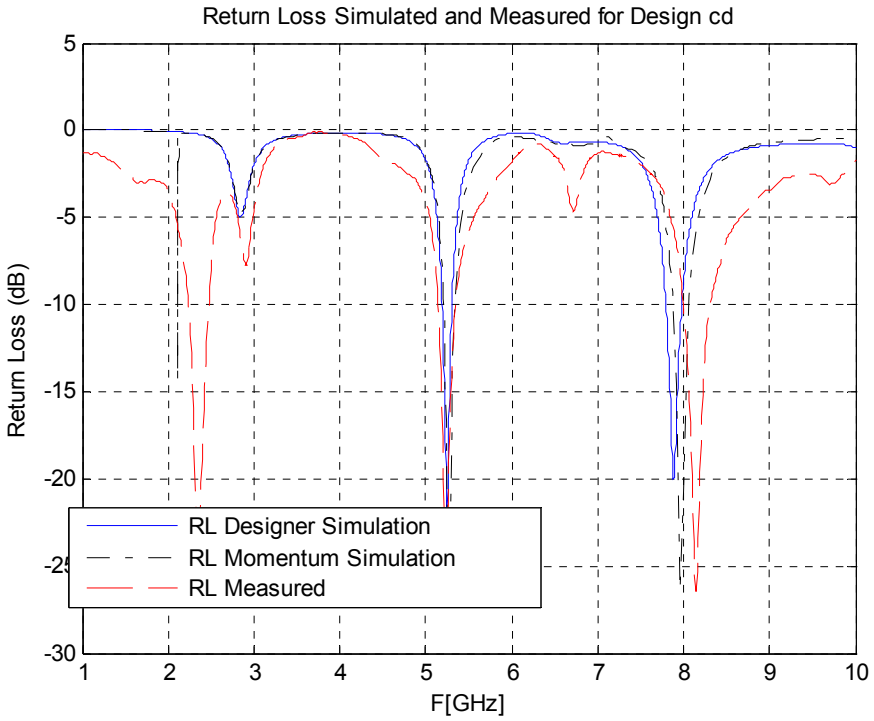

(b)

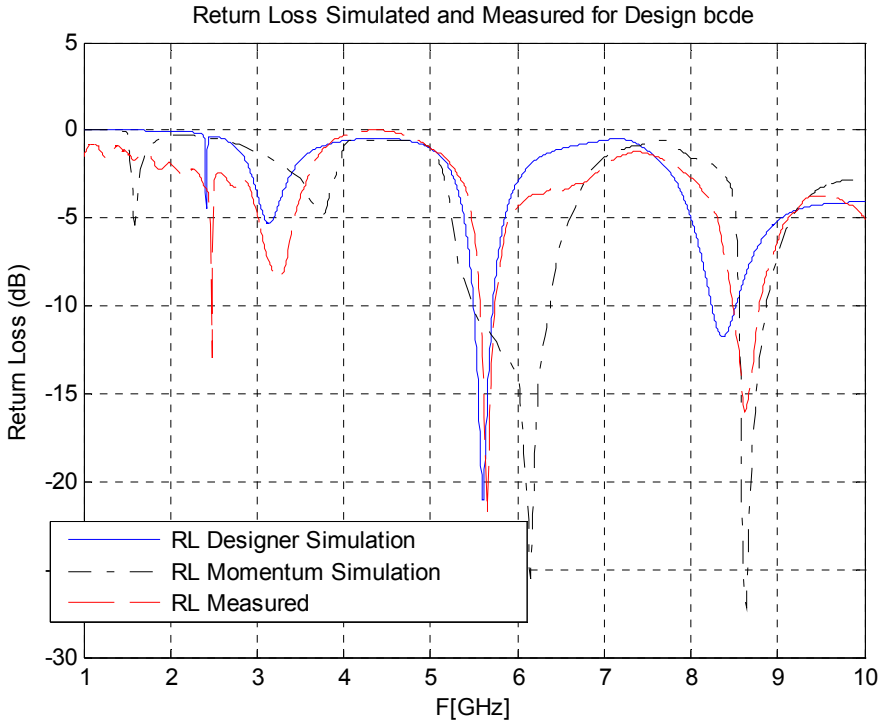

(c)

Figure 4.7.2. Continued

4.8 Summary

The results obtained of analyzing the RSRA using three approaches are presented in this chapter.

The intuitive analysis for the RSRA Case 1 and 2 was applied and the effect of the five main factors was observed in the antenna return loss and resonance frequency. The effect of changing each factor was summarized in Table (4.1.2) and Table (4.1.3). The second approach allowed identifying the confidence frequency bands in which the linear regression was a reliable tool to inference the significant factors in the antenna response. Linear models for the resonance frequency and antenna input impedance were computed in the third approach. This approach used punctual responses and two replicates of the same design.

A matching technique is presented in this chapter; this technique had been applied in folded slot antennas and it worked also for the RSRA cases. In addition, the equation models deduced in Sections 4.3.1 and 4.3.2 can be extended to the RSRA Case 3; this antenna presented the impedance scaling property. This happened either varying the distance between the parasitic ring and the feeding antenna or adding parasitic rings outside the feeding antenna. The electric field distribution on the substrate side, radiation pattern and gain was analyzed for the three RSRA cases. Finally, several prototypes were fabricated and tested. Reasonable agreement between the simulations and measured results was observed.

Chapter 5. Conclusions and Recommendations

5.1 Conclusions

The characterization of RSRA using DOE was presented in this thesis. Three different RSRA structures were considered; these structures used the principle of improving the antenna input impedance bandwidth by adding parasitic elements or parasitic rings. The characterization predicted the antenna performance according to changes in the physical dimensions and relative permittivity of the substrate. 2^5 factorial designs was the type of experiment performed; the statistical analysis was based on design simulations from two different electromagnetic simulators. The data was analyzed using three different approaches.

The first one was an intuitive approach using a geometrical representation of the DOE input factors. Only the five main factors were considered to simplify the analysis; however this analysis was enough to identify the factors that affected the antenna tuning, multiband operation, input impedance bandwidth and return loss response. These results were summarized in Table (4.1.2) and Table (4.1.3).

The second approach, intended to overcome the fact that DOE only deals with punctual responses. In this approach, the Return Loss response of each design simulation is considered as an individual datum, and as it is known this response is a continuum function through frequency. The return loss response was divided in 2000 frequency points. For each frequency point a linear regression model was computed. According to the adjusted determination coefficient over 0.6, one and two factor interaction linear

regression models are computed in confidence frequency bands. In these bands, based on testing hypothesis on individual regression coefficients the significant factors were presented. Knowing these factors, the antenna response can be optimized. In addition, codified coefficients were calculated; with these coefficients the antenna response can be predicted in a specific frequency.

The third approach computed linear regression models for the resonance frequency and the antenna input impedance using punctual responses. Several models validated the first approach inferences. In this approach also, it was possible to use a DOE software to optimize the response.

In addition, a matching and impedance scaling techniques were presented for the RSRA. The antenna electric field distribution, radiation pattern and gain were studied. Finally some prototypes were fabricated and tested.

5.2 Recommendations

The mathematical models computed for the structures studied in this research can be used as a starting point to develop further theory to characterize log periodic RSRA as well as cavity backed RSRA. In the second approach it was not possible to calculate more simplified models to predict or optimize the return loss response; it is recommended to develop a mathematical theory based on functional data analysis to overcome this flaw.

References

[1] P. Bhartia, R. Garg, Inder Bahl and A. Ittipiboon., Microstrip Antennas Design Handbook Norwood M.A. Artech House, 2001, ch 7.

[2] R. C. Johnson and H. Jasik, Ed., Antenna Engineering Handbook. New York: Mc-Graw-Hill, 1961, chs. 8, 9.

[3] S.B. Cohn, "Slot line on a dielectric substrate", IEEE Transactions on Microwave Theory and Techniques, October 1969, pp. 768-778.

[4] Janaswamy, R., and D. H. Schaubert, "Characteristic Impedance of a Wide Slot Line on Low Permittivity Substrates, " IEEE Trans., Vol. MTT-34, 1986, pp. 900-902.

[5] Tsai, H., and R. York, "Multi-Slot Antennas for Quasi-Optical Circuit." IEEE Microwave Guided Wave Lett., Vol. 5, 1995, pp. 180-182.

[6] H. C. Liu, T. S. Horng, and N. G. Alexopoulos, "Radiation from Aperture Antennas with a Coplanar Waveguide Feed," 1992 IEEE AP-S Symp. Dig., pp. 1820-1823.

[7] I. S. Misra and S.K. Chowdhury, "Study of Impedance and Radiation Properties of Concentric Miscrostrip Triangular-Ring Antenna and its Modeling Technique Using FDTD Method", IEEE Transactions on Antennas and Propagation, April 1998, pp. 142-143

[8] Fries, M. K., Gräni, M., and R. Vahldieck, "Slot-Antenna with Switchable Polarization,"Antennas and Propagation Society International Symposium 2002, vol. 2, 2002, pp. 440-443

[9] I. Carrasquillo-Rivera, R. A. Rodríguez-Solís, and J. Colom-Ustaris, "Tunable and Dual Band Rectangular Slot Ring Antenna", Submitted to IEEE AP-S Symp. Monterrey, CA June 2004.

[10] K.C. Gupta, "Design of frequency-reconfigurable rectangular slot ring antennas", Antennas and Propagation Society International Symposium, 2000. IEEE , Volume: 1 , 16-21 July 2000 pp. 326.

[11] H. Tehrani, K. Chang, "Multifrequency operation of microstrip-fed slot-ring antennas on thin low-dielectric permittivity substrates", IEEE Transactions on Antennas and Propagation, September 2002, pp. 1299-1308.

[12] Morishita, H., K. Hirasawa, and K. Fujimoto, "Analysis of a Cavity-Backed Annular Slot Antenna With One Point Shorted ", IEEE Trans. on Antennas and Propagation, Vol. AP-39, 1991, pp. 1472-1478.

[13] C.E. Tong, and R. Blundell, "A self-diplexing quasi-optical magic slot balanced mixer", IEEE Transactions on Microwave Theory and Techniques, March 1994, pp. 383-388.

[14] C.E. Tong and R. Blundell, "An annular slot antenna on a dielectric half space," IEEE Transactions on Antennas and Propagation, July 1994, pp. 967-974.

[15] K. D. Sthephan, N. Camilleri and T. Itoh, "A quasi-optical polarization-duplexed balanced mixer for millimeter-wave applications," IEEE Trans. Microwave theory and Techniques, vol. MTT-31, No 2, Feb 1983.

[16] S. Raman and G. M. Rebeiz, "Single and dual polarized millimeter wave slot ring antennas," IEEE Transactions on Antennas and Propagation, November 1996, pp. 1438-1444

[17] S. Raman and G. M. Rebeiz, "Single and dual polarized slot-ring subharmonic receivers," IEEE MTT-S Digest, 1997, pp. 565-568.

[18] S. Raman and G. M. Rebeiz, "Integrated millimeter-wave polarimetric radar receivers," IEEE National radar conference, Ann Arbor, Michigan, May 13-16, 1996, pp 232-237.

[19] K.C. Gupta, R. Garg, I. Bahl, P. Bhartia., Microstrip Lines and Slot lines. Second edition. Arthech House, 1996, ch 7.

[20] M. H. Yeh, P. Hsu and J.F. Kiang, "Analysis of a CPW-fed slot ring antenna", Microwave Conference, 2001. APMC 2001. 2001 Asia-Pacific , Volume: 3 , 3-6 Dec. 2001

[21] Moosbrugger, P.J.; Lo, Z.; Carpenter, L.A.; Barton, R.R., "Experimental Design of a Two-layer Electromagnetically Coupled Rectangular Patch with a Global Response Surface Modeling Technique"
Antennas and Propagation, IEEE Transactions on , vol. 45 , Issue: 5 , May 1997 pp. 781 - 787

[22] N. López-Rivera, and R. A. Rodríguez-Solís, "Impedance and resonance frequency characterization for Folded Slot Antennas through DOE techniques", IEEE AP-S Symp. Dig., 2003, Vol. 2, pp. 545-548.

[23] Montgomery, D.C. (2001), "Design and Analysis of Experiments", (5th edition), New York: Wiley

[24] Ansoft Corpartion
www.ansoft.com

[25] Agilent Technologies
www.agilent.com

[26] Stat ease
www.statease.com

[27] Rogers Corporation
www.rogers-corp.com

Appendix A:

t test for Three Factors Interactions. RSRA Case 1

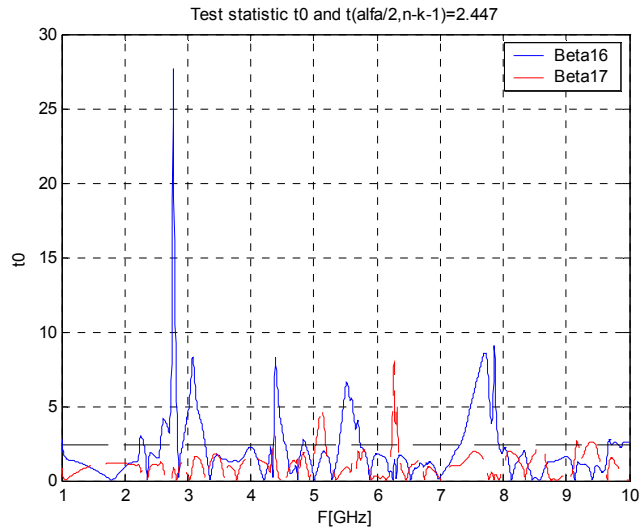

(a)

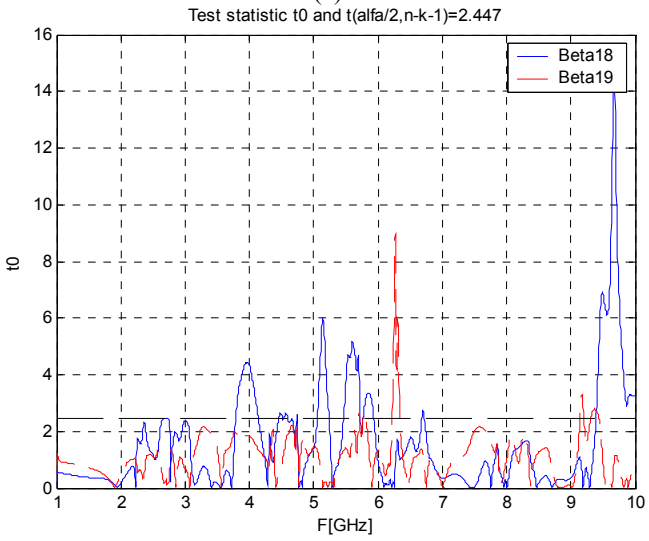

(b)

Figure A.1. T test for Three Factor Interaction. (a) β_{16}, β_{17}, (b) β_{18}, β_{19}, (c) β_{20}, β_{21}, (d) β_{22}, β_{23}, (e) β_{24}, β_{25}

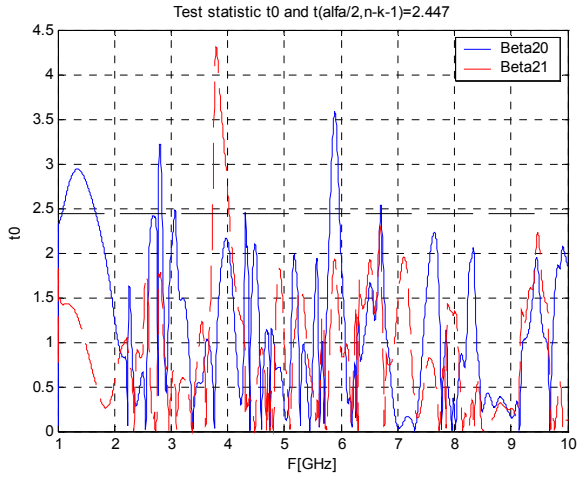

(c)

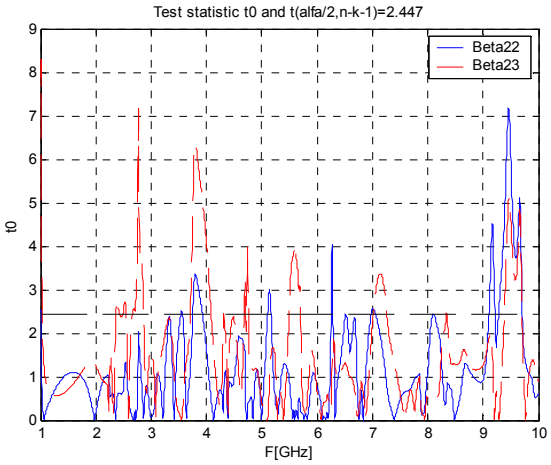

(d)

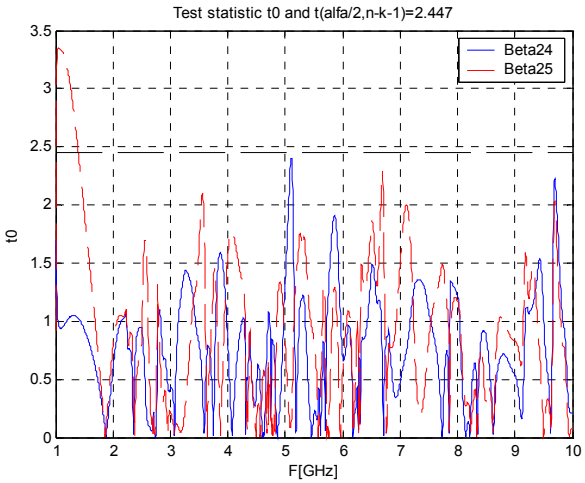

(e)

Figure A.1. Continued

Appendix B

Determination Coefficients for 5 Regressors. RSRA Case2

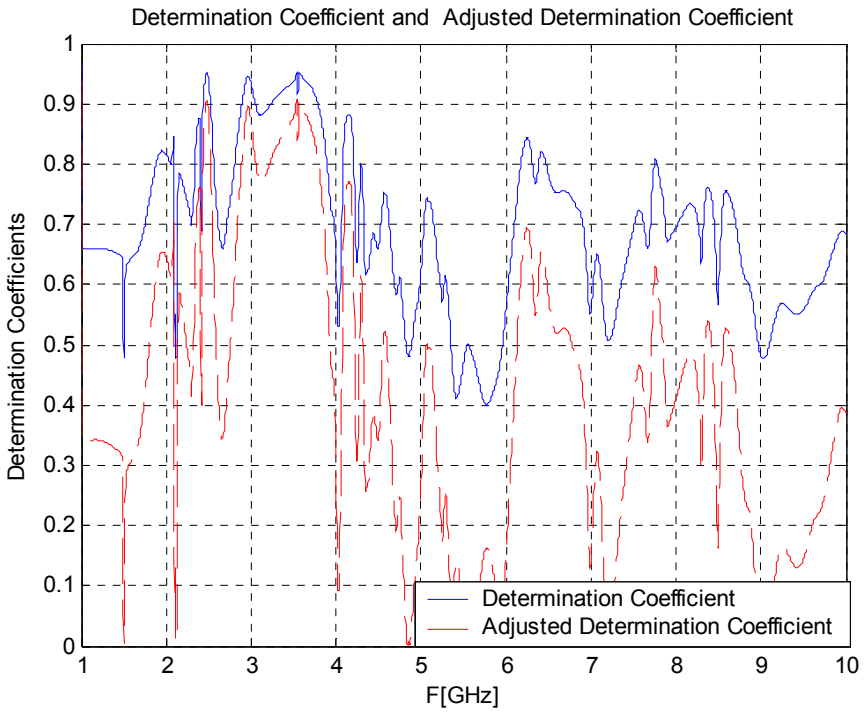

Figure B1. Determination Coefficients for 5 Regressors.